Republic of Iraq
Ministry of Higher Education and Scientific Research
University of Babylon
College of Materials Engineering
Department of Polymer Engineering and Petrochemicals Industries

Preparing and Studying the Tribological and Mechanical Properties of the Transparence Polymeric Nano Composite Coating

A Thesis

Submitted to Department of Polymer Engineering/ University of Babylon in Partial Fulfillment of the Requirements for the Master Degree in Materials Engineering \ Polymer

By

Ahmed Fadhil Abbas Hadi

B.Sc. Materials Engineering/Polymer Engineering and petrochemical industries

Supervised by

Asst. prof. Dr.
Ammar Emad Kazem Al-kawaz

Prof. Dr.
Zoalfokkar Kareem Mezaal

2023 AD

1444 AH

بِسْمِ اللَّهِ الرَّحْمَٰنِ الرَّحِيمِ

" يَرْفَعِ اللَّهُ الَّذِينَ آمَنُوا مِنْكُمْ وَالَّذِينَ أُوتُوا الْعِلْمَ دَرَجَاتٍ وَاللَّهُ بِمَا تَعْمَلُونَ خَبِيرٌ"

صَدَقَ الله العَليُ العَظيم

سورة المجادلة: الآية 11

Dedication

I would like to dedicate this thesis to all for their support and encouragement

To my kindest Mother

To my dear Brother

To my love my wife

To my dear daughter Mian

and special love to my friends who support me

and all people I love and my father

Ahmed Fadhil Abbas

2023

Acknowledgment

First of all, profusely all thanks for **ALLAH** Lord of all creation who enable me to achieve this work.

I would like to express my gratitude to my supervisors, **Asst. Prof. Dr. Ammar Emad Kazem Al-kawas and Prof. Dr. Zoalfokkar Kareem Mezaal**, for guidance, advice and enthusiastic encouragement throughout this investigation

I would like to thank the **Materials Engineering College in Babylon University** for giving me the opportunity to get the M.Sc. degree in materials science. Sincere thanks are also expressed to the staff of the material engineering college especially Polymer laboratories for their encouragement during this work.

I would like to thank all persons who stood beside me and offered their support in one way or another and all my friends for their assistance. Special thanks for **Dr. Ahmed T. Jaiad, Salam Salah, Ban Jawad and Ahmed Amer.**

I also wish to convey my utmost appreciation and thanks to my Family for their love, help, support and extraordinary patience during the years of my study.

AHMED FADIL ABBAS
2023

Abstract

This work includes preparing and studying a transparence polymeric coating that has good tribological and mechanical properties, and the coating enhanced with nanoparticles has the ability to absorb UV radiation while keeping transparency.

Reducing friction coefficient to enhance the wear resistance behavior for coating for mobile and computer screen applications also increasing the life span of car lamp covers and glass, plastic windows and coating of solar cells.

The solution-casting technique was used to create the nanocomposite coating made of GO, Graphene oxide modified (MGO), hybrid filler of MGO and Bees wax (BW) and polymer PMMA. By using a solution mixing procedure, composite coating samples with GO, MGO nanoparticles at different weight percentages (0, 0.25 , 0.5, and 1 wt %) and 1 wt% of MGO with (0.1,0.25 and 0.5 wt %) of BW were created. The distribution of nano and the fracture failure were assessed using scanning electron microscopy (SEM) method.

The chemical structure of the PMMA and nanocomposite coating was examined using the (FTIR) method also Hardness, FTIR, DSC, UV, nanoindentation, contact angel and pull off and wear tests were done for samples. Additionally, the mechanical characteristics of PMMA nanocomposites coating were investigated in the nanoparticle addition and to investigate the connection between tribological and mechanical behavior.

The outcomes demonstrated that the inclusion of the GO, MGO nanoparticles improved the PMMA tribological performance. The wear and friction coefficient of PMMA nanocomposites coating were found to be lower than those of pure PMMA coating. Coefficient of Friction decreased by 26% for PMMA\MGO\BW 0.5 wt% and this sample has lowest wear rate and coefficient of friction. According to the microstructure data, the ultrasonic

treatment had a significant role in achieving excellent dispersion and reducing the agglomeration of the nanoparticles.

There has been a noticeable improvement, as seen by the findings of mechanical properties such as hardness, elastic modulus, and pull off. UV test showed that there is decreasing in transparency with increasing filler content and the absorption of UV increasing with addition of GO, MGO fillers and hybrid filler of MGO and BW.

The results of the wettability indicate that the addition of beeswax improved the wettability resistance of PMMA. The improvement in hardness (Vickers) by 55% for PMMA\1 wt % MGO\BW 0.5 wt% . Elastic modulus has improved by 38% for sample PMMA\ MGO\BW 0.5 wt% , and the results of the wettability tests showed that there is increasing with addition of modified Graphene oxide and beeswax. T_g increased about 20% for PMMA\MGO 1 compared with pure PMMA.

List of Contents

List of Symbols

Symbol	Description	Unit
A	Cross- Sectional Area of Specimen	mm^2
Aa	Nominal Contact Area	mm^2
Ac	Counter Area	mm^2
A_r	Real Contact Area	mm^2
E	Modulus Of Elasticity	GPa
ε	Strain	__
F_n	Normal Force	N
T%	Transparency	
G_c	Impact Strength	J/m^2
H	Hardness	_
L	Sliding Distance	m
P	Pressure	MPa
Hsp	Scratch Hardness	
Ra	Roughness	µm
µ	Friction of Coefficient	
v	Velocity	m/s
W. R	Wear Rate	gm\cm
θ	Diffraction Angle	Degree
T_g	Glass Transition Temperature	°C
σ	Stress	MPa
°C	Degrees Celsius	°C

List of Abbreviations

Symbol	Description
BW	Bees Wax
APTMS	(3- aminopropyl) trimethoxysilane
ASTM	American Society For Testing And Materials Specifications
CA	Contact Angle
CF	Carbon Fiber
E	Modulus Of Elasticity
F	Normal Force
FTIR	Fourier Transform Infrared Spectroscopy
GO	Graphene Oxide
MGO	Graphene Oxide Modified
PMMA	Poly (Methyl Methacrylate)
PEI	Polyethylenimine
DSC	Differential Scanning Calorimetry
PPS	Polyphenylene Sulfide
PTFE	Polytetrafluoroethylene
SEM	Scanning Electron Microscope
Silane	Trimethoxysilanes
T_h	Thickness of The Film
TiO_2	Titanium Dioxide
UV	Ultraviolet
VF	Volume Fraction
XRD	X-Ray Diffraction

Chapter One

Introduction

1. Introduction

Coating technology employs organic coatings to offer surface protection, decorative finishes, and a variety of other uses for goods and trade. Numerous commonplace items are only useable and hence sellable due to their surface treatment [1].

Lately, the development of multifunctional polymer coatings has gotten a lot of consideration because of the value of these materials in applications, for example, drag decrease in microfluidic gadgets, self-cleaning surfaces, and the counteraction of consumption and fouling [2]

Using thin coatings allows the designer of a mechanism to take full advantage of the mechanical characteristics of the underlying substrate without compromising lubrication conditions. This argument is, perhaps, the strongest advantage that the usage of thin film coatings provides over the usage of bulk materials. To make full use of this argument, more wear resistant, higher load bearing ability and even lower friction characteristics coatings must continuously be developed [3].

Polymethyl methacrylate (PMMA) is among the best polymers for solar applications. It provides exceptional optical qualities, great machining precision, and inexpensive prices. The coating of soft material serves primarily to enhance its mechanical durability. Additionally, anti-reflective coatings are important for many solar applications [4].

Polymers are now often used in a variety of tribological applications. This is a fast-growing field that offers the appealing benefits of self-lubrication and enhanced cleaning. Furthermore, the intrinsic weakness of polymers might be successfully reduced by utilizing various unique fillers; polymer composites are increasingly

being employed as sliding components, which were previously solely made of metallic materials [5].

Today, polymer composites are one of the most widely used engineering materials, with a significant market share. They offer a unique combination of benefits, including simplicity of manufacture, good performance and cost-effectiveness, which polymers, metals and ceramics cannot match. On the other hand, polymers cannot provide the qualities required for tribological applications on their own. Inorganic particle fillers are used to improve properties and reduce the cost of polymer goods [6].

In the past, polymeric/inorganic composite materials have garnered considerable interest for diverse purposes. Polymer matrices have been infused with inorganic fillers in the form of nanoparticles, nanotubes, and fibers to gain diverse functional characteristics [7].

The addition of fillers or fibers to thermoplastic polymers helps to reinforce the surface, hence improving the polymer's tribological performance. Fillers, such as particles, are frequently added to polymeric materials to improve processability and mechanical compound qualities while also lowering material prices. The behavior of fillers is influenced by their shape, surface area, surface chemistry, and distribution of particle sizes [8, 9].

Thermoplastics have various advantages over thermoset matrices, including higher impact tolerance, decreased fracture propagation, recyclable materials, superior chemical resistance, and rapid forming process availability [10].

Polymers toughened with nanoparticles are rising in popularity as a result of their extraordinary capabilities resulting from nano-scale formations. One of the most appealing properties of nanoparticles is their extraordinarily high specific surface area, which allows for the creation of a large quantity of interphase in a composite and, as a result,

a strong link between the fillers and the lattice even with a somewhat low load nano filler. When nanoparticles are incorporated into a polymer–matrix, the wear rate of the polymer is frequently reduced [11].

In recent years, graphene oxide has garnered a great deal of attention not only because of its exceptional inherent qualities, but also because it has been used to generate a diverse assortment of materials [12].

As a graphene derivative, graphene oxide (GO) is an oxidized form of graphene having oxygen-containing functional groups connected to its edges and surface, such as epoxy, hydroxyl, and carbonyl [13].

This facilitates the manufacture of many homogeneous GO layers using straight forward solution coating techniques, such as spray coating, spin coating, and solution casting, as well as the quick dispersion of GO in polar solvents [14, 15].

Several uses of coated GO light waveguides in photonics have been demonstrated. This category includes humidity sensors, waveguide polarizers, saturable absorbers, and optical modulators [16, 17].

In this study, graphene oxide and preparation of modified graphene oxide nanoparticles were incorporated into PMMA matrices as a reinforcement and addition of bees wax as a lubricant in order to create polymer/graphene oxide nano composite coatings for Teflon and glass substrates. The influence of graphene oxide concentration, beeswax, and polymer matrices on the mechanical, optical, and tribological properties of coatings was examined.

1.2 Aims of the Work

This work is dedicated to prepare and study the tribological and mechanical performance of polymer nanocomposite coating. Studying the effect of graphene oxide, modified graphene oxide and graphene oxide\ beeswax hybrid filler on the tribological, mechanical and optical properties of the resultant coating and reducing friction coefficient to enhance the wear resistance behavior for coating for mobile and computer screen applications also Increasing the life span of car lamp covers and glass, plastic windows and Coating of solar cells.

1.3 Scope of the Work

To achieve the above aims, the following activities has been done:

1. A survey of the relevant literature.
2. Choosing simple technique, which is solution casting coating method.
3. Carrying out the required structural mechanical and tribological tests to determine various properties, such as hardness, wear state, nano indentation, SEM, UV and so on.

Chapter Two
Theoretical Part and Literature Review

2.1 Introduction

Polymers are a class of materials with a wide range of applications in daily life. Due to their use in several fields of research, technology and industry. polymeric materials have thus far had a significantly greater impact on society. Additionally, the demand for lightweight composites made of high strength polymeric materials is steadily rising because of these materials' superior mechanical qualities, low processing temperatures, high performance, cheap cost, and exceptional environmental stability [18].

Utilizing nanoscale particles in polymeric coatings has recently proven to be a successful way to enhance their mechanical, optical, physical, anticorrosion, electrical, and thermal characteristics [19].dry lubricants have been used classically in applications involving vacuum, high temperature, contamination sensitive and chemically aggressive conditions, because in these environments' fluid lubrication is not feasible [20].

In the area of dry lubrication, solid lubricants are used in the form of bulk materials and in the form of thin coatings, the selection between these two forms of material usage is mostly dependent on the design requirements and characteristics of the specific mechanical system to be studied.

Base materials for solid lubrication are chosen due to their natural characteristics of low resistance to shear forces. This is the sought behavior to promote effective lubrication. This natural characteristic can rise from atom arrangements (typically lamellar solids) or molecular structures.

An example of material that provides dry lubrication due to atom arrangement is graphite. Lubrication characteristics are delivered due to

the weak London forces that govern interaction between carbon planes promoting low resistance to relative sliding motion [22 ,21].

The exponential increase in the polymer composites usage reflected and supported the extraordinary transformations that happened in the 20th century. The use of composite materials has increased recently due to its better advantages, which include low weight, strong mechanical and chemical resistance, and high thermal capabilities, which go beyond the base material alone. Composite materials are used in a number of applications.

The composite material may be made with a variety of properties and improved in one area without impacting another, depending on the application and purpose of usage. Nowadays, composite materials are used extensively in the aerospace and aviation industries [23].

The field of nanotechnology has attracted attention due to the potential to develop both human lives and the planet as a whole [24].polymer/graphene synthesized nanocomposites and graphene-doped polymers such as epoxy, polyethylene (PE), and polymethyl methacrylate (PMMA) are also available [25].

2.2 Poly Methyl Methacrylate (PMMA)

It is a kind of polymer made of methyl methacrylate. PMMA, Plexiglas, and Lucite are trade names for poly methyl methacrylate, which belongs to the vinylidene polymers family (acrylics) [26].

This type of polymer has unique optical qualities, including transparency of around 92 percent, theoretical limit for incident visible region, very little UV absorption. PMMA can be utilized instead of glass, coating, and as a resistance for electron beam or ion-beam resists in microelectronics chip fabrication [27].

Because of the methyl ester pendant groups, which prohibit molecules from forming crystalline bonds with one other, PMMA is classified as an amorphous substance [28].

PMMA from the standpoint of a hydrocarbons, poly [1-(methoxy carbonyl)-1-methyl ethylene], and from the perspective of an ester, poly (methyl2-methylpropenoate monomer of isocyanate [29].

PMMA was developed by Hill and Crawford at the beginning of the 1930s, while German chemist Otto Rohm used it for the first time in 1934 [30]. PMMA is a thermoplastic that is optically clear (transparent) and frequently used in place of inorganic glass due to its high impact strength, low weight, shatter resistance, and favorable production characteristics [31].

PMMA is a promising polymer with potential uses in coating, conductive devices, sensor, analytical separation, and pneumatic actuation [32].

The appealing optical and physical characterizations of poly(methyl methacrylate), which are important for determining its area applications, make it a necessary and fascinating polymer. PMMA is a high stiffness, strong insulation. There are certain drawbacks to poly(methyl methacrylate), such as brittleness and poor chemical resistance, although these can be improved via chemical or physical alteration. Each unit has both hydrophilic (carbonyl) and hydrophobic (methylene) groups [33]

PMMA is an environmentally friendly substance. The external lenses of cars and trucks are made of PMMA. it is used to make the spectator shield in ice hockey arenas. Many motorcycles helmet visors and the windows on many airplanes and police cars used for riot control are made of PMMA. Medicine also makes use of PMMA.

It is having been utilized to replace intraocular lenses in eyes because of its high compatibility with human tissue. PMMA is a common material used to make hard contact lenses. PMMA-containing bone cement is used to affix implants and replace missing bone. PMMA effectively distributes stress with natural bone because its Young's modulus is close to that of bone. PMMA is frequently used for dentures [34].

2.2.1 PMMA Physical Properties

PMMA which is a transparent, colorless polymer with 100 °C glass transition temperatures and, at ambient temperature, a density of 1.20 g/cm^3. The polymer has a melting point of 130 degrees Celsius [35] .PMMA has high exposure resistance to sunlight because of how little it changes when exposed to UV rays. It also has excellent optical qualities [36].

PMMA has a high Young's modulus and a low elongation at breakage, which contribute with its mechanical strength. Being one of the toughest thermoplastics with exceptional scratch resistance, it does not break when ruptured. The majority of laboratory chemicals' aqueous solutions have no effect on this polymer, demonstrating its respectable chemical resistance. It is only moderately resistant to esters, ketone, and chlorinated and aromatic hydrocarbons [37].

The tactility of a polymer, particularly vinyl polymers, is defined as the relative stereochemistry. Glass transition temperature (Tg), solubility, hydrolysis, and crystallinity of a polymer are all physical properties that not depend only on the monomer type but on the secondary and tertiary structures, or link stereochemistry [38].

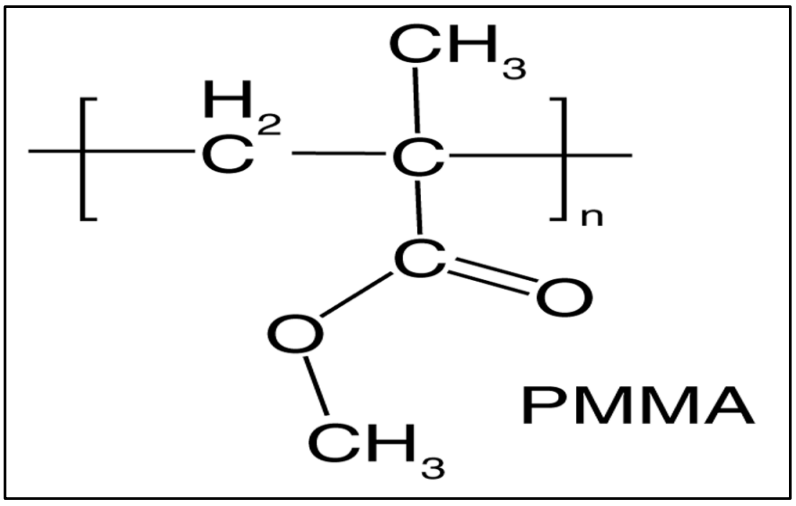

Figure 2.2: A chemical structure of the repeating unit of PMMA polymer [39].

2.2.2 Optical Applications of PMMA

Many academic fields, including medicine, engineering, astronomy, and pure science, use optical science and place great importance on it. additionally, practical applications include those found in lasers, microscopes, fibers, lenses, and polymers. The optical activity of a substance is determined by the refractive index of the substance and is the result of the interaction of the substance with light. PMMA is employed in optical applications due to its high refractive index, good UV light resistance, chemical stability, and exceptional mechanical characteristics. Organic polymers are excellent substrates for immobilizing semiconductors for heterogeneous photocatalytic applications because they are often inexpensive, lightweight, and simple to produce [40].

2.3 Applications of PMMA in Nanotechnology

In the realm of nanotechnology, a significant advancement was made possible by the discovery of interactions between polymers and nanomaterials. This interaction created polymer nanocomposites that improved material properties with a small number of nanoparticles.

Strength, flame retardancy, scratch resistance, optical characteristics, electrical conductivity, thermal stability, and solubility can be improved.

Due of nanocomposites promise in nanotechnology, many researchers focus on their fabrication and uses. Plastic chip electrodes (PCEs) were made using PMMA and graphite using a straightforward solution casting technique. Also PMMA using in coating of soler cell .This material was characterized by AFM, SEM, microscopy, mechanical, and electrical properties, and TGA. The created electrode was affordable, useful for many different applications, and replaceable [41].

2.4 Graphene Oxide (GO)

The most popular precursor for making graphene materials right now is graphene oxide (GO). Sulfuric acid and potassium permanganate are the two main ingredients used in the modified Hummer's technique, which is often used to create GO by intercalating and oxidizing graphite powder [42].

Graphene oxide, which is often produced by exfoliating graphite, opens the door to the flexible, inexpensive properties. In recent times, fillers for creating composites have used graphene oxide and graphene bucky paper. The bucky sheets are composed of a self-contained, porous, and thin carbon fillers network connected by van der Waals forces.

Numerous processes, including as vacuum filtering, evaporation-induced, resin infiltration, spin coating, and self-assembly utilized to create graphene oxide and products with graphene that resemble paper [43].

GO is highly desirable for bendable, flexible thin film optoelectronics, generated on plastic or paper-like substrates. Similar to carbon nanotube network architectures, graphene and graphene oxide sheets may combined to generate polycrystalline thin films with multi-layered network structures.

Thin film transistors, transparent conductors, electrodes, chemical/biological sensors [44].

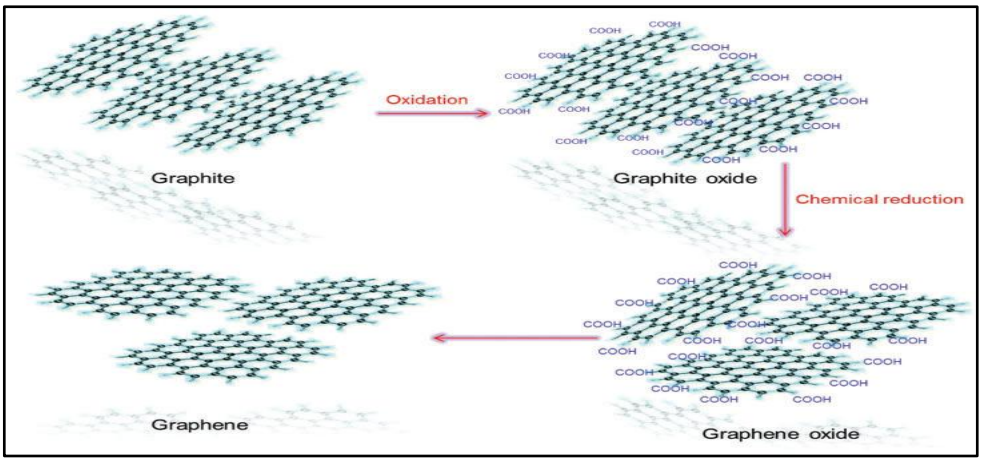

Figure 2.3: Graphene cycle [45].

photodetectors, non-volatile memory systems, field emitters, and paper-like materials based on graphene and graphene oxide each have special properties [46].

Graphite exfoliation yields GO, graphite intercalation chemicals, and graphene. At first, GO created by exfoliating graphite with HNO_3 and H_2SO_4 [47]By reducing the interplanar forces, the chemical alteration of the GO surface resulted in lamellar stacking. Therefore, under thermal, ultrasonic, and other intense conditions, these oxidized GO layers may be removed with ease. It has been crucial to prepare GO in order to synthesis graphene.

Offman and Hummer suggested an alternative method of GO oxidation that involved contacting graphite with strong sulfuric acid and

potassium permanganate ($KMnO_4$). The modified Hummer technique is the most often used method for GO production [48].

Alkaline is solution used to decrease a GO dispersion; they created reduced GO. They came to the conclusion that this process created thin lamella carbon with very little hydrogen and oxygen. The so-called "graphite oxide soot" resulting from the rapid combustion of graphite oxide was investigated. According to electron microscopy, this soot was revealed to include graphene nanoplatelets, which are comprised of multi-layer hexagonal sheets of carbon (approximately 12.6Aº, or 2-3 layers). Graphite and its intercalation compounds, however, attracted a lot of attention since they offered a practical path for ion storage. Graphite intercalation compound was a new name for a single carbon layer in the graphite structure [49].

2.4.1 GO Physical Properties and Reactivity

Hydrophilic and intensely oxygenated graphite oxide can be exfoliated in water to create a stable dispersion. The dispersion comprises graphene oxide sheets [50].

The most typical GO dispersion medium is water, and there are two methods for dispersing GO in water, mechanical stirring and sonication. However, several applications show that sonication is inferior to mechanical stirring because it produces flaws and shrinks the size of the GO sheet (from microns to a few hundred nanometres) [51].

Numerous solvents, such as tetrahydrofuran (THF) and N, N-dimethylformamide, can be used to dissolve GO. Therefore, it is believed that GO is amphiphilic in nature, with the edges being more hydrophilic and the center being more hydrophobic, and that it may have a surfactant-like function [52].

2.5 Coatings of Polymers and Their Composites

In general, coatings can be classified as either hard‖ or soft coatings and polymer-based coatings belong to the soft coatings.

Using the Archard wear model, we would expect hard coatings such as diamond-like carbon (DLC), Ti–N and WC/C synthesized through physical vapor deposition (PVD) techniques are effective in preventing both abrasive and adhesive wear of metal sliding contacts [53].

DLC coating has a significantly lower scuffing load and higher COF compared with a PTFE-based coating under simulated unidirectional sliding swash plate compressor environment. In addition, hard coatings (DLC) are more sensitive with the environment conditions and hard coatings are relatively expensive and exhibit difficulties in coating them on substrates with low surface energy or high roughness. Some metallic alloys with different preparation methods can decrease wear rate and COF [54, 55].

Tribological performance improvement is not very sufficient for extremely low wear and COF applications. Thus, alternative solutions such as inexpensive soft polymer coatings need to be explored.

Polymer coatings are widely used as tribological protective coatings, such as erosion/corrosion resistance coatings for automobile transparent protective coating for touch panel screens and optical applications , hydrophobic coatings for moisture repellent and dirt resistance

Bio-implant materials like artificial joints , bearing materials for compressor bearings or thrust pad bearings . Most of the researchers have been using Nano/Micro indentation/ scratch or moderate conditions such as low PV (pressure times velocity) and low

temperature to investigate these polymer coatings‘ tribological performance [56, 57].

2.6 Nanocomposite

Nanocomposites can be used to create monophasic or multiphasic ceramics, glasses, or porous materials, each having specifically designed and enhanced characteristics. In comparison to monophasic or micro composite alternatives, a range of nanocomposites, including those made of sol-gel, intercalation, entrapment, electro ceramic, and structural ceramics, display better characteristics. It is anticipated that the use of nanocomposites in materials processing will have a significant influence on ceramic materials used in electro ceramics, catalysis, sensors, and other fields of technology [58].

A multiphase solid material or a structure with nanoscale repeat distances between its various phases, when one of the phases has one, two, or three dimensions of less than 100, is referred to as a nanocomposite (nm). Due of their desired electrical characteristics, nanocomposites are frequently employed in semiconductor and electronics applications.

Nanocomposite may be produced as transparent conductive films (TCF), which are a highly transparent, cost-effective replacement for traditional materials in flexible displays and touch panels. Compared to traditional materials, the market for nano composites is growing much faster, with market volume in 2018 expected to be between 3.5 and 5 times that of 2010 [59]. Figure 2.5 show the growth of nano composite.

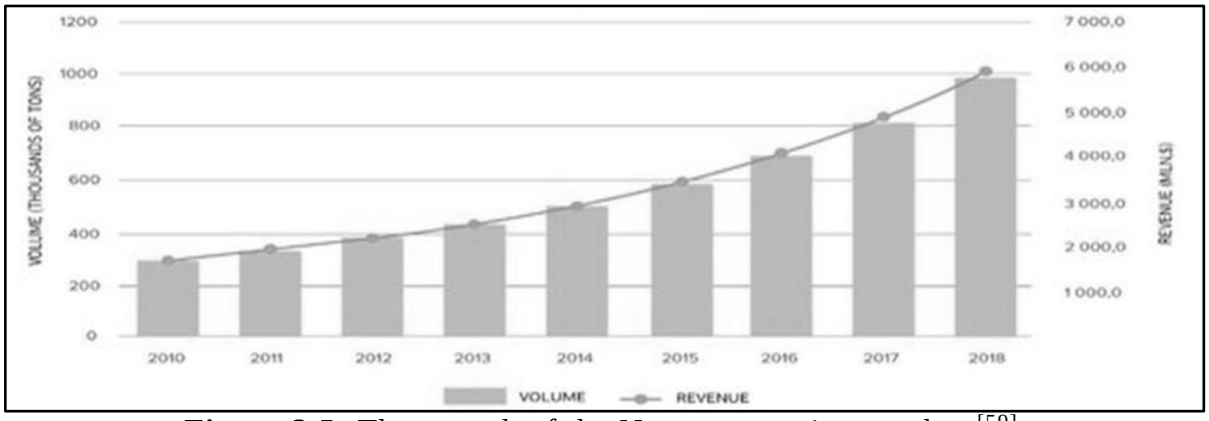

Figure 2.5: The growth of the Nano composites market [59].

Multiple phases that have at least one, two, or three dimensions in the nanoscale range offset a nanocomposite material. Phase interfaces are produced when material dimensions are reduced to the nanoscale level, and they are crucial for improving the characteristics of the material.

The surface area to volume ratio of the reinforced material used to create nanocomposites has a direct impact on our understanding of how structure and property relate to one another. Opportunities for overcoming barriers in the medical, pharmaceutical, food packaging, electronics, and energy industries are provided by nanocomposites on whole new scales [60].

2.7 Types of Nanocomposites

According to the kind of matrix, nanocomposites are divided into three categories

However, nanocomposite types according to the reinforcing type include [61].

2.7.1 Nanoparticle-Reinforced Composites

The most often used composites in everyday materials are probably particulate composites, those are strengthened with microscopic particles of various substances. Particles are often incorporated to increase the yield strength and matrix elastic modulus [62].

It has been demonstrated that new material characteristics may be acquired by decreasing the particle size to the nanoscale [63].

2.7.2 Nanoplatelet-Reinforced Composites

The two most well-known varieties of nanoplatelet-reinforced composites are nano graphite and nano clay. Both clay and graphite may be found as layered materials in their bulk forms. The layers must be divided and distributed evenly throughout the matrix phase in order to make the most use of these components.

The inter-layer gap in a clay particle is at lowest in the classic miscible condition. The distance widens and is referred to as the intercalated condition when injecting polymer resin into the gallery separating the neighbouring layers. A clay is regarded as having exfoliated after the layers have completely separated [64].

Different filler materials are used, but montmorillonite, a form of nano clay, is the most popular. Clays are hydrophilic in their natural form, whereas polymers are hydrophobic [65].

2.7.3 Nanofibers-Reinforced Composites

Many different polymers, such as poly (ethylene terephthalate), polycarbonate, acrylonitrile-butadiene-styrene, poly (ether sulfone), polypropylene, poly (phenylene sulfide), nylon, and epoxy, have been reinforced using vapor-grown carbon nanofibers.

It is well known that carbon nanofibers may have a variety of morphologies, from structures with a chaotic bamboo-like structure to highly graphitized, in which the conical shells of the nanofiber are nestled within one another. Typically, the diameter of carbon nanofibers ranges from 50 to 200 nm [66].

2.8 Fabrication of Polymer Nanocomposite

The creation of innovative polymer-nanocomposites (PNCs) has attracted a significant amount of study over the past decades. In difference to typical composites, the PNCs have fillers fewer than 100 nanometers in size. Polymer-nanocomposite has the benefit of enhancing the pure polymer's qualities without compromising its processability, intrinsic mechanical properties, or light weight [67].

The size and characteristics of the nanofiller, as well as the interface between the nanofiller and the matrix, are the most important aspects of the design and behavior of PNCs. Carbon nanotube (CNT)-based PNCs have been extensively studied in recent years. The intrinsic bundling of CNTs, the restricted availability of high-quality nanotubes, and the expensive cost of these materials have limited their applicability [68].

Graphene has garnered interest as a candidate for the creation of innovative PNCs because its outstanding features and the accessible availability of progenitor, graphite. Extremely low graphene loadings could substantially enhance the physical, electrical, and mechanical properties [69].

Due to its remarkable reinforcement in composites, graphene and its derivatives-filled polymer nanocomposites have demonstrated vast application potential in the domains of electronics, aircraft, car, defense

industries, green energy, etc. Integration of individual graphene into polymer matrices is of utmost importance if its characteristics are to be fully exploited in applications. Graphene surface-to-volume ratio was higher than carbon nanotubes, making it possibly more useful for enhancing the electrical, mechanical, thermal, microwave absorption properties of polymer matrices, and gas permeability [70].

2.9 Graphene-Polymer Nanocomposites Synthesis

Utilizing three separate synthesis techniques, graphene-polymer nanocomposites were produced. Solution blending, melt blending, and in situ polymerization are the most common techniques for producing

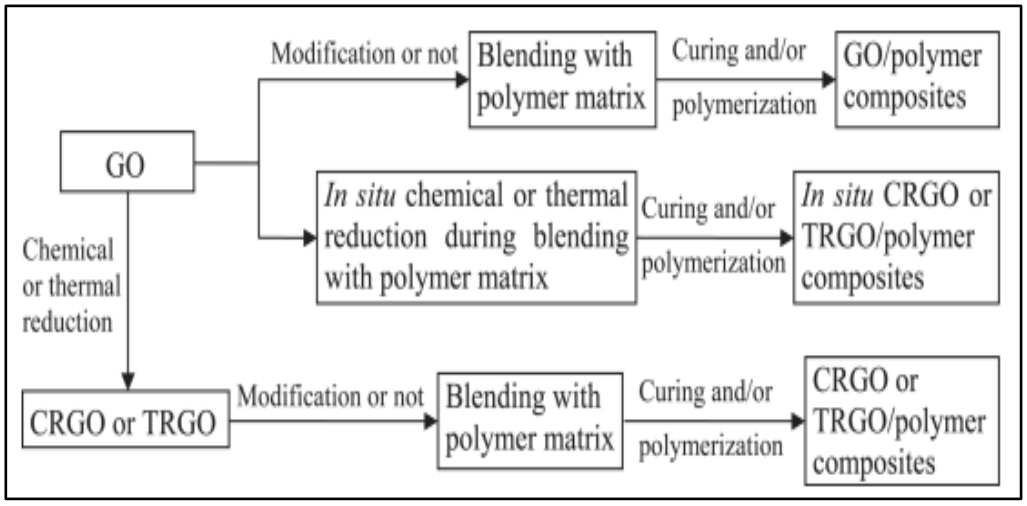

polymer matrix composites.

Figure 2.6: Generic manufacturing methods for filler-filled polymer-based composites (GO) [71].

2.9.1 Solution Mixing

The most basic approach for preparing polymer composites is solution mixing. The procedure involves three steps: ultrasonication-assisted filler dispersion in a suitable solvent, polymer integration, and remove of solvent by distillation or evaporation Polymer covers graphene sheets during the solution mixing process, and after the

solvent evaporates, the graphene sheets reassemble, create the nanocomposite by sandwiching the polymer [72].

A polymer and filler's solvent compatibility plays a crucial role in generating a proper dispersion. This method may be used to create polymer composites from a variety of polymers, including poly (vinyl alcohol) Polyvinyl fluoride, Polyethylene , Poly (methyl methacrylate) [73].

GO is compatible with water-soluble polymers like PVA because of the oxygen functional groups. By mixing PVA powder right into an exfoliated aqueous solution of GO at 85 °C, GO-PVA composites were created. The bulk of the GO sheets are completely exfoliated and clearly well-dispersed in the PVA matrix, with just a tiny number of restacks, according to field emission scanning electron microscopy (FESEM) images. XRD measurements of composites verified the molecular dispersion of GO in the PVA matrix. Chemical functionalization can increase the solubility and polymer interaction of GO [74].

GO was grafted with polymer utilizing a solution mixing method. Functionalization of graphene sheets is advantageous for dispersion in water and organic solvents with less agglomeration and for obtaining composites with greater graphene loading. Ultrasonication can aid the homogenous dispersions nevertheless, extended exposure to huge power of ultrasonication might result in defects in graphene that harm the characteristics of the composite [75].

Functional groups on GO that include oxygen may disrupt the conjugated structure, reducing carrier mobility and concentration. Additionally, the linked groups change graphene's electronic structure and act as potent scattering sites that interfere with electrical current. GO sheets are often insulating as a result [76].

2.9.2 Melt Blending

In particular for thermoplastic polymers, melt blending is a more practical and adaptable method. Fillers are dispersed in the polymer matrix using a high temperature and shear force. High temperature softens the polymer matrix, allowing for straightforward dispersion of the reinforcing phase [77].

Another method disadvantage is the rolling, bending, or even shortening of graphene sheets during mixing as a result of intense shear pressures, which is not conducive to greater dispersion [78].

The impact of blending techniques on the characteristics of graphene/polyethylene nanocomposites has been explored. The bulk of melt-blended samples seem to be phase separated, and occasionally full exfoliation happens. In addition, they found that melt-blended composites did not demonstrate significantly increased electrical conductivity, but solvent-blended graphene could reduce the surface resistance of polymer at concentrations, incorporating graphene into a PE matrix enhanced the tensile modulus, regardless of the blending technique [79].

Nevertheless, it’s have created graphene/poly (lactic acid) (PLA) nanocomposites with improved properties by melt mixing. The researchers have employed a master-batch technique for melt-blending graphene into PLA. The graphene was successfully dispersed, resulting in nanocomposites with greatly improved crystallinity, electrical conductivity, mechanical properties, crystallization rate, and flame resistance. The properties are determined by graphene dispersion and loading [80].

2.9.3 In Situ Polymerization

It is a frequently employed method for fabricating graphene polymer nanocomposites such as epoxy, PMMA [81] poly (butylene terephthalate) (PBT) , PE etc. This process involves inflating graphene or a derivative of it in a liquid monomer before dispersing a suitable initiator. Heat or radiation can cause polymerization to occur.

During in situ polymerization, the intercalation of monomers into the layered structure of graphite increases interlayer spacing and exfoliates graphene platelets, resulting in well-dispersed graphene in the polymer matrix. Using multiple chemical processes, the in situ polymerization approach enables covalent connection between functionalized sheets and polymer matrix.

Major disadvantage of this technology is the rise in viscosity as the polymerization process progresses, which complicates handling and restricts load fraction . In addition, the method is sometimes performed in the presence of solvents, a major issue in the solvent mixing technique is solvent removal [82].

Using in situ polymerization to create chemically modified graphene/epoxy composites, the lowest electrical conductivity percolation threshold has achieved for epoxy reported. Research revealed a universal method for fabricating highly dispersed graphene/polymer nanocomposites with precise structural control [83].

2.10 Polymer/GO Composite

Graphene oxide paper compositions demonstrated extraordinary electrical conductivity together with amazing mechanical rigidity and flexibility when they were left to stand alone. Due to these properties, GO paper may be useful for electrochemically active materials that are

flexible, such as batteries, supercapacitors, medical devices, and fuel cells [84].

Due to the smaller active surface of unitary graphene and the lower electrical conductivity of GO, these materials are incapable of sustaining heightened electrochemical activity. To enhance the GO and graphene paper materials' electrochemical characteristics, a second phase that is both electrochemically active and electrically conductive is required.

The mechanical and thermal characteristics of the resulting nanocomposites can be improved by adding graphene oxide filler components to a polymer matrix. This is in comparison to the qualities of pure polymer. Low concentrations of GO can completely alter the chemistry of a polymer matrix, resulting in novel features such as antibacterial and fire-retardant qualities [85].

GO sheets are known to possess phenolic and carboxylic hydroxyl functionalities. When the aniline monomer is immersed in the polymer's aqueous phase, hydrogen bonds or van der Waals forces adsorb it to the site containing the functional groups described above. As a result, these locations act as seeding dots for polyaniline nanoparticles [86].

2.11 Mechanical Features of Composites with Graphene Oxide and Polymers

One of the most resilient substances ever made, graphene oxide may improve the mechanical properties of polymer matrices even when subjected to extremely low loads. The most significant improvements are in tensile strength and elastic modulus.

Graphene oxide/polymer composites, in addition to ways for graphene reinforcing polymer matrices The different manufacturing procedures lead to an increase in the tensile strength and elastic

modulus of polymer composites with different graphene loadings. This is owing, in part, to the vast disparities that exist between the structure and fundamental characteristics of graphene, as well as between its surface modification, the polymer matrix, and the process of polymerization [87].

The abundance of functional groups in GO promotes strong interfacial contact and load transfer from the host polymers to the GO; the functional groups have the power to significantly alter the van der Waals interactions between the GO sheets, which facilitates the dispersion of the GO sheets in polymer matrices; and the high molecular weight of GO makes it more resistant to aggregation [88].

GO may not be preferable to clay for mechanical reinforcement due of clay's cheaper cost. GO is lighter and more flexible than clay, making GO/polymer composites better structural materials. Graphene/polymer composites may be multifunctional. Electrical and thermal conductivity should also be improved [89].

GO has better thermal and electrical conductivity. Due to variations in surface chemistry, which lead to variations in the dispersion states of fillers in matrices, the interfacial interactions between fillers and matrices, and the crystallinity of the polymer matrices, the efficacy of GO/polymer composites to improve mechanical properties differs from that of GO composites. The effect of GO to nanocomposite loading enhances tensile strength [90].

2.12 Modification of Nanographene Oxide

Graphene oxide (GO) and Graphene are well-known, atomically thin, two-dimensional barrier materials with excellent gas barrier and mechanical properties [91].The surface of fibers that have a high degree

of crystallinity is chemically inert and smooth to the microscopical eye. As a consequence of this, their adhesive bonding with the vast majority of matrices is poor; hence, a surface treatment is often carried out in order to strengthen the reinforcing effect [92].

Chemically activating the surface of the fiber and coating with coupling agents or finish formulations to make chemical bonds with resins on the surface of the fiber. This method improves mechanical performance and surface activity concurrently. The nanostructured interface created by the grafted carbon nanotubes enhanced the interlaminar strength in modified fibre bismaleimide composite [93].

Greater specific surface area of graphene platelets, enhanced mechanical interlocking at the nano-filler–matrix interface, and the two-dimensional shape of graphene platelets have been linked to this increased efficiency. Produced through the controlled oxidation of graphite, graphite oxide (GO) is an oxygen-rich carbonaceous layered substance. Each layer of GO is made up of a sheet of graphene oxide, which is graphene that has been oxidized [94].

The surface of graphene oxide, which is generated through controlled oxidation of graphite, contains epoxide and other oxygen-containing functional groups that react with these functionalities on the fibre surface [95]In an oxidative media, graphene oxide may be entirely exfoliated to form aqueous colloid suspensions of few-layer carbon sheets by sonication or magnetic stirring [96].

Due to oxygen functional groups presence, the graphene oxide (GO) surface chemistry is extremely diverse. Several functionalization techniques may be employed [97]. Ultrasonication is a straightforward method for synthesizing graphene oxide from expanded graphite [98].

The primary purpose of adapting Hummers' approach with ultra-sonication was to employ ultra-sonication-supplied shear forces to

breakdown the van der Waals connection and disassemble the graphite oxide flake [99].

The resulting GO's surface properties are greatly reliant on the shape of the starting material. Variations in morphology result in modifications to the characteristics of GO [100].

There are enormous differences between GO nano-sheets and ordinary GO (obtained from the graphite powders). Normal micrometer-sized GO collisions travel to the water's surface [101].

Graphene oxide (GO) with epoxy, hydroxyl, and carboxylic groups opens a novel chemical modification path. Such as advancements in GO structural geometry, physiochemical properties, and functionalization, as well as graphene-based new carriers for enzyme immobilization [102].

Separating graphite layers is the first stage in making graphene oxide, followed by oxidation to increase layer spacing [103].The electrical properties, electrochemical properties, and mechanical properties of GO may all be traced back to these oxygenated groups. These oxygenated functional groups found in GO increased several of its features [104].

The relative amount of these oxygenated groups is very sensitive to the synthesis pathway as well as the stoichiometric conversion rate . Oxygenated groups can be more modified chemically to confer various functionality on GO sheets [105].

These functionalities, whether covalent or noncovalent, open up a wide variety of doors for GO, such as the immobilization of a variety of electroactive species for the design of active electrochemical systems, the preparation of a stable dispersion in organic solvents, and the stabilization of GO sheets from agglomeration in organic solvents by nanoparticles coating [106].

The presence of nanoscale items and macromolecules on the surface of GO, which are readily accessible for further modification known as chemical functionalization, exemplifies the diversity of GO functionalization strategies. These modifications of GO have broadened its application in many technologies, including composite materials, polymer grafting, and as building blocks for thin films [107].

The most common technique for covalent bonding is the use of a suitable cross-linker, depending on the functional groups on the surface of the nanomaterial support.

GO has a natural tendency to produce severe aggregations at relatively high loading because to its large surface area and Van der Waals' interaction. Unquestionably, the most urgent problem that has to be solved right away to ensure a successful use of GO in coating is improving GO dispersion. GO can be chemically treated with polymeric solubilizing groups to increase its dispersion [108].

Silanes are frequently used as reinforcing agents to modify the surface of GO. The silanes alteration can increase GO's compatibility and covalent bridges to the matrix, leading to a significant improvement in coatings' corrosion protection effectiveness [109].

3-Glycidoxypropyltrimethoxy silane was used to modify the TiO_2-GO nanocomposite (GPTMS). TiO_2-GO nanocomposite that has been uniformly dispersed in epoxy resin with the use of GPTMS, which includes functional groups like silicone and epoxide, can produce a nanocomposite with anticorrosion capabilities. Silane-functionalized nanoscale particles are used to create nanocomposites [110].

2.13 Fabrication of Surface Coating

It has always piqued interest to see how organic and polymer coatings develop on conducting substrates. The coatings can be used to decorate surfaces, change optical activity, protect against heat and corrosion, and more.

Enhancing the interfacial laminar shear strength and toughness of brittle composites are two other significant uses. Initially, manual or mechanical application methods were used to cover substrates with organic and polymer coatings. However, manual or mechanical application of coatings had drawbacks that went beyond what was already problematic [111].

Coating and printing must be distinguished in this situation. The distinction may initially seem rhetorical, but when the filmmaking process is examined, its physical relevance should become readily clear. Historically, the term "printing" has been used to describe a technique in which an ink layer is transferred from a stamp to a substrate via a reverse process.

A postage stamp is a perfect illustration of something that does this. Contrarily, coating is the process of applying an ink layer to a substrate by pouring, painting, spraying, casting, or spreading the ink evenly across the surface. Coating does not frequently entail the production of a complex pattern, but printing may also imply this. Screen printing, pad printing, gravure printing, flexographic printing, and offset printing are examples of printing processes.

Examples of coating methods include spin coating, doctor blading, casting, painting, spray coating, slot-die coating, curtain coating, slide coating, and knife-over-edge coating. The only technique that may be included in both categories is inkjet printing. It is a coating process at

its core, but because of its capacity to reproduce intricate patterns and connection to office printing on paper, it is also appropriately called a printing method, which is why it has that word in its name [112]. The coating process can be classification as following:

2.13.1 Solvent Casting

This is perhaps the simplest method of filmmaking. The benefit is that no equipment other than a horizontal work surface is required. Simple application of a solution to a substrate is followed by drying. While it is feasible to produce both high-quality and thick films. The method lacks control over film thickness, resulting in frequent picture-framing effects at the margins of the film and precipitation during drying. In situations when liquid surface tension predominates, drying is not uniform. In addition, if crystallisation or precipitation be avoided, the coating ingredient must be extremely soluble in the solvent used [112].

The continuous solvent cast technique, the oldest method for making plastic films, was created more than a century ago in response to the demands of the then-emerging photography industry. After 1950, thermoplastic polymer new film extrusion techniques took over as the primary way to produce plastic films, and solvent cast technology's significance waned. Solvent cast technique is currently gaining more and more appeal for the creation of films with exceedingly high quality criteria.

Uniform thickness distribution, optimum optical purity, and incredibly minimal haze are some of this technology's benefits. The films are very flat and dimensionally stable, and the optical orientation is practically isotropic. It is possible to prepare the cast film in-line with

an optical coating scheme. New materials and enhanced solvent casting and coating procedures have been developed as a result of the rapid expansion of new liquid crystal display applications.

The fundamental components of cast film production are described, and technical aspects of dope preparation, die design, casting support, film drying, and solvent recovery are covered. The main uses of films produced using various polymer/solvent combinations are outlined The last polymer layer. The resulting films are isotopically oriented and flat. If the basic components are soluble yet non melting, this process can be used to create high-temperature resistant films.

However, this approach also has a few drawbacks. The solvent volatility has a significant impact on film formation. Less volatile solutions will take longer to evaporate, delaying the drying of the polymer layer in the process. Additionally, less volatile solvents have a tendency to leave more solvent residue in the finished film. This method's high energy and thus high expense are due to solvent recovery. Despite all drawbacks, solvent casting produces polymer films with superior properties than those made using other techniques [113]. Figure 2.7 showed the solvent drying produce polymer film.

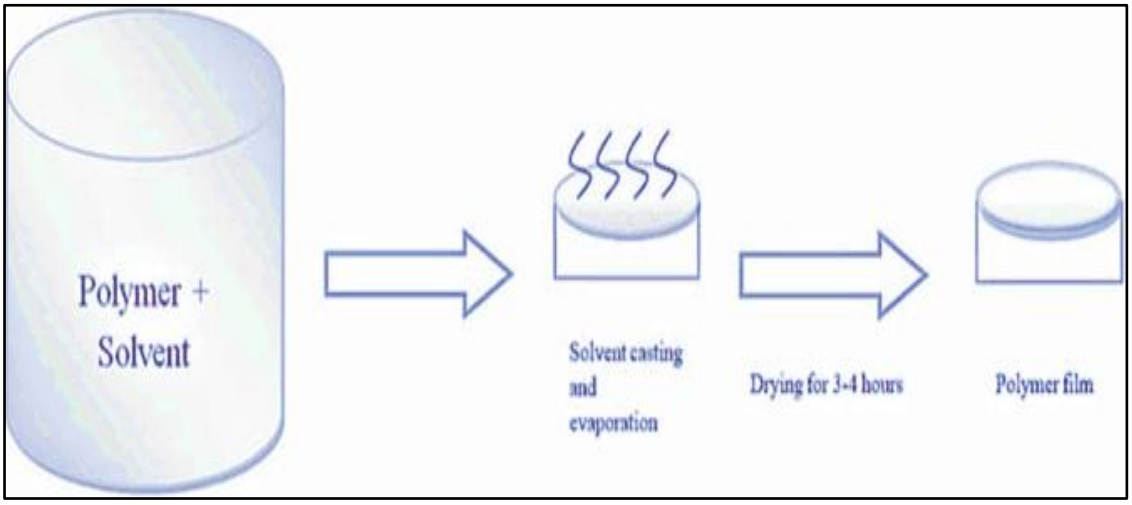

Figure 2.7. Solvent drying to produce polymer film [113].

2.13.2 Spin Coating

Spin coating is a technique for creating thin films that evenly cover flat surfaces with organic compounds [114]. Figure 2.8 show the Stages of spin coating on substrate

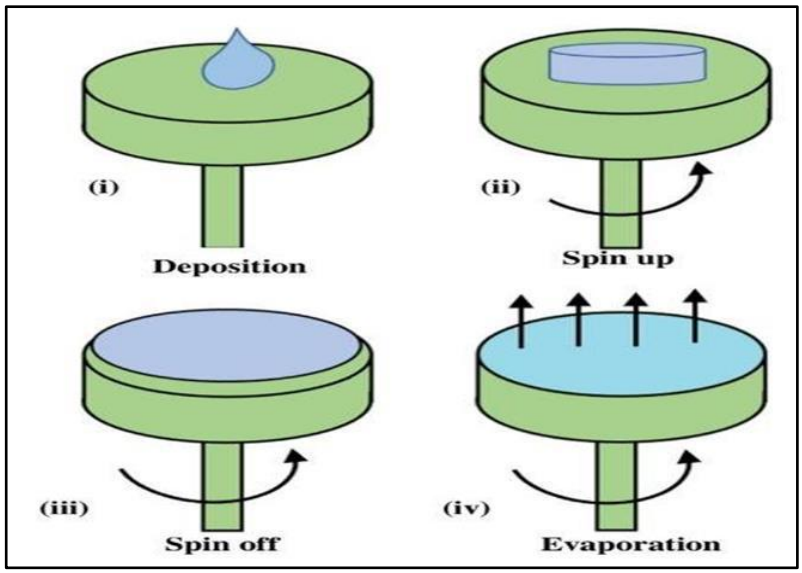

Figure 2.8: Stages of spin coating on substrate [114].

The material is placed on the turntable in the first stage, after which the spin up and spin off stages take place sequentially while the evaporation stage continues the entire process. Utilizing centrifugal force, the applied solution on the turntable is dispersed. The layer thins as a result of fast rotation. The applied layer's drying process comes after this stage.

Rapid rotation makes it feasible for the solvent to evaporate uniformly. Low volatile components of the solution remain on the substrate's surface whereas high volatile components are evaporated or simply dried off the substrate.

The coating solution's viscosity and rotational speed regulate the thickness of the layer that is deposition [115].

The size of the substrate is one of the key drawbacks of spin coating. High-speed spinning is more challenging as the size goes up because film thinning gets more challenging. There is virtually little material efficiency in spin coating. Typically, throughout the procedure, (95-98)% of the material is tossed off and disposed away, and just (2-5% of the material is dispensed onto the substrate [116].

2.13.3 Spray Coating

Spray coating is used in industry to cover complex-shaped polymeric substrates [117]. Figure 2.9 show Spray coating on substrate

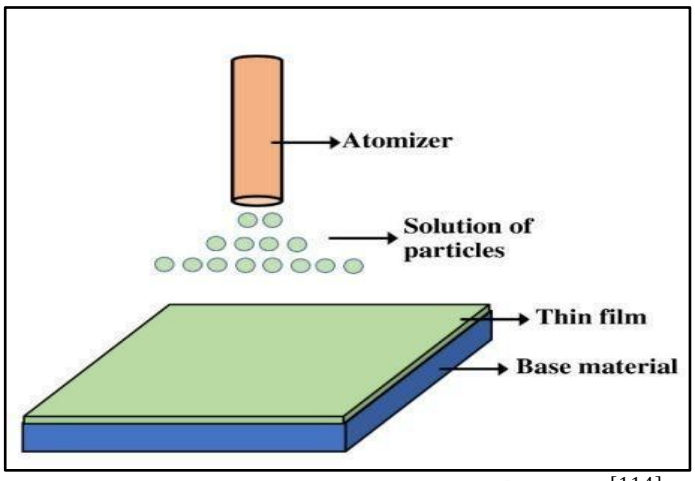

Figure 2.9: Spray coating on substrate [114].

2.14 Trimethoxysilanes (TPTMS)

Trimethoxysilane (TPTMS) are employed for surface modification to generate hydrophilic surface qualities or to attach functionalities that may be further obtained by various typical organic coupling techniques[118].The reaction of the silane surface modifiers is more regulated but also more difficult than that of organic modifiers like carboxylic acids since it necessitates an activation phase through the hydrolysis of the alkoxy groups prior to binding to the surface [119].

A solution of methanol (1.45 mol) in pentane (50 ml) was added to a solution of trichlorosilane (0.485 mol) in pentane(200 ml) that was constantly agitated at 0 °C in order to produce trimethoxysilane. A nitrogen flow is utilized to remove the generated HC1. The distillation of the combination provides 0.29 mol of trimethoxysilane with a boiling point of 87 ° C and a yield of 60%. At 0 degrees Celsius, triethoxysilane was produced by combining a solution of trichlorosilane (0.5 mol) in hexane (1000 ml) with solutions of ethanol (1.5 mol) and N, N-diethylaniline (1.5 mol) in hexane (500 ml). Before filtration, the mixture is agitated continuously for 24 hours at room temperature. With a distillation yield of 78%, triethoxysilane has a boiling point of 131°C and a mass of 0.39 mol [120].

Three-aminopropyl trimethoxy silane was added in varying quantities to change the Fe_2O_3 nanoparticles (APTMS). After adding different amounts of modified and unmodified nanoparticles to the polyurethane matrix, the mechanical characteristics of the resulting nanocomposites were examined.

The FTIR spectra and XPS investigations proved that APTMS was effectively grafted onto nanoparticle surfaces and formed chemical bonds with them. Furthermore, silane surface treatment of the nanoparticles considerably enhanced the mechanical properties of the polyurethane coating. The greatest obvious improvement was brought about by changing the nanoparticles [121].

On the properties of acrylic-based polyurethane/silica composites, the effects of surface modification of nanosilica particles with various silane coupling agents, such as methyltriethoxysilane (MTES), octyltriethoxysilane (OTES), Vinyl triethoxy silane (VTES), and methacryloxy propyl trimethoxy silane (MATMS), were examined. They noticed that the OTES and MTES modified nanosilica particles

dispersed uniformly in the polyurethane matrix when the organic coating on the nanoparticles was thicker.

They came to the conclusion that a key element in influencing the mechanical characteristics of polyurethane is the size of the silane chains. The addition of MTES and OTES surface modified nanoparticles reduced the coating's storage modulus because long-chain silane molecules were plasticized. This implies that the chemical composition and chain length of the silane coupling agents have a considerable impact on the properties of the nanoparticles in the coating matrix [122].

2.15 Beeswax

At first, the only natural wax used in commerce was beeswax. The term "wax," which comes from the Old English word "weax," originally solely applied to the wax produced by the European honeybee Apis mellifera, but it started to be used for other natural compounds as early as the 19_{th} century, including ozocerite, which had certain qualities similar to beeswax. Since ancient times, beeswax has been valued as a commodity. One early example is the inclusion of beeswax on the 9_{th}-century Viking ship discovered at Oseberg Beeswax is being used in a variety of industrial, pharmaceutical, and medical applications[123].

Making proper knowledge of its make-up crucial. Additionally, beeswax often costs roughly twice as much as vegetable waxes and eight times as much as petroleum wax, respectively [124].

One of the most popular recycling methods for turning plastic trash into liquid or gaseous fuels is pyrolysis. However, the technique takes close attention and a lot of work. To save energy, polymethylene methacrylate (PMMA) is co-pyrolyzed with beeswax at a 1:1 ratio using a thermogravimetric analyzer (TGA). Beeswax considerably lowers the

reaction's activation energy when it is added to polymers. The thermodynamic parameters of the thermal breakdown of plastics are observed to be affected by the combination of beeswax. In comparison to similar waste plastics, the plastic and beeswax combination has a lower enthalpy value [125].

Using a number of approaches, the mechanical characteristics of beeswax are determined and compared as a function of temperature. The coefficient of friction of beeswax is measured and compared to the coefficients of plasticine and Nylon 6–6. It is demonstrated that the frictional behavior of beeswax deviates and instead resembles that of a traditional soft, elastic polymer [126].

2.16 Tribology of Materials

Tribology may have been implied by the word tribos, which is Greek for "rubbing." It could depict both the engineering and the physics of surfaces interacting with one another through relative movement. In order to understand how surfaces, interact with one another and to prescribe improvements in a particular application, it may be necessary to examine the friction, grease, and wear for planning surfaces [127].

Tribology is a multidisciplinary field that includes mechanical engineering (particularly the study of wear resistance in relation to machine parts like gears, journals, and roller bearings), materials science, surface technology, coatings, surface topography research, and the science of lubricants and additives. When two surfaces are brought into contact, the contact first forms at the asperities' greatest points, allowing the load to be sustained by asperities' deformation. As a result, the visible (or noticeable) zone of touch only makes up a small portion of the true (or real) region of contact [128].

The study of wear, friction, and lubrication is referred to as tribology. Systems exhibit wear and friction when the two solid bodies move in relation to one another. Wear and friction mostly cause a loss of energy and resources. Systems exhibit wear and friction when the two solid bodies move in relation to one another. Wear and friction mostly cause a loss of energy and resources [129].

2.17 Tribology of Polymer Nanocomposite

Because of their quick growth and superior tribological, mechanical, and corrosion qualities, polymers have frequently taken the place of numerous traditional metals sliding components. Due to the successful use of unfilled polymers in engineering, composite materials were created using polymers, allowing for the changing of characteristics by the addition of one or more reinforcing fillers. High hardness, strength, or elasticity are provided by the fillers, and a self-lubricating effect is added by the polymeric matrix [130].

Polymers are frequently thought of as a solid lubricant for materials, rather than just being employed in dry environments. Due to their ability to deliver very low wear rates and friction coefficients in a variety of operational circumstances with high dependability, polymers are frequently used as materials for dry or self-lubricating bearings and bushings [131].

Due to their elasticity, ability to accommodate stress loading, minimal friction, and resistance to wear, polymers are being employed more often in tribological applications. To fit a specific purpose, polymers may be altered both on their surface and in their bulk using a variety of chemical and physical techniques. The ability to manage their

friction and wear characteristics made them appealing options and extremely promising materials for tribologists [132].

Around the middle of the 1990s, the use of nano-particles in polymers for improving tribology performance was introduced, and this field has since grown fairly promising in terms of its potential for the future. The vast majority of the time, a polymer nanocomposite's superior mechanical capabilities depend on the filler's (nanoparticles or nanofibers) exceptionally large contact area with the matrix (a polymer). Higher interface results in greater phase bonding and, as a result, stronger and more durable characteristics than those of an empty polymer [133].

2.18 Friction

Every mechanical system that has pieces moving relative to one another has friction. In most mechanical applications, friction is detrimental, but in many other situations, it is crucial to ensuring the system's primary function [134].

According to Figure 2.11, friction force is the opposing force tangential to the common boundary of two bodies when one body moves or tends to move in relation to the surface of the other under the influence of an external force. The coefficient of friction is the dimensionless ratio of the friction force (F) to the normal force (N) pushing the two bodies together [135].

$$\mu = F/N \quad \text{..... (1)}$$

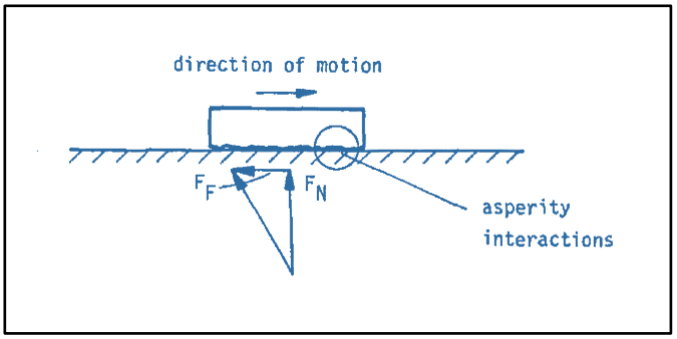

Figure 2.10: A Solid Body During Sliding [132].

2.19 Wear

Wear is damage to a solid surface that typically includes material loss that happens over time as a result of relative motion between surfaces of things that are in touch. It is simple to picture how the asperities would constantly slide on top of one another and eventually remove material. Even though one contact surface is significantly tougher than the other, wear still occurs and material will be lost from both [136].

Wear is established on the chemical makeup and mechanical behavior of the contacting surfaces when contact occurs during rolling, sliding, or impact action. In reality, wear begins by altering the surface's qualities through contact [137].

As shown in figure 2.11 wear volume loss can be calculated from equation below:

$$\textbf{Volume loss, mm}^3 = \frac{\textbf{mass loss,g}}{\textbf{density,g/cm}^3} \times \textbf{1000} \quad \textbf{..... (2)}$$

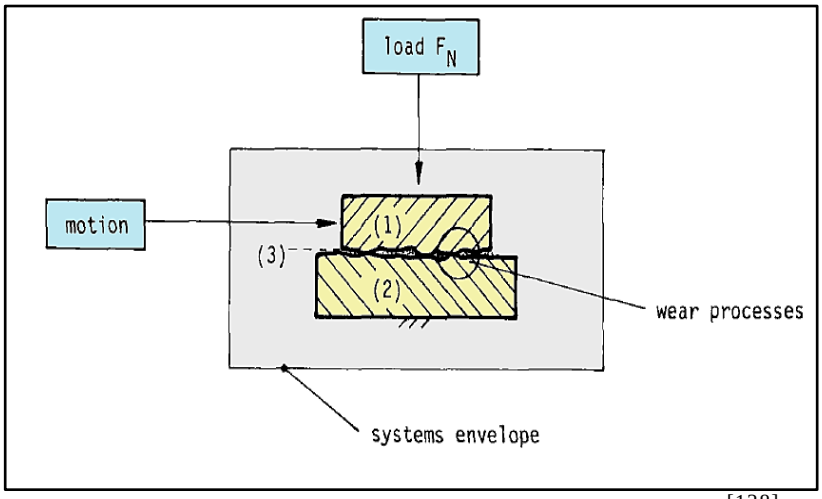

Figure 2.11: A simple tribo-mechanical system [138].

2.19.1 Wear of Polymer Composite

Polymers are advantageous for several sliding scenarios because of their capacity to self-lubricate while gliding across metallic surfaces. Thus, polymer-metal sliding techniques may be used to achieve low friction coefficient of connected with reasonable wear resistance without the need of an outside grease.

The inclusion of other elements, such as inorganic particles composites like clays, fibers, and even particles of different polymers, can affect the characteristics of polymers. When filler particles are added to polymers, it frequently results in a better-bonded and more uniform transfer layer than when the polymer is left empty. This leads to increased wear resistance in the first scenario and lower wear resistance in the second scenario [139].

2.19.2 Wear test models

It depends on the type of tribological loading being compared that determines which wear test is utilized in practice. Tribological loading examples include sliding, rolling, sliding while rolling, and oscillating sliding.

When assessing the wear of plastics, sliding wear test methods, such as the pin-on-disc and block-on-ring tests, are widely employed. Figure 2.12 depicts the testing principles for the pin-on-disk and block-on-ring tests [140].

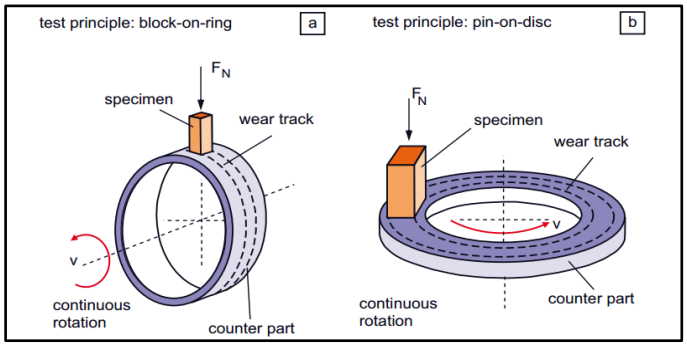

Figure 2.12: Test principles of (a) block-on-ring(b) pin-on-disk wear tests [140].

Figure 2.13 depicts a fretting wear testing machine that may be used to analyze wear caused by vibrations. The counter body of this machine is typically ball-shaped and oscillates over the specimen being tested [140].

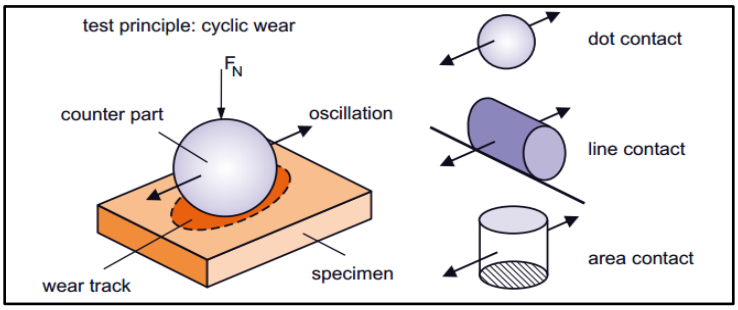

Figure 2.13: Testing principles of oscillating wear experiments [140].

2.20 Literature Review

Chau, et al. , [141], 2008 Described how to make a silica-PMMA nanocomposite. In an organic solvent, the surface-modified silica nanoparticles can be thoroughly mixed before being integrated into the polymer resin. The nano-composite demonstrated enhanced mechanical properties and may be used with other functional acrylic materials. According to DSC research, silica concentration rise along with the hybrids' glass transition temperature. In nanocomposite with 10 wt% silica content, good transparency (>90%) and hardness grade (>5H) are observed.

Jeon, et al. , [142], 2008 CreatedFilms and hard coating for UV/thermal dual curing were created. The coated sols included nanoparticles modified with organosilanes (such as methacryloxy-propyl trimethoxy silane, vinyl triethoxy silane, and 3-glycidoxy-propyltrimethoxy silane). On poly(methyl methacrylate) substrates, hard coating films with pencil hardness over 8H and transparency above 90% in the visible light spectrum were created using this coating solution. Additionally, UV/thermal dual curing allowed for a speedy 35-minute cure of the coating solution at 100 °C. On the hardness and transparency

of the resultant films, the effects of the additive and initiator are detailed.

Gonçalves, et al. , [143] **2010** Graphene oxide, a novel two-dimensional allotrope of carbon, is generating a lot of interest. The availability of large amounts of graphene (G) that can be easily processed by chemical exfoliation to produce graphene oxide is particularly alluring (GO). In this study. AFM, FTIR, and contact angle were used to describe the surface of the PMMA-grafted GO (GPMMA). The ability of these new nanocomposites to be uniformly disseminated in polymeric thick matrices and to foster strong interfacial adhesion, which is especially important in stress transmission to the fillers, is what makes them interesting.

The mechanical investigation of the resultant films demonstrated that loadings of GPMMA as low as 1 wt% are effective reinforcing agents, producing films that are even harder than pure PMMA films and composite films of PMMA made with GO. In point of fact, the addition of GPMMA fillers at a weight-to-weight ratio of 1 percent led to a considerable improvement in the elongation at break, which resulted in a material that was significantly more ductile and, as a result, more durable.

Kim, et al. [144]**, 2011** examined the tribological behavior of coatings made by directly casting PMMA-grafted-MWCNT nanocomposite materials onto metal surfaces was examined. To add the contact force, amino-functionalized MWCNTs were first covalently functionalized with PMMA. Due to robust interfacial contacts in the nanocomposite, PMMA-MWCNT had a greater dispersive capacity in polyimide matrix than pure MWCNT composite.

The maximum amount of PMMA-g-MWCNT that could be used was 5 weight percent because too much MWCNT causes the nanocomposites

to be brittle and fragile. Dry circumstances were used to conduct sliding testing in ball-on-disk arrangements. A 12.7 mm steel ball was subjected to a normal contact force of 9.7 N, resulting in a Hertzian circular contact stress of 0.65 GPa. The sliding tests were conducted at a speed of 0.02 m/s until the coefficient of friction stabilized. In this investigation, the nanocomposite coating with 3 wt% MWCNT reinforcement was the most stable and had the lowest coefficient of friction. As a result of the formation of a thin, uniform friction film on the wear track during sliding, the conclusion that the friction film is essential for the nanocomposite coatings to exhibit a stable frictional behavior.

Gonçalves, et al. [145]**, 2012** investigated that if functionalized carbon nanotubes (f-CNTs) and graphene oxide (GO) might be used as reinforcing agents for poly(methyl methacrylate) (PMMA) as a matrix. The results for changes in the mechanical characteristics that were measured for the reinforced composite (storage modulus, bending strength, and elastic modulus) were mixed.

The nanofiller functions as a scavenger of the radicals created during the polymerization reaction due to the delocalized bonds. Because of this, it hypothesize that this result is the result of each of the nanofillers preventing the polymerization process from occurring in the composite. In addition, it demonstrated that the mechanical characteristics of the GO-reinforced containing 0.5 wt% when the radical species concentration was doubled.

Yang, et al. , [146]**, 2013** studied Functionalized reduced graphene oxide (RGO) was created by treating graphene oxide with dodecyl, octyl, and propyl trimethoxysilane and then reducing the result with hydrazine hydrate. The results showed that the alkyl groups were

effectively grafted onto the surface of RGO and that graphene's lipophilicity increased with the length of the alkylated chains.

By solution mixing, the RGO- was also introduced into the polypropylene matrix as a reinforcing element. The resultant nanocomposites showed a notable improvement in mechanical, thermal, and crystallinity properties. This study offers a fresh approach for enhancing graphene's solubility and dispersion in polymer matrixes.

Stojanović, et al , [147], 2014 showed that melt compounding technique is used to create PMMA/silica nanocomposites with great optical transparency and improved mechanical characteristics. A methacryloxypropyltrimethoxy silane coupling agent was used to modify the surface of SiO2 particles in a supercritical carbon dioxide–ethanol combination using a standard method.

The deagglomeration and dispersion of nano silica, which results in the ideal particle-matrix bonding in composites, are greatly influenced by the dispersion of silica nanoparticles in ethanol at low temperatures. Composites coated using the supercritical coating process and loaded with 5 wt% silica nanoparticles were found to have the best mechanical and optical qualities.

Kesong Hu , et al .[148], 2014 showed that flexible nanocomposites have been created as a result of the introduction of graphene-based nanomaterials for new applications requiring better mechanical, thermal, electrical, optical, and chemical performance. If correct structural and interfacial organization is accomplished, these nanocomposites demonstrate exceptional structural performance and multifunctional features by synergistically integrating the traits of both components. Here, it has been provide a brief overview of the materials used to create the graphene-polymer nanocomposites, their fundamental

interfacial interactions, and the accompanying theoretical models for predicting their mechanical properties.

Then, using the weak and strong interfacial contacts present in functionalized graphene sheets, we address several assembly approaches available for successfully inserting the strong and flexible graphene-based components into polymer matrices. In addition to discussing mechanical performance, its provide a brief overview of the various physical (thermal, electrical, barrier, and optical) characteristics that are influenced by interfacial interactions and processing conditions.

Hu, et al. [149]**, 2014** investigate GO and grafted GO (rGOPDA-g-PMMA) were employed to investigate the root cause of the improved mechanical properties of poly (vinyl chloride) (PVC). Dopamine was employed to reduce the quantity of GO while polydopamine was used to cover the GO surface .to synthesize rGO-PDA-g-PMMA, surface-initiated atom transfer radical polymerization and mussel-inspired chemistry were combined.

The resulting derivatives were characterized by thermogravimetric analysis, Fourier transform infrared spectroscopy, X-ray diffraction, and Raman spectroscopy. Solution blending was employed to make PVC nanocomposites with GO derivatives, and casting was used to produce the nanocomposite films. The mechanical properties of the nanocomposites were investigated using tensile testing as well as dynamic mechanical thermal analysis.

Harb, et al. , [150]**, 2016** found that the surfaces of the films protective coatings based on PMMA–silica nanocomposites reinforced with carbon nanotubes were extremely smooth and that CNTs were dispersed uniformly in the nanocomposites. The nominal composition of the films was validated by X-ray photoelectron spectroscopy (XPS), and nuclear magnetic resonance demonstrated that CNT loading had no

effect on the connectivity of the silica network. Thermogravimetric analyses and mechanical testing showed that coatings containing CNTs had higher thermal stability, hardness, adhesion, and scratch resistance than coatings without CNTs did .

Al-Kawaz, et al. , [151]**, 2016** showed that the Carbon nanotubes (CNTs) may become more chemically compatible after chemical functionalization. (MWCNTs) functionalized with (PMMA) are created by “grafting from" in situ atom transfer radical polymerization it enables two factors are used to regulate the thickness of the polymer layer grafted onto MWCNTs: feeding ratio the volume fraction of the solvent to the ratio of MMA to MWCNT.

This study compared the impact of various PMMA-grafted-MWCNT/PMMA, PMMA-grafted-MWNCT fillers incorporated into a PMMA matrix, and produced using a method for solution mixing. The tribological capabilities of 20 mm coatings of on PMMA, these nanocomposites were deposited. To keep the PMMA clear, the amount of embedded fillers is kept to a minimum. With an increase in the weight percent of polymer grafted to the surface of MWCNT, it was discovered that the coefficient of friction tended to decrease. Additionally, when the weight percentage of PMMA-coated MWCNT grew, the elastic modulus did as well.

Hang Hu , et al. [152]**, 2018** studied 3-glycidoxy-propyl trimethoxy silane (GPTMS), functionalized graphene oxide (FGO) was created. It was then incorporated into polysiloxane coatings to improve their mechanical properties, notably their scratch resistance, using sol-gel and epoxy/amino curing techniques. TEM, FTIR, and XPS provided evidence for the graphene oxide (GO) surface's functionalization. In comparison to GO, FGO was shown to be more compatible with and to

make a stronger contact with the polysiloxane matrix based on the microstructures that were seen using OM and SEM.

Using nanoindentation, macro scratch, and progressive load scratch tests, the mechanical performance of FGO/polysiloxane nanocomposite coatings was evaluated, revealing a considerable improvement over either pure polysiloxane or GO/polysiloxane coatings. Only 0.75 wt% of FGO is required to obtain a 40% increase in microhardness (233 MPa), an 83% improvement in scratch resistance (1100 g), and a 144% rise in 1^{st} scratch critical normal load (4.88N). In addition, elastic recovery and scratch damage morphology were studied to shed light on scratch behavior and the reinforcing process.

Nazri, et al. , [153] **2018** studied (GO) is well known for possessing a number of unique properties that are advantageous in a range of applications. it is produced by the graphite chemical oxidation. The GO's plane is joined by oxygen functional groups, setting it different from graphite and graphene's crystal structures. In this work, GO was produced utilizing a modified version of Hummers' method from natural graphite powder. Investigations were done into how different response durations, such as 24, 48, 72, and 96 hours, affected GO yields.

The results showed that different GO samples exhibited distinctive morphologies, attachments of functionalized groups, crystallinity, and UV-Vis absorption peaks A scanning electron microscope (SEM), Fourier Transform Infrared Spectroscopy (FTIR), X-Ray Diffraction (XRD), and UV-Vis were used to analyze GO.

The surface of GO (48 hours) had a platelet-like appearance, according to the SEM results, as opposed to GO (72 hours), where wavy wrinkled and layered-flakes, as well as crumpled structures, were visible. Due to the extended oxidation duration, FTIR studies showed that there were more numerous oxygen-containing functional groups in

GO (96 hours) than GO (24 hours). Additionally, the GO absorption peak was seen at about 230 nm, and its strength increased with reaction time.

Loste, et al. , [154], 2019 found that Incorporating inorganic nanoparticles into polymer matrix enhances their fascinating and complementary properties. Transparent polymer nanocomposites are important in many applications. To achieve high transparency in nanocomposites, the aggregation of nanoparticles that causes light scattering must be reduced.

This review introduces light scattering, refractive index modification, and transparency assessment methods for nanocomposites. Several aggregation-restraining approaches focus on creating transparent nanocomposites. Several strategies have been employed to govern polymerization, nanoparticle formation, and the polymer-nanoparticle interface, together with polymer casting or processing. Optical characteristics of inorganic nanoparticles have gained the greatest interest.

Polymer/nanoparticle systems are also reported for creating transparent polymer nanocomposites with advanced optical features, such as UV or IR filtering, photoluminescence, extreme refractive index, dichroism, or nonlinear optical properties.

Boussehel , [155], 2019 described how surface modification impacts polystyrene composites with olive pomace flour (OPF). First, the OPF was treated with 3-(Trimethoxysilyl)propyl methacrylate (TMSPMA). Composite samples were generated by mixing treated OPF with polystyrene (PS). The structural and property changes brought about by this treatment were seen and discussed using morphological, thermal, mechanical, and FTIR studies.

As OPF concentration rose, composites' tensile strength and elongation at break reduced but their Young's modulus increased; silane coupling agent-prepared composites were more thermally stable than untreated composites; and OPF's surface modification by TMSPMA boosted filler-matrix interaction.

Shah, et al. , [156]**, 2020** (GO) is anticipated to significantly improve the permeability and selectivity for O_2/N_2 separation. In order to improve separation efficiency, GO functionalized with 3-(Trimethoxysilyl)propyl methacrylate (TMOPMA) was utilized as an inorganic filler and inserted into a PVC/PAMPS based MMM. Different membrane compositions were created, and the combination of 0.5 g of PVC, 1.0 g of PAMPS, and 0.015 g of filler produced the optimum morphology.

SEM, EDS, FTIR, Raman, and XRD spectroscopy were used to analyze the produced membrane and inorganic filler. Additionally, gas permeation tests were conducted to determine how well the synthetic membrane separated O_2/N_2. At 5 bar pressures, the greatest permeabilities for O_2 and N_2 were 4097 and 3373 bar, respectively. With the rise in permeability, a tendency toward slow growth was seen for selectivity. The results showed a tendency toward improving selectivity when feed gas pressure increased along with the permeability of gases through the membrane.

Chathuranga, et al. [157]**, 2021** , studied that in many synthetic materials, strength and toughness have traditionally been seen as mutually incompatible qualities. This contradiction has been resolved in natural materials like nacre by tuning internal architecture at the nanoscale. In this study, a nanocomposite of graphene oxide (GO) and poly (methyl methacrylate) (PMMA) with a "brick and mortar" microstructure and improved interfacial strength is created. Tensile

strength and toughness are respectively 55% and 42% higher than those of traditional GO/PMMA nanocomposites, at 261 7 MPa and 5 0.2 MJ m3, respectively. The nanocomposite also exhibits remarkable wet-environment stability. Consequently, this work enhanced mechanical characteristics.

2.25 Concluding Remarks

In previous studies, graphene or graphene oxide was used with the polymer as a reinforcing material, and the properties of the composite material were improved in terms of mechanical or thermal properties. Coatings were also made and strengthened using different fillings. In addition, the graphene oxide was improved and the results were compared before and after the improvement and its use in composite materials. Different methods of coating were used.

In the current work, a simple and inexpensive method of coating was used, which is the solution coating method. A composite coating of PMMA polymer was also made with a nano-based filler material, graphene oxide, and it was taken into account that the coating be transparent. Also, the filler was improved in terms of diffusivity and was modified with silane. Also, beeswax was used as a lubricant that helped spread the nano in the base material and improved flexibility.

Chapter Three
Experimental Part

3.1 Introduction

This chapter includes:

1-Listing the used materials (PMMA, graphene oxide, silane, and beeswax) and mentioning their properties.

2-Describeing the procedures used to prepare the substrates.

3-The experimental procedure that followed to prepare the coating

4-Listing the required tests and the devices to evaluate thin films such as FTIR, DSC, SEM, Contact Angle, UV, Wear test, and Nano indentation.

The experimental component entails the synthesis and characterization of nanocomposite materials as well as the examination of the mechanical, structural, and tribological characteristics of thermoplastic poly (methyl methacrylate) PMMA and PMMA nanocomposite with (0.25%, 0.50%, and 1% wt.%) GO nanoparticles no modified.

PMMA with (0.25, 0.5, and 1 wt. %) GO modified nanoparticles with (1) wt. % GO modified nanoparticles with (0.1, 0.25, and 0.5) wt. % beeswax The characterization of nanoparticles includes the use of nanoindentation, SEM, and FTIR. Pin-on-disc sliding test used to determine tribological characteristics. The mechanical tests include those for hardness, pull off, elastic modulus, and scratch resistance. Optical properties are such as UV.

3.2 Work plan

A work process has been chosen in order to accomplish the thesis' goal. Figure 3.1 presents experimental part and test.

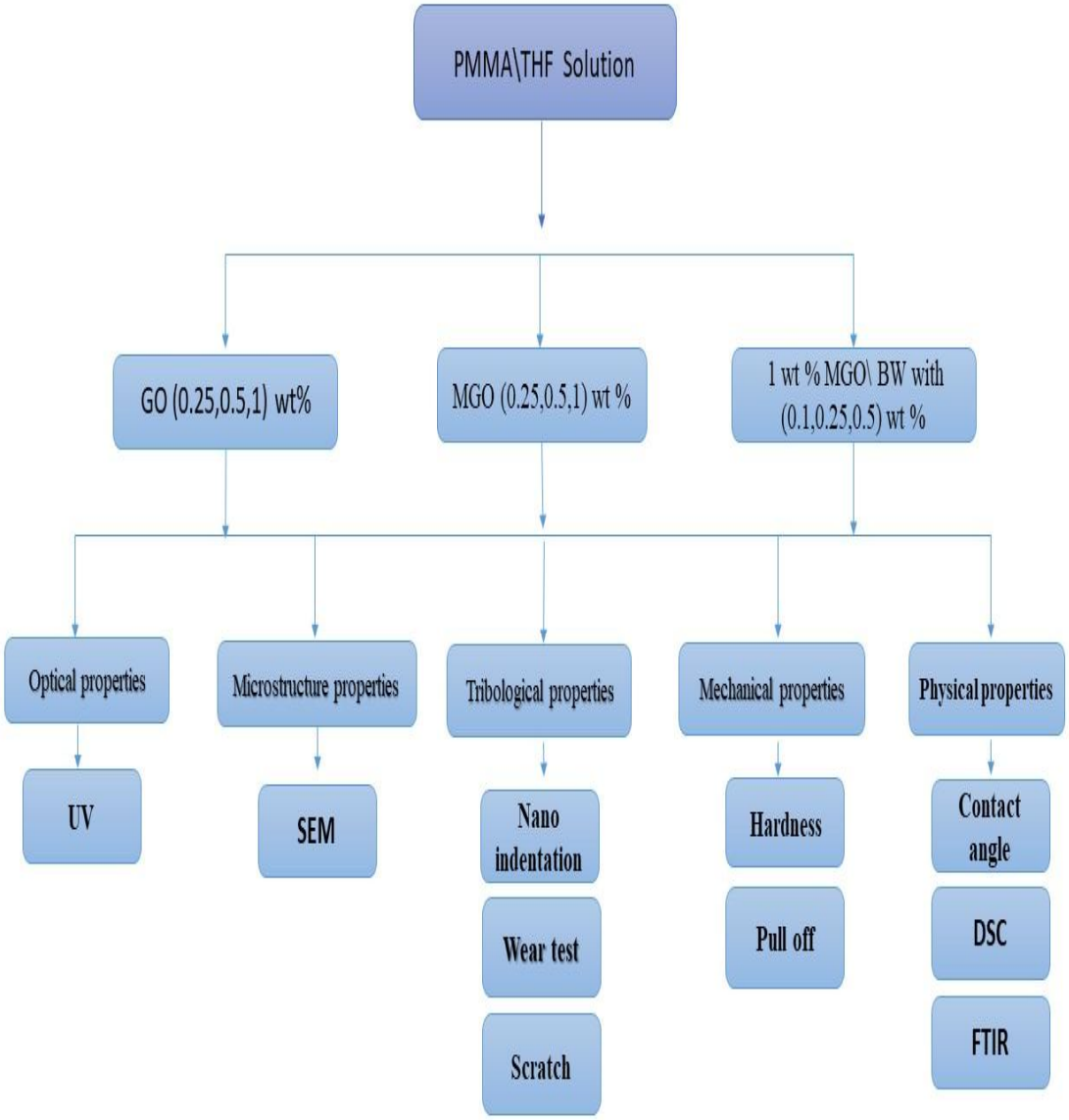

Figure 3.1: Flowchart of experimental part and tests.

3.3 Materials Used in this Study

3.3.1 PMMA matrix

The Guangzhou Ideal Technology Co. Ltd./China offered kind of PMMA that was employed in this investigation has the characteristics listed in table 3.1

Table 3.1: Properties of PMMA.

Property	Units	Value
Modulus of Elasticity	GPa	3.5
Glass Transition (T_g)	°C	100
Friction coefficient		0.78
Density	g/cm^3	1.18

3.3.2 Graphene oxide

Nanoparticles (GO) was used to reinforce the (PMMA) matrix. It supplied as a powder by (Platonic Nanotech /India). The characterization of GO is shown in Table 3.2 and Graphene oxide shown *in Figure 3.2.*

Figure:3.2 Graphene oxide

Table 3.2: Graphene oxide (GO) Nanoparticles

Product name	**GO powder nanograde**
Appearnce	Black powder
Particle size	50-100 nm
GO content	≥ 99 %

3.3.3 (Trimethoxysilyl)propyl methacrylate (TMSPMA)

Silane (Trimethoxysilyl)propyl methacrylate (TMSPMA) is a hydrophobic compound. Silanes can significantly enhance thermoplastic and other materials wetting, compression, shear, mechanical, and wet electric characteristics. The acrylate's extra functional group makes TMSPMA's 98% purity. It was purchased from the local market. Its from ALDRICH company. Figure 3.2 shows the TMSPMA and TMSPMA structure.

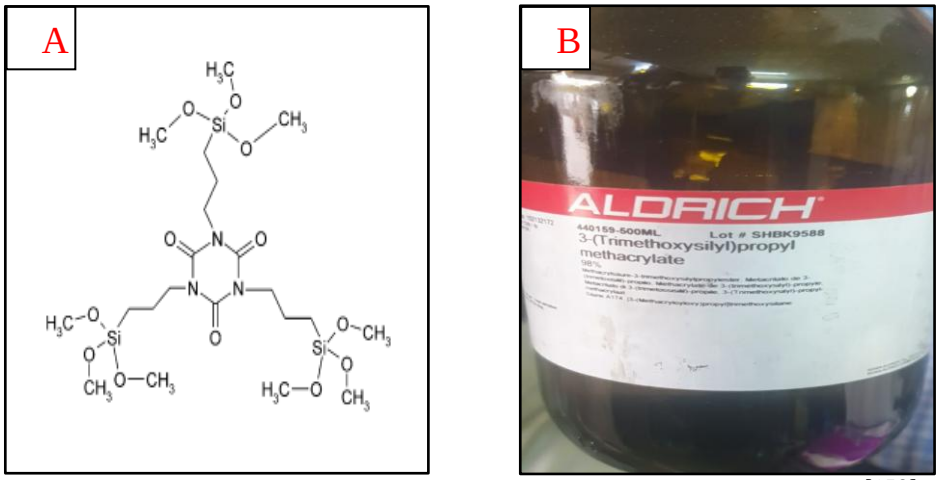

Figure 3.3: (a) (Trimethoxysilyl)propyl methacrylate structure [158] , (b) TMSPMA

3.3.4 Beeswax

The principal compounds' primary components include saturated and unsaturated monoesters, diesters, saturated and unsaturated hydrocarbons, free acids, and hydroxy polyesters. The chemical formula is $C_{15}H_{31}COOC_{30}H_{61}$. It was purchased at the local market. Figure 3.4 shows the beeswax picture.

Figure 3.4: Beeswax

3.3.5 Tetrahydrofuran (THF)

C_2H_4O were used as surfactant agent for PMMA \ PMMA with graphene oxide thin film preparation with the properties maintain in the Table (3.2)

Table 3.2: THF Properties

Property	value
Purity %	99
Density	0.888 g/mL
Boling Point	66°C

3.4 GO Modifications

The graphene oxide was modified with silane (Trimethoxysilanes) by dispersing 1.8 g of graphene oxide in 1.8 liters of deionized water and sonicating the solution for 30 minutes. The GO solution is added to the ethanol and silane solution and stirred at 70 °C for 2 hrs**.** Then 3 ml of hydrochloric acid (HCL) is slowly and carefully added to the solution and left on the sterilizer.

The solution was allowed to be cool, then filtered to get the modified graphene oxide (MGO) using a Buchner funnel as shown in Figure 3.8. The Buchner funnel technique consists of a funnel with filter paper at the top, a nozzle in the funnel via which a vacuum line is attached to extract the air, and then the solution is introduced to the funnel. Through the top filter, where the liquids are withdrawn to the funnel and the graphene particles remain trapped in the filter paper, the procedure takes place throughout the vacuum's work.

MGO was then removed from the filter paper and dried in an oven at 80 Cº for four hours, resulting in an activated graphene oxide that was ready to use [54]Figure 3.9 shows the procedure of modified graphene oxide and the Buchner funnel.

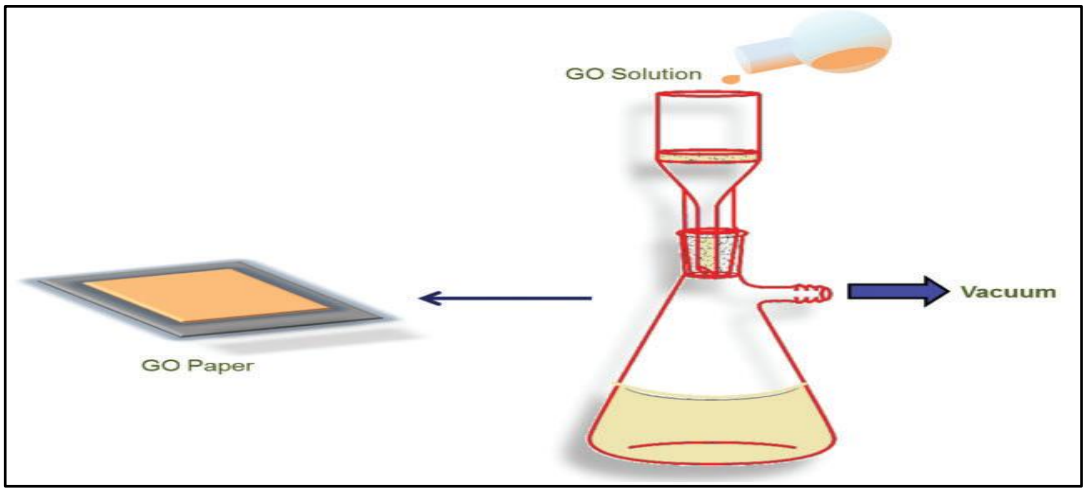

Figure 3.8: GO Modification process

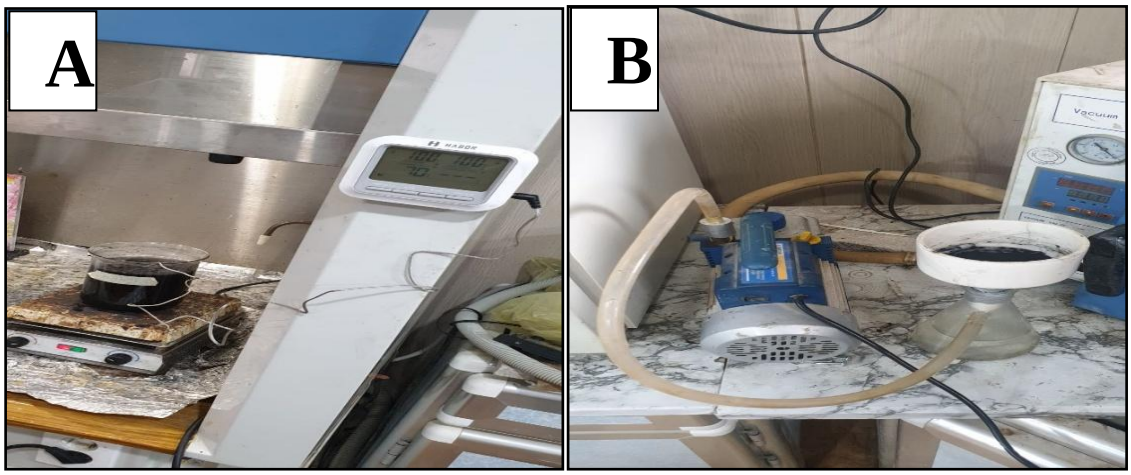

Figure 3.9: (A) Modified of graphene oxide **(B)** Buchner funnel

3.5 Beeswax Extraction

The bees wax was extracted from the honey by first bringing the honey with the cells to be dissolved in an ethanol solvent and stirred at 70 Cº for an hour, after which the bees wax was melted and honey dropped to the bottom because honey don't dissolve in ethanol while the wax remaining on top. The wax was removed, and then the process was repeated.

The same procedure was used to remove impurities and honey from the wax. After a day, the top layer of wax was removed and placed in a glass container, after which it was removed again and baked at 60 degrees Celsius for two hours. It is then dried to remove the ethanol, and it is ready to use.

Figure 3.10: Beeswax extraction

3.6 Preparation of PMMA Nanocomposites

In order to prepare the nanocomposite, the nano GO powder was dried at 100 °C for 2 hours under vacuum. The filler was weighted in the required proportions and PMMA nanocomposite with (0.25, 0.5 and 1) wt. % GO , (0.25, 0.5 and 1) wt. % GO modified and (1) wt.% GO modified with (0.1,0.25,0.5) BW. The procedure for preparing PMMA nanocomposites consisting of the polymeric materials were carefully washed with alcohol to remove oils, dust, grease or any surface contaminants.

The material is in the form of particles. They were then weighed according to the appropriate proportions for mixing. Preparing PMMA Nano composite with PMMA particles weighing 10 g were dissolved in THF solvent with a volume of 5 ml and stirred for 4 hours to make the composite material. The GO solution was prepared by dissolving the GO in 5 ml of THF as the solvent.

The solution was then placed in a sonication dispersion device for 30 minutes, and after that, the solution was included. An hour was then spent mixing the polymeric solution. After coating a glass, the solution was poured into the polymeric mold. The modified graphene oxide samples were made using the same procedure, but the graphene oxide was already modified when it was introduced. We'll go through how to modified graphene oxide in the next part. Beeswax was collected from honey for the addition, and the procedure for obtaining beeswax will be discussed in the future part.

After sonicating the modified graphene oxide in THF solvent for an hour, it was poured over the polymeric solution, added to beeswax, and left on the curtains for an hour. Then, it was poured into the polymer mold and the glass plate was coated. This procedure is repeated for each one of the samples.

PMMA containing (1) wt.% GO modified nanoparticles with (0.25, 0.5, and 1) wt.% beeswax. The MGO was then blended with Tetrahydrofuran (THF) solvent and bees wax using an ultrasonic instrument at 30% of the total energy (1,200 w) for 30 minutes and 40 °C to disperse the particle aggregates. Some activities were carried out before dumping the samples into the molds to prepare the mold for casting. To begin with, the samples were poured into two molds. The first was composed of Teflon polymeric material.

Because of the Teflon material is characterized as a hydrophobic substance, the material does not stick to it, and also because the spilled solution consisting of PMMA polymer does not interact with the mold and THF solvent, nanomaterials of graphene oxide, waxes, and lubricants, this mold was used for its advantages in the ease of extracting samples from the thin films from the mold. Glass plates were

utilized to coating the material on, and the molds were cleansed of dust and contaminating substances before pouring the material.

Before pouring the material, the molds were cleaned using acetone. The plates were also put on a flat surface before pouring to guarantee that the casting was exactly even in the mold. The application of a grading scale (the water balance) is a tool used by construction workers to check that the surface is level before the material is put into the molds. Molds as shown in Figures (3.7)

Figure 3.7: (A) Glass mold, (B) Teflon mold, (C) coating on glass mold , (D) coating on Teflon mold

Table 3.4 Code Sample

No.	Code Sample	Full Name
1	PMMA	Pure PMMA
2	PMMA\GO 0.25	Pure PMMA\graphene oxide 0.25 wt%
3	PMMA\GO 0.5	Pure PMMA\graphene oxide 0.5 wt%
4	PMM\GO 1	Pure PMMA\graphene oxide 1 wt%

5	PMMA\MGO 0.25	Pure PMMA\graphene oxide Modified 0.25 wt%
6	PMMA\MGO 0.5	Pure PMMA\graphene oxide Modified 0.5 wt%
7	PMMA\MGO 1	Pure PMMA\graphene oxide Modified 1 wt%
8	PMMA \MGO\BW 0.1	Pure PMMA\graphene oxide Modified 1 wt% \Bees Wax 0.1 wt %
9	PMMA\MGO\BW 0.25	Pure PMMA\graphene oxide Modified 1 wt% \BeesWax 0.25 wt %
10	PMMA \MGO\BW 0.5	Pure PMMA\graphene oxide Modified 1 wt% \BeesWax 0.5 wt %
11	GO	graphene oxide
12	MGO	graphene oxide Modified
13	PMMA\MGO\BW	Pure PMMA\graphene oxide Modified 1 wt% \ Varity Wight percentage of beeswax

3.7 Testes Devices

3.7.1 Scanning Electron Microscopy (SEM)

The JEOL 6400F Field Emission Phonon used to examine the dispersion of GO, MGO nanoparticles in the PMMA matrix and MGO\BW in the matrix, as illustrated in Figure 3.11. This experiment was carried out by collecting the resulting material on 1 cm x 1 cm pieces of aluminum foil morphology of thin films according to (ASTM 986-04).To minimize charge interruptions the samples were coated with a gold using gold-sputtering equipment Images were magnified from 5,000 to 50,000 times their original size. sample.

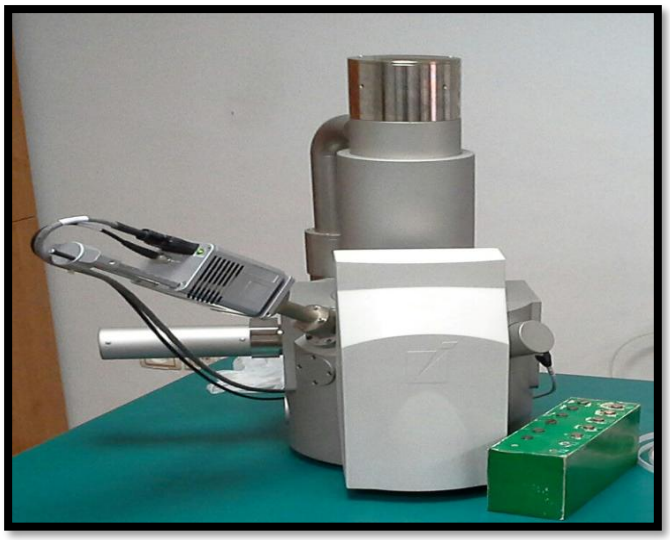

Figure 3.11: The Scanning Electron Microscopy Machine.

3.7.2 Infrared Fourier Transform Spectrometry (FTIR)

FTIR test is done by utilizing IR Affinity-1 Shimadzu –Japan Figure (3.12). To know the type of interaction between components and bonds types of it. A graph of transmittance against wave number produced by FTIR spectroscopy reveals the chemical structure. This test carried out according to ASTM E1252 The appropriate material was determined by comparing this chart to the standard chart.

Figure 3.12 : FTIR spectroscopy analysis device

3.7.3 Wettability Test

Contact angle (Lablabs fitting mode) was used to evaluate the wettability of the nanocomposite samples using “SL200B Optical Dynamic / Static Contact Angle Meter” as shown in Figure (3.13) with a contact angle range of 0 to 180 . This device computes and compares the left and right contact angles, determines their average value, and provides a Real-time data graph enabling video recording of contact angle changes.

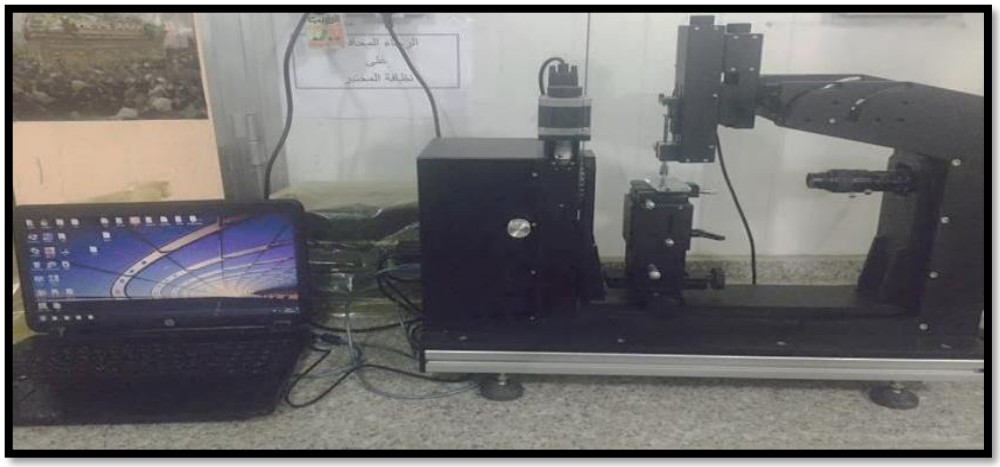

Figure 3.13: Contact Angle Measurement Device.

3.7.4 Pin-on-Disc Test

Figure 3.14 depicts the sliding test carried out on the pin-on-disc wear machine (ASTM G99). Under dry circumstances, the wear samples were evaluated. The pin specimen is 5 centimeters in length and 6 millimeters in diameter. The counter face was comprised of steel carbide with a diameter of 35 mm that remained constant during all testing. The experiments were conducted at room temperature. During the test, the sliding time was 20 min, and the sliding rotations per minute rpm 300 m/s. 3 MPa was the nominal contact pressure. Before each test, a brand-new disc was utilized.

These tribological processes can be analyzed individually for polymers and chemicals. As illustrated in the following equation, The

friction coefficient (COF) may be calculated as the frictional force (Ff) divided by the normal load (FN).

$$\mu=\frac{Ff}{FN} \qquad (1)$$

The deformation of fills reveals that adhesion, solid isotope crusts, and debris plowing between two surfaces are all examples of atomic-level mechanical interactions. Friction is significantly influenced by the shear technique and the rupture of the material surrounding the contact zone between the two surfaces.

$$\text{Wear rate } (W.R) = \Delta W/ \pi D.N.t \quad gm/cm \qquad (2)$$

where: - D is the sliding circle diameter in cm, t is the sliding period in minutes, and N is the speed of the steel disc (rpm).

Figure 3.15: Pin-on-Disc Sliding

Table 3.3: Device Elements

No.	Description	No.	Description
1	Pin specimen	5	Emergency stop
2	Disk specimen	6	Applied load
3	Disk holder	7	Load cell
4	Pin holder	8	Balance weight

3.7.5 Nanoindentation

Nanoindentation is a great way to learn about mechanical property measurement at the nanoscale, including for things like ultra-hard coatings with very thin layers. The four types of mechanical deformation (elastic, plastic, viscous, and fracture) which are most commonly encountered during indentation testing are first considered. The initial nonlinearity beyond which the reaction can no longer be considered linear.

Hardness, or contact Hardness (Hc), is the standard unit of indentation plasticity; it is defined as the peak load (Pmax) divided by the contact area under load (Ac), Hc = Pmax/Ac. Instrumented indentation measurements can be taken immediately after thermal stabilization using the novel top surface referencing technique.

In addition to the modulus, the present approach may be utilized to determine the hardness of a material H. Using its conventional meaning, hardness:

$$H = \frac{P_{\max}}{A}, \qquad (3)$$

where A is the predicted hardness imprint area and P_{max} is the maximum indentation force, h_c total displacement h is represented as

$$h = h_c + h_s \qquad (4)$$

where hc is the vertical distance along which contact is created and h_s is the surface displacement at the edge of the contact (now known as the contact depth) which links Er to A and S to the observed contact area and modulus.

The slope of this line, which is determined by the derivative dP/dh at point (Pmax, hmax), indicates the surface's elastic stiffness and is denoted by the following equation:

$$S = \frac{dP}{dh} = \frac{2}{\sqrt{\pi}} E\sqrt{A_c} \qquad (5)$$

For the indenters (assuming perfect geometry), the contact area A_c is given by:

$$A_C = 24.5\ h_c^2 \qquad (6)$$

$$hc = h_{max} - h_s \qquad (7)$$

The reduced elastic modulus is then obtained using the stiffness.

$$E_r = \frac{\sqrt{\pi}}{2\beta}\frac{S}{\sqrt{A}} \qquad (8)$$

Figure (3.17) is a graphic depiction of data from an indentation experiment showing load vs indenter displacement. Peak indentation load is denoted by Pmax, indenter displacement is denoted by h_m, d_X, final contact impression depth is denoted by h_f., and initial contact impression

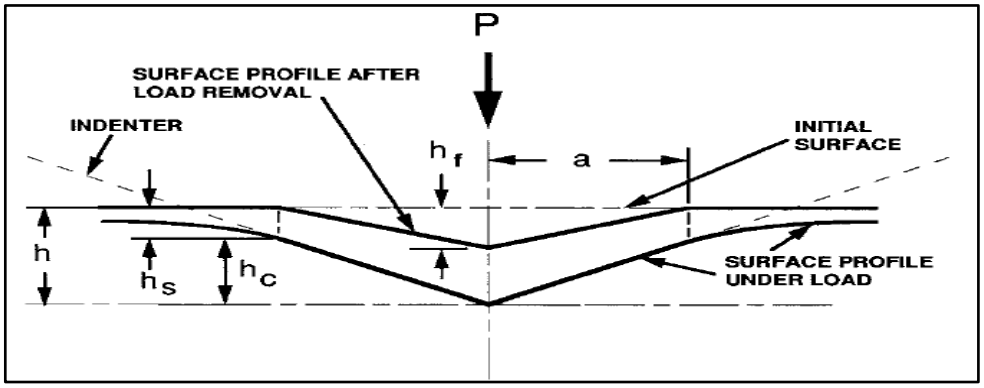

Figure. 3.17 Diagram of a segment through an indentation that shows the different amounts used in the analysis

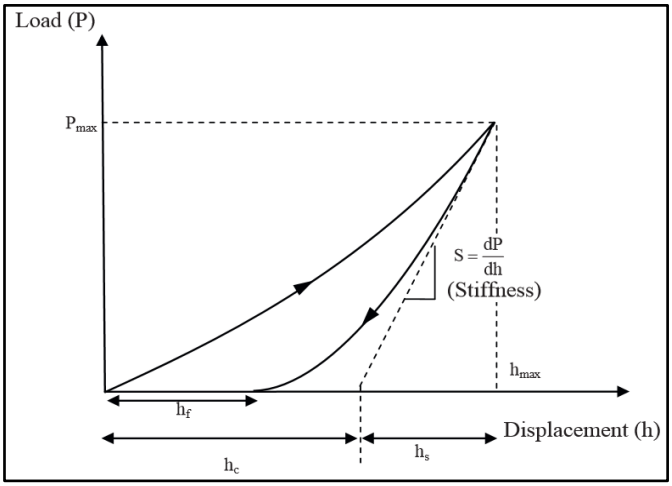

Figure 3.18 Indentation curve

3.7.6 Differential Scanning Calorimetry (DSC)

The test was done using a SH1MADZ-4 DSC-60 equipment in accordance with ASTM D3418-03 (Figure 3.18). The samples of pure materials (PMMA) and PMMA nano graphene oxide in powder form were analysed under nitrogen gas and a heating rate of 10 °C / min between 25 and 350 °C.

Figure 3.19 : Differential scanning calorimetry (DSC) device.

3.7.7 Ultraviolet-visible spectrophotometer test

UV-Visible – CECIL 2700 computerized spectrophotometer used to assess the sample's optical characteristics. The sample is positioned in a certain location on the UV/VIS instrument. depicts the operating principle of a double beam spectrophotometer, which employs two beams of light: a reference beam and a beam that passes through the sample as a sampling beam. this test was done in Iraq and Iran . Figure 3.20 shows the principle of UV.

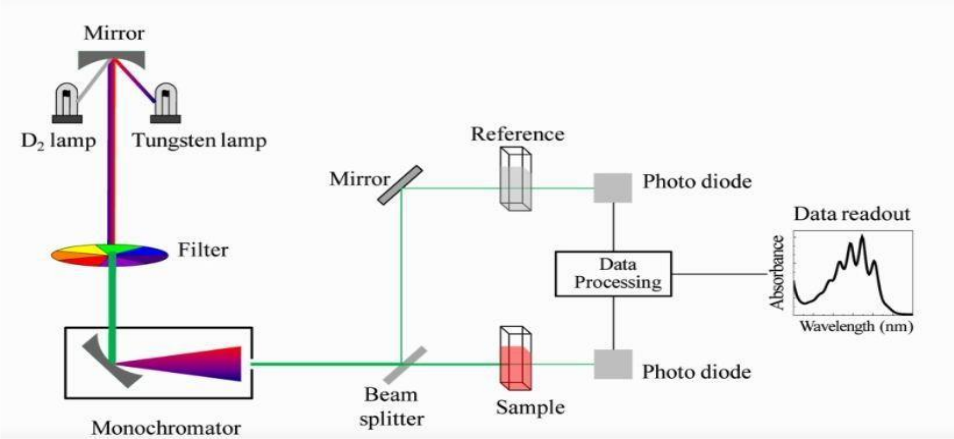

Figure 3.20 The principle of UV.

3.7.8 Hardness (Micro Vickers Hardness) Test

The hardness of PMMA and its nanocomposite were tested. Each hardness value is the mean of four independent samples. The test is made according to ASTM standard C1327-90, using digital micro Vickers hardness tester (TH-717),at 0.5kg with a dwelling time of 15 second. Vickers hardness is calculated using the following equation.

$$H_v=1.\ 854\ (P/d^2) \qquad (9)$$

Where, H_v, is the Vickers hardness (MPa), P, load (N), d, diagonal length of the indentation impression (μ m)

Figure 3.21 : Vickers Device

3.7.9 Scratch Test

Hardness is frequently used to determine a material's resistance to irreversible or plastic deformation. There are three different ways to quantify hardness. The material's capacity for being scratched, indented, and rebounding. The scratch hardness test measures the resistance of a material to scratches and abrasion caused by sharp object contact.The ISO 1518 standard is used to describes a method for determining how resistant a single coating or multi-coat system of paint, varnish, or a similar product is to penetration by the scratching with, a stylus loaded to a certain load.

Figure (3.23) show the Scratch Device and According to Figure (3.22) , the test sample's surface is exposed to a continuous normal force from the stylus, which creates the relative sliding motion that creates the scratch track. Only the front half of the indenter is completely supported by the material due to the dynamic nature of scratching; the back half is either only partly or not supported at all. The formula for universal scratch resistance is as follows $\mathbf{H_{sp}=\frac{4\,q\,p}{\pi\,w^2}}$ **(10)**

H_{sp} is considered the scratch of hardness, W stands for the measured scratch width, P represents the applied normal load, and q represents a factor ranging from 1 for elastic materials to 2 for plastic materials (q is considered to have a mean value of 1.5). Due to the fact that most polymers are naturally viscoelastic or viscoelastic in this study [54]

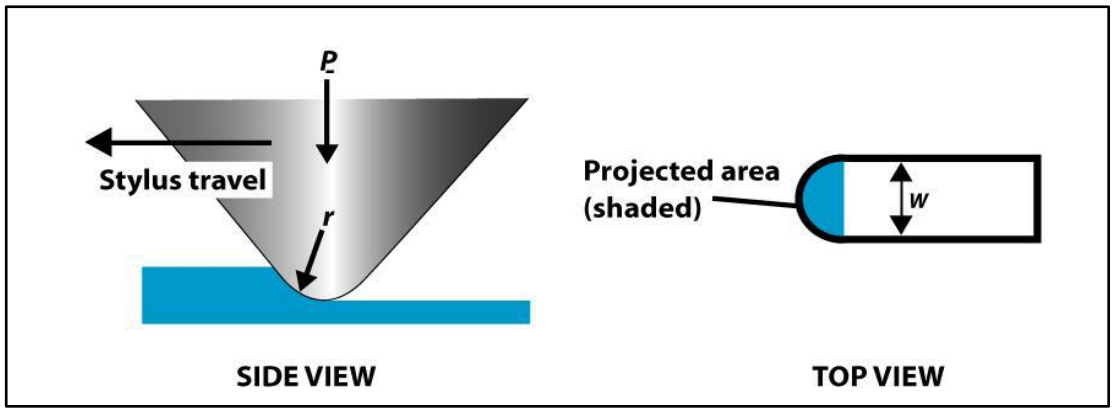

Figure 3.22 Scratch Tip

Figure 3.23: Scratch Device

3.7.10 Pull Off Test

Pull off automated coating adhesion meter included a "pull-off"-style pulling head, was used to evaluate the adherence of the applied coatings. Pull-off measurements were taken three times on each specimen .The pull-off test's classification in accordance with this standard. The obtained samples' failure kinds are displayed.

When assessing coating adherence using a pull-off adhesion gauge, the pull-off test can be performed once a suitably prepared dolly has been attached to the prepared coating.

When performing a pull-off test on a coating applied to a thin substrate, it is imperative to employ a thin substrate base ring or thin substrate skirt; otherwise, the applied force might distort the substrate and cause the coating to fail prematurely.

Bond testers are more advanced testing tools that can be used when higher precision is required. A bond tester provides more control and increased automation. This technology may also be used to assess direct tensile strength and/or adhesion between two layers. The test standard is ASTM D4541-22. Figure 3.24 explain Pull off sample and Figure 2.25 pull-off Device.

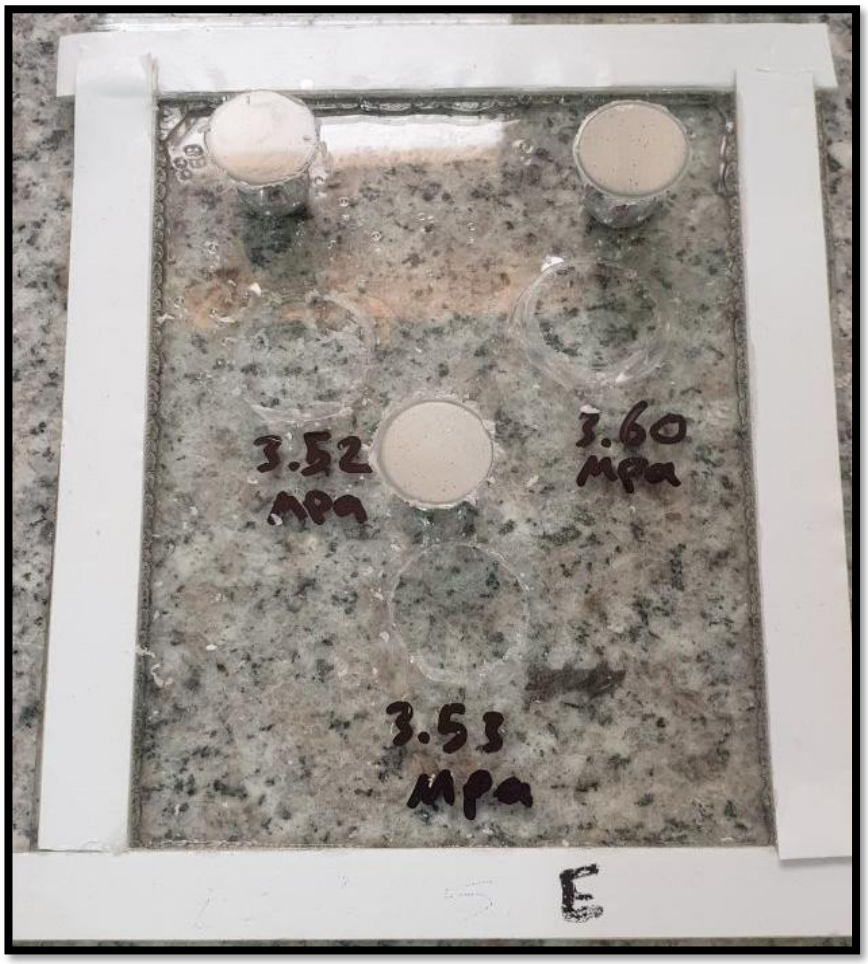

Figure 3.24 Pull off sample.

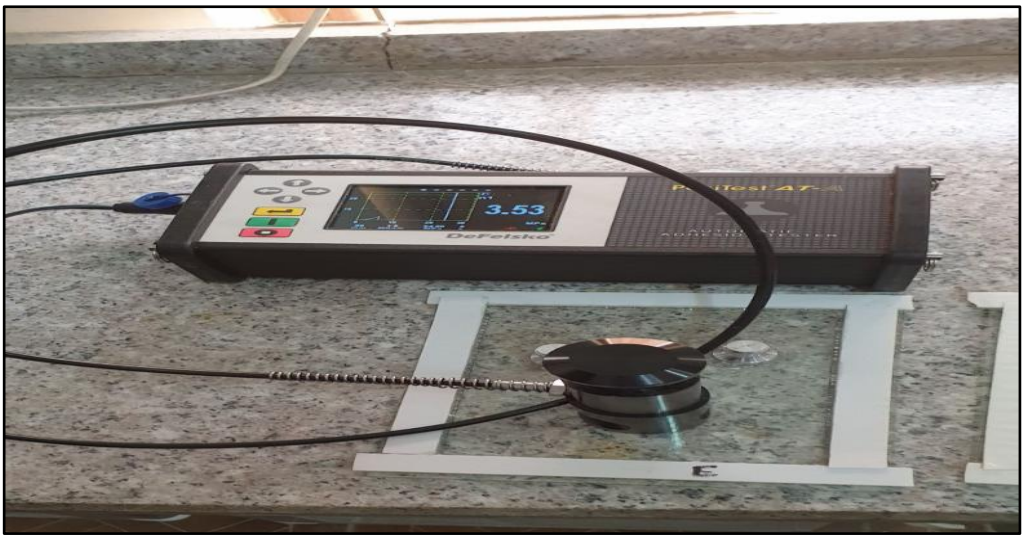

Figure 3.25: pull-off Device

Pull off = F/A

Where F is the applied force and A is the contact area.

Chapter Four

Results and Discussions

4.1 Introduction

This chapter presents the results obtained from the prepared samples. Tribological, mechanical and optical, properties of nanocomposite coating PMMA reinforced with different wight percentages of GO , MGO and MGO\BW hybrid. Studying the structure properties using FTIR, thermal properties by DSC, the mechanical properties for the prepared samples which included Hardness and Pull off, tribological properties including Wear test and Scratch test, optical properties using UV the Wettability properties using contact angel test, the morphological properties using SEM and elastic and viscoelastic behavior by using nanoindentation.

Results And Discussion

4.2 FTIR

Figure 4.1 showed that The FT-IR spectra of GO and MGO reveals a prominent peak at 3417 cm^{-1} as well as a number of peaks of lesser strength at, for GO band at 1622 cm^{-1} refers to the stretching vibration mode C=C for conjugated alkene structure, the stretching of carboxylic acid groups, a drop in the intensity of the peak at 3425 $cm^{-1}$and a decrease in the intensity of the peak at 1636 cm^{-1} compering with MGO.

Form Figure (4.1), FTIR spectra demonstrate that MGO has not undergone any chemical reaction. GO has oxygen-containing functional groups, including hydroxyl (O-H), carbonyl (C-O), and C-O-C groups, which correspond to absorption peaks at 3400, 1636, and 1232 cm^{-1}. The peak at 1625 cm^{-1}represents GO's skeleton, while the peak at 1438 cm^{-1} is due to the C-OH bending vibration [159]. GO 3400 cm^{-1} absorption peak becomes less pronounced after MGO alteration.

Figure (4.2) showed the distinctive peaks of the PMMA polymer and Graphene oxide films were determined. The peaks at 3442 and 1730 cm^{-}

[1] related to the stretching vibrations of CH_2 and C=O groups, whereas the peak at 2925 cm^{-1} corresponds to the asymmetrical stretching of C-H bonds in the CH_3 group.

The asymmetric deformation vibration of methyl group is appeared around 1427 cm^{-1} and the C-O-C symmetrical stretching appeared at 1150 cm^{-1}. Band at 942 cm-1 is due to the C-O-CH_3 rocking [160].

FTIR was used to examine the molecular structure of (pure PMMA, PMMA\GO, PMMA\MGO and PMMA/MGO/BW) and to understand the bonds between Pure and composite materials. The 1148 cm^{-1}peak is the C–O bond stretching vibration in C–O–C.

PMMA/GO reduces GO's C–O, C–O–C, and –OH FTIR peaks. GO network growth decreases C=O 1728 cm^{-1} FTIR peak. FTIR spectra of GO/PMMA and MGO/PMMA nanocomposite coatings demonstrate the appearance of two peaks at 2877 cm^{-1} indicates the formation of Si-O-C bond [161].

Beeswax has organic compounds. Figure 4.2 shows PMMA\MGO\BW FTIR spectrum. 1175 Cm^{-1}relates to C=O stretching and CH bending of esters, whereas 1750 Cm^{-1} is due to C=O stretching of esters and free fatty acids Absence of a new peak in PMMA\MGO\BW FTIR spectra proved composite was a mix of two components [162].

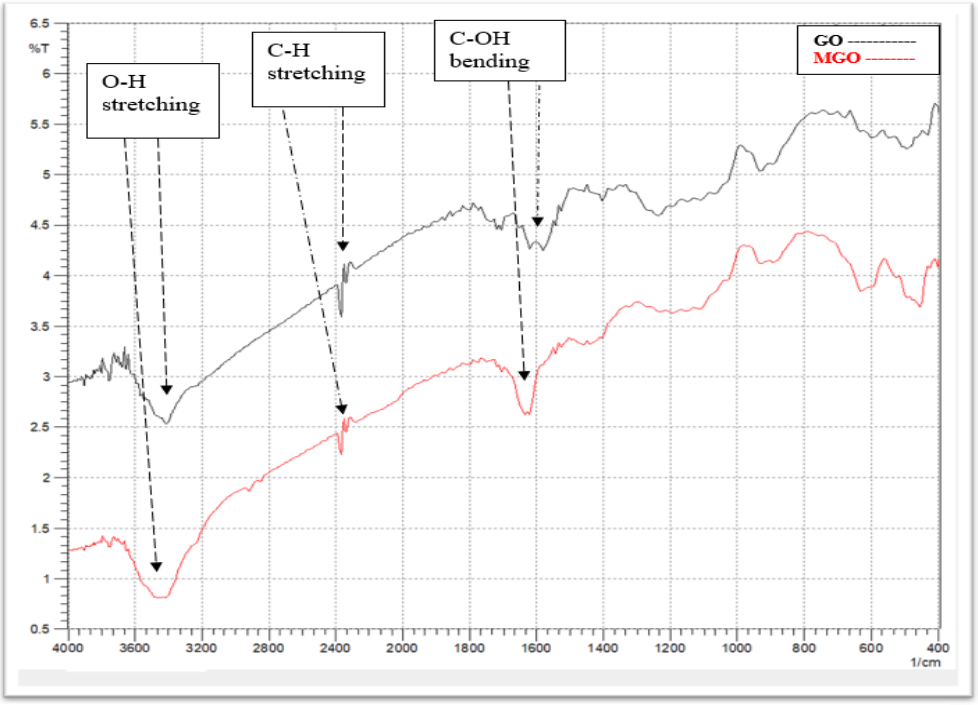

Figure 4.1: FTIR For GO and MGO

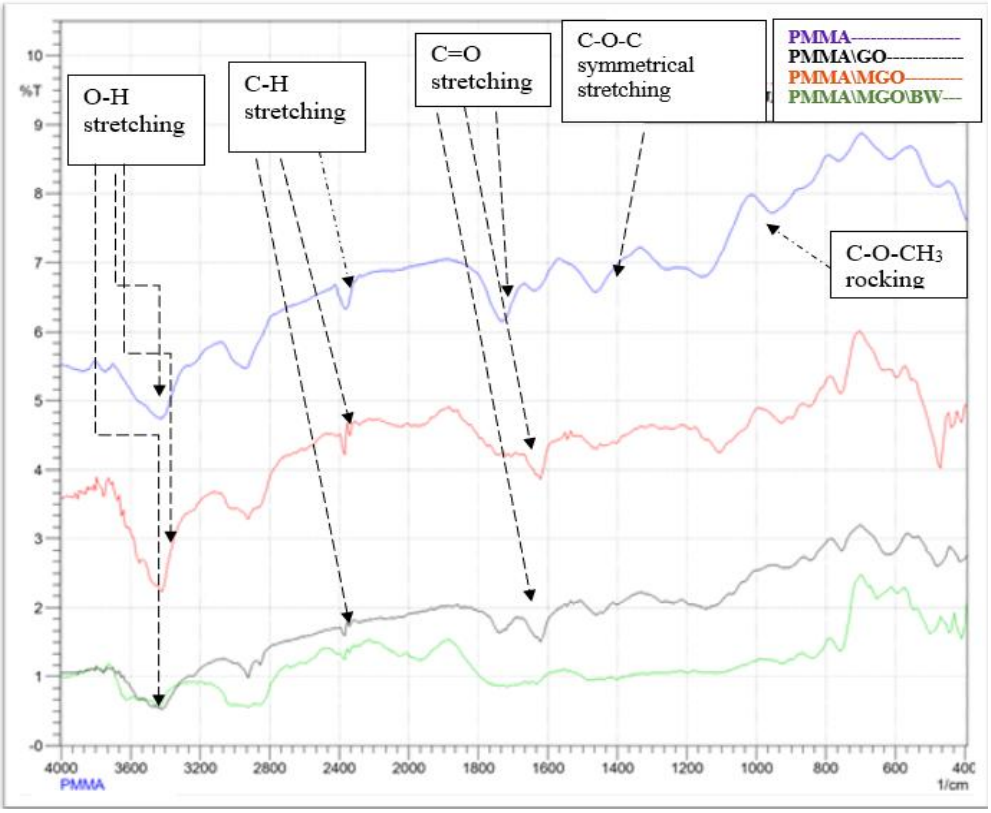

Figure 4.2: FTIR For PMMA, PMMA\GO 0.5 wt% , PMMA\MGO 0.5wt % , PMMA\1 wt% MGO\BW 0.5

4.3 DSC Test

Figure (4.3) shows the DCS analysis of pure PMMA wich used to determine PMMA and PMMA nano-composites glass transition temperatures. The results showed that Neat PMMA has a Tg of 99 °C . this agree with [163]

Figure 4.4 is PMMA containing 0.25 wt% GO nanoparticles had a glass transition temperature (T_g) that was approximately 10 °C higher than that of pure PMMA. The T_g values for PMMA containing 1 wt% GO and 1 wt% MGO. were approximately 18 °C and 19 °C higher, respectively.

Because of the large specific surface area of nanoparticles and their homogeneous dispersion within the matrix, these particles are able to effectively act as nucleating agents, as shown in Figure 4.5 Additionally, increasing in T_g can be attributed to the nanoparticle's occupation of a space in the PMMA lattice, which in turn restricts the mobility of chain diffusion.

So it is clear, that T_g values increased linearly from 99 Cº (for PMMA [164]. up to 117 Cº (for sample with 1 wt% MGO.) 19% . This increment in T_g give an indicator about the improvement of the mechanical properties of the prepared samples as well as the thermal stability and this agree with . When Graphene Oxide amounts increased within the composite structure, the steric hindrance increased, so the polymeric chain restricted and cannot be sliding above each other's, which leads to increase T_g and this agree with [165].

Table 4.1 T_g for PMMA and it's composites

Sample	Tg
PMMA	98.61 ºC
PMMA\GO 0.25 wt%	109.96 ºC
PMMA\GO 1 wt%	116.53 ºC

PMMA\MGO 1 wt%	117.58 °C
PMMA\1 Wt% MGO\BW 0.5	107.72 °C

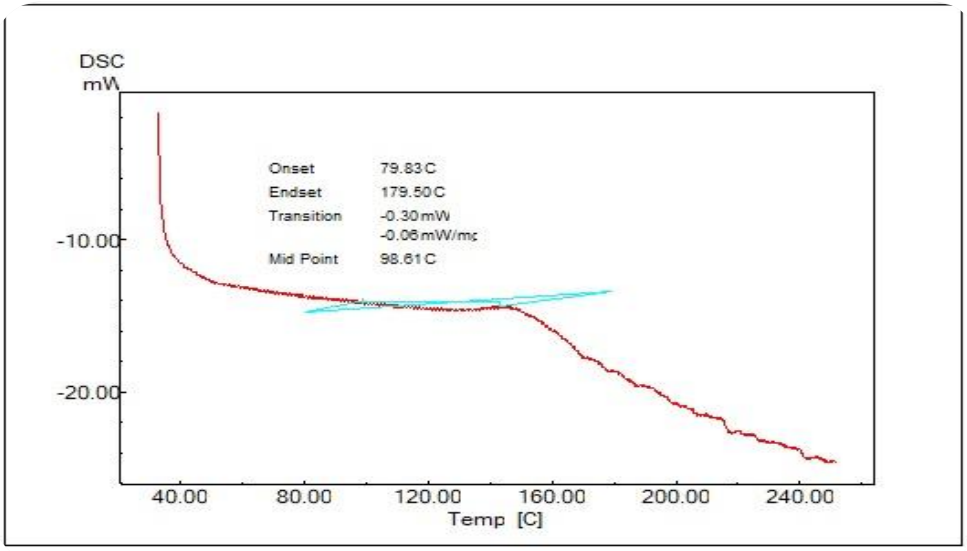

Figure 4.3 DSC curve For PMMA

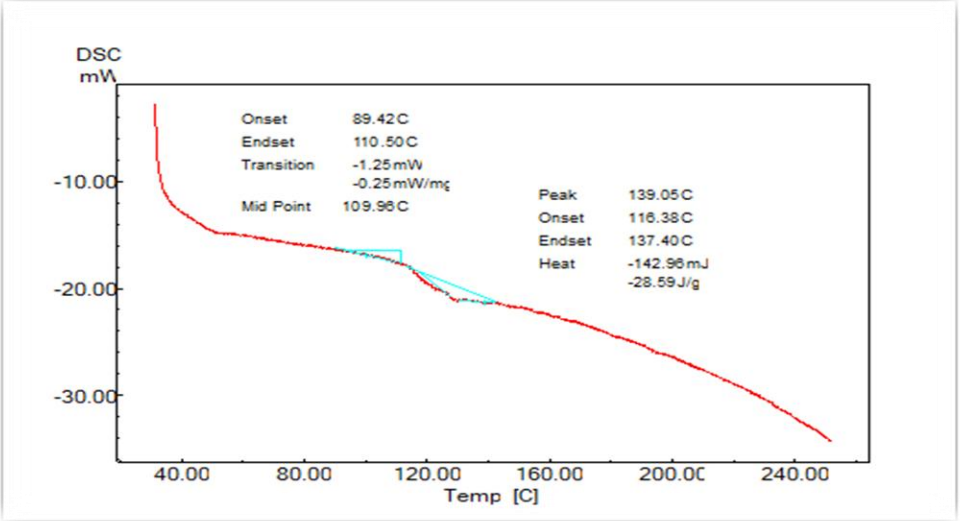

Figure 4.4 DSC curve for PMMA\GO 0.25 wt%

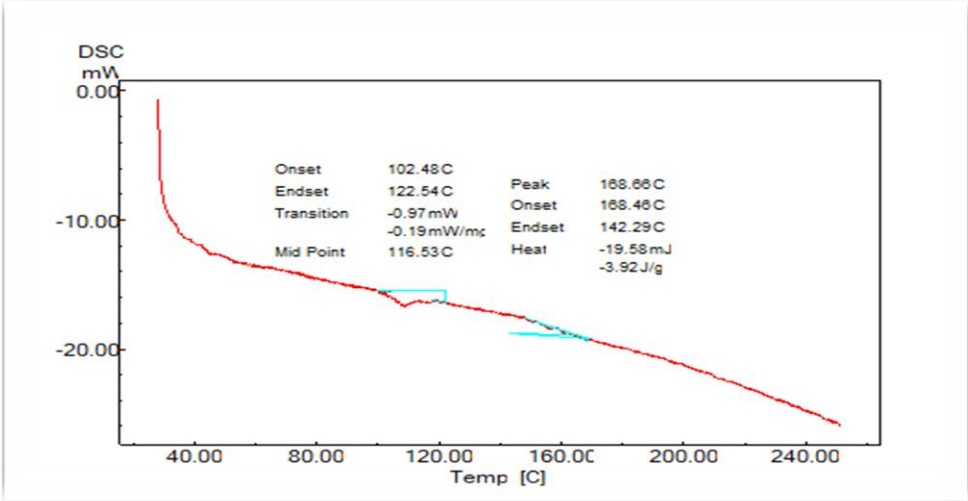

Figure 4.5 DSC Curve For PMMA\GO 1 Wt%

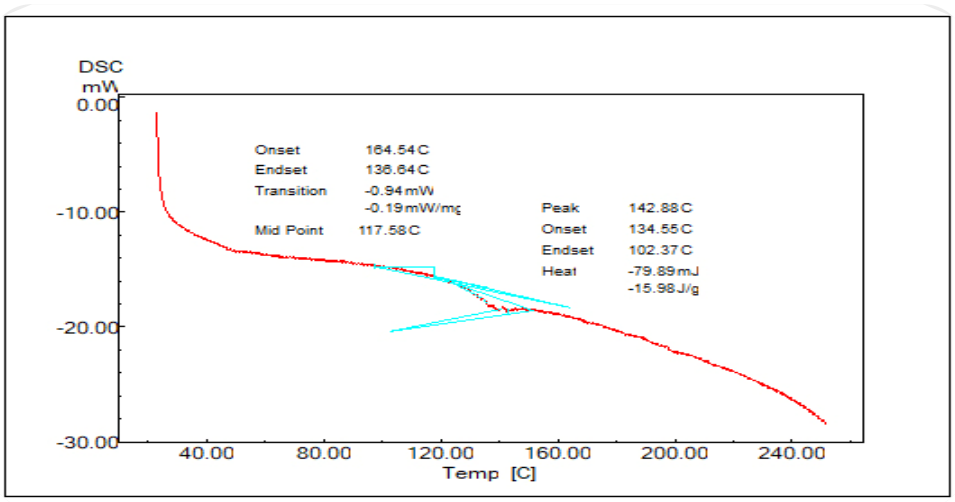

Figure 4.6 DSC Curve For PMMA\MGO1 Wt%

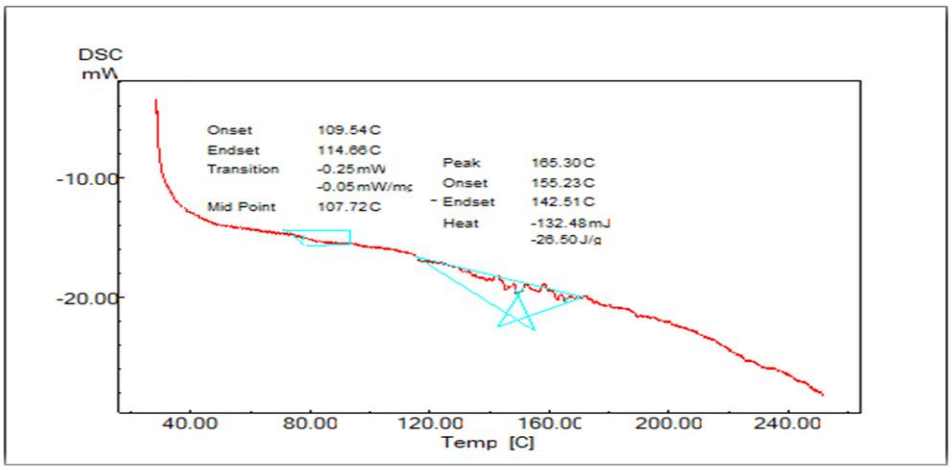

Figure 2.7 DSC Curve For PMMA\1 Wt% MGO\BW

4.4 Hardness Test

Material hardness is defined as the resistance of material against surface deformation caused by external load. The Vickers hardness test for PMMA nanocomposite is shown in Figure 4.8 The hardness of the PMMA increases with the increasing nanoparticles content addition. The measured values of the micro hardness with change in GO content the increase in GO content led to increase in density, and micro hardness from 11 to 18.4 HV.

Figure. (4.8) showed the hardness of the pure PMMA and PMMA reinforced with GO and MGO. the increase in GO and MGO content caused to increase of hardness value. The hardness value increased by 96% for PMMA\GO 1 wt and 100% for PMMA\MGO 1wt%. Addition of wax led also to increase in hardness from (21.3) for 0 wt% wax to (23.7) 0.5 wt% beeswax as shown in Figure (4.9)

The addition of beeswax had a significant effect on the improvement of the dispersion of MGO, as well as the improvement of the mechanical properties of the resulting compound, as it improved the hardness by 110 % in comparison with pure PMMA.

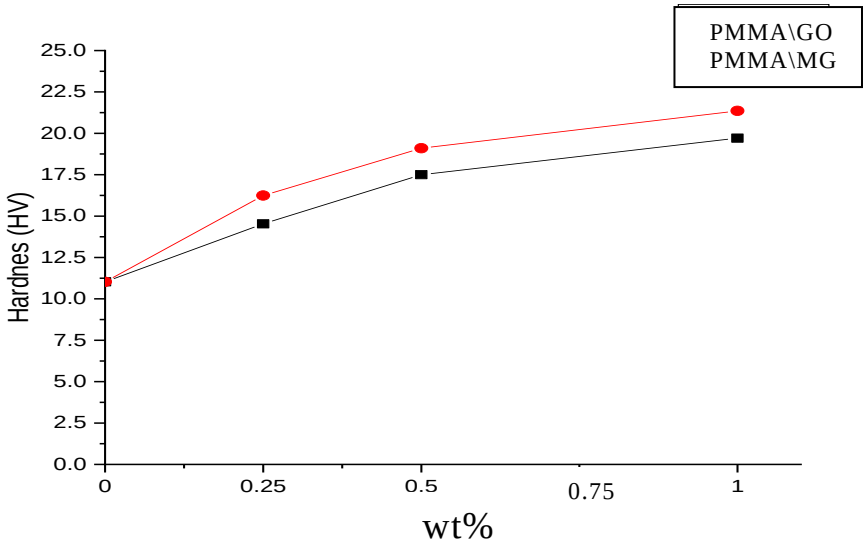

Figure 4.8 Micro Hardness test For PMMA\GO And PMMA\MGO wt%

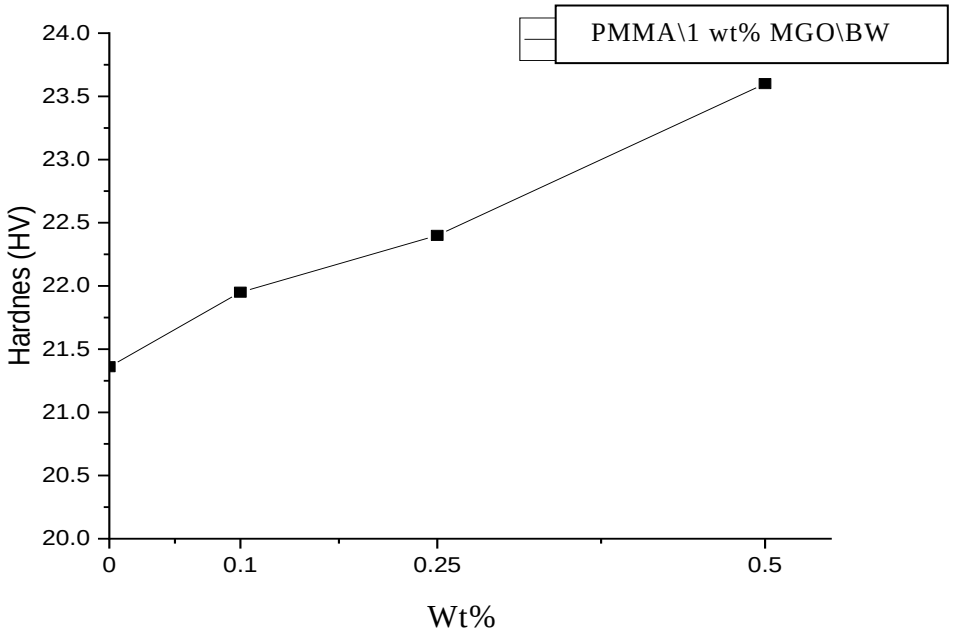

Figure 4.9 Micro Hardness test For PMMA\1 wt% MGO\BW (hybrid composite)

4.5 Coefficient of Friction and Wear result

According to the findings, the friction coefficient reduced in a linear faction when the weight percentage of GO increased. Specifically, the coefficient of friction changes from 0.78 for pure PMMA to 0.68 for PMMA that had been reinforced with GO 1 wt %, as shown in Figure (4.10). This might be attributed to cleavage of graphene oxide layers which behave as a solid lubricant

As shown in Figure (4.10). addition of MGO can cause a significant reduction in friction coefficient of (PMMA/MGO) nanocomposite was decreased (from 0.78 to 0.67) and the coefficient of friction decreases as the MGO content increases.

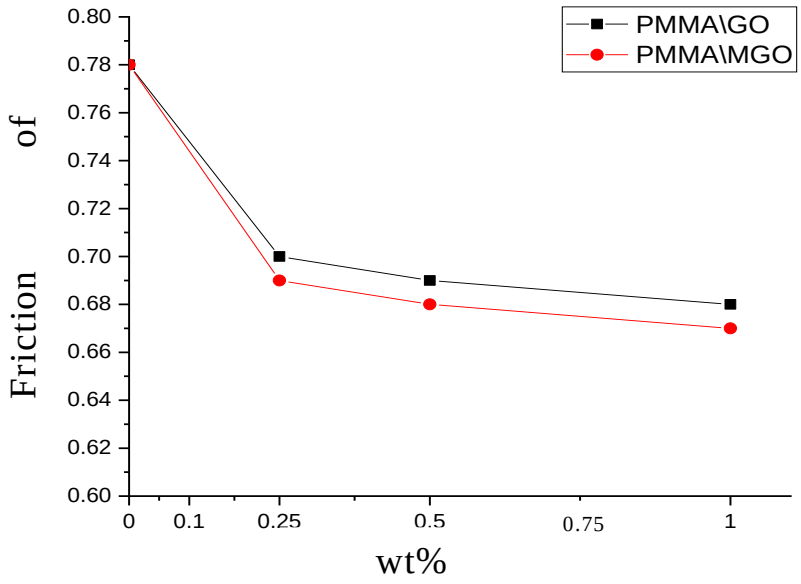

Figure 4.10 Friction of Coefficient. For PMMA\GO And PMMA\MGO

The presence of beeswax with the PMMA\1 % MGO nanocomposite leads to decrease in the coefficient of friction. Beeswax plays a significant role in enhancing the dispersibility of MGO in PMMA matrix and also decrease the interfacial shear stress at contact zone which can reduce the coefficient of friction .

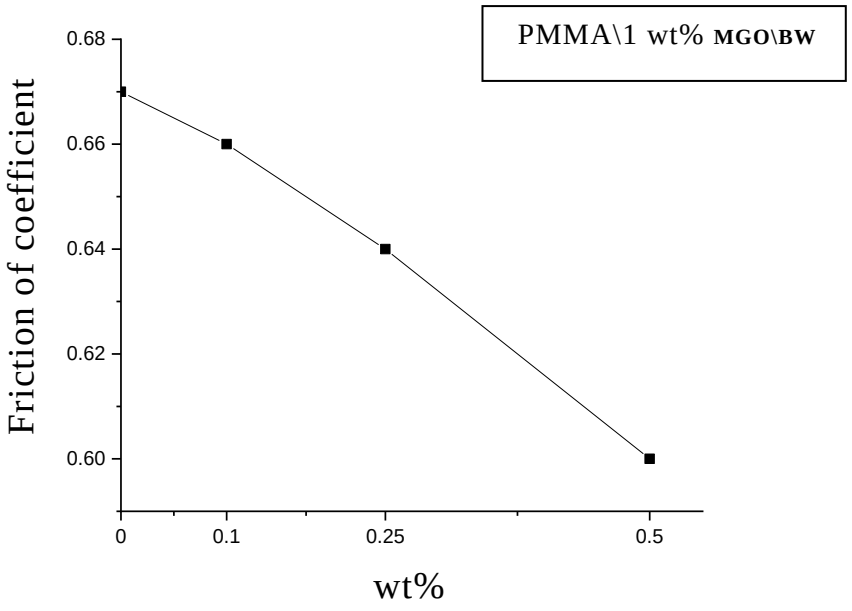

Figure 4.11 Coefficient of Friction For PMMA\1 wt% MGO\BW

The wear rate losses of PMMA\GO and PMMA\MGO Nanocomposite decrease as the GO ,MGO content increases, and this behavior is related to the role of GO and MGO as a solid lubricant. GO and MGO maybe decreased the interfacial shear stress at the contact zone. Figure 4.12 showed (0.25%, 0.50%, and 1%) GO and MGO PMMA. GO can enhance the wear resistance when sliding. GO nanoparticles worked as a solid lubricant on the samples surface during testing, and their resistance to rubbing during sliding decreased wear volume loss. The wear rate decreased by 58% for PMMA\GO 1 wt % and decreased by 69% for PMMA\MGO 1 wt% as compered for pure PMMA.

The inclusion of nanofillers and wax increases the wear resistance of PMMA because the GO and MGO nanoparticles operate as a barrier material that prevents the PMMA matrix large-scale fragmentation due to the mean contact pressure. Due to the composites limited thermal conductivity, produced heat localizes and softens the contact surface. Consequently, the shear strength of the interfacial surface layer required for the sliding technique would be drastically reduced.

Figure 4.13 shows the greatest reduction in wear volume correlates to the decrease in friction coefficient seen in PMMA nanocomposites (0.5 wt.%) beeswax by 34% for PMMA\MGO 1wt% which has the lowest wear volume. This reduction in friction coefficient and wear volume was a result of the ultrafine GO nanoparticles partially smoothing the counterpace. Also, lubricating wax increases in addition of wax reduce the rate of wear since wax acts as a lubricant.

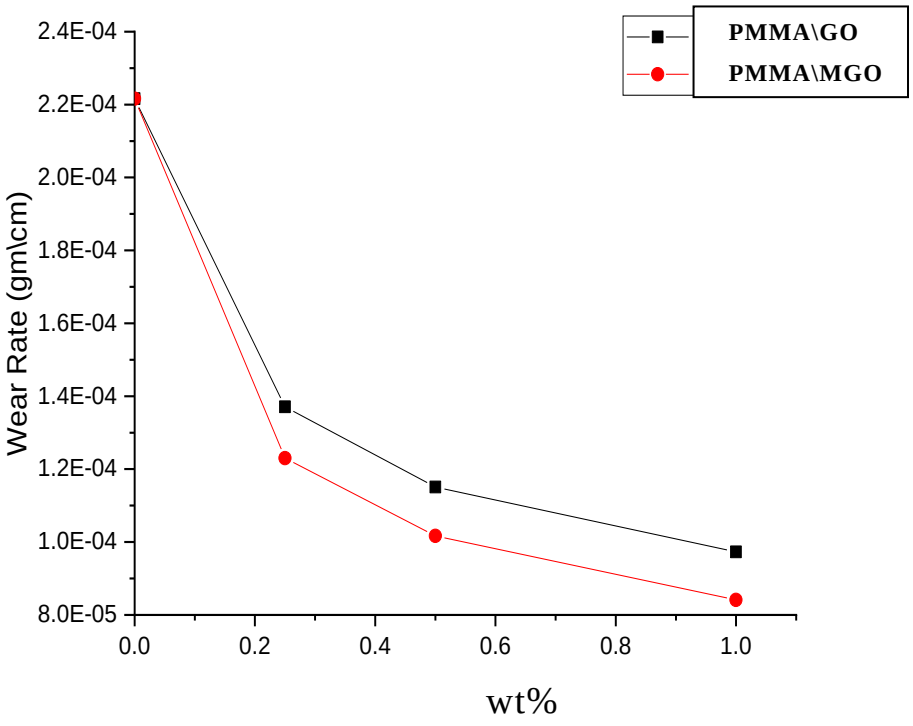

Figure 4.12 Wear rate for PMMA\GO and PMMA\MGO *wt %*

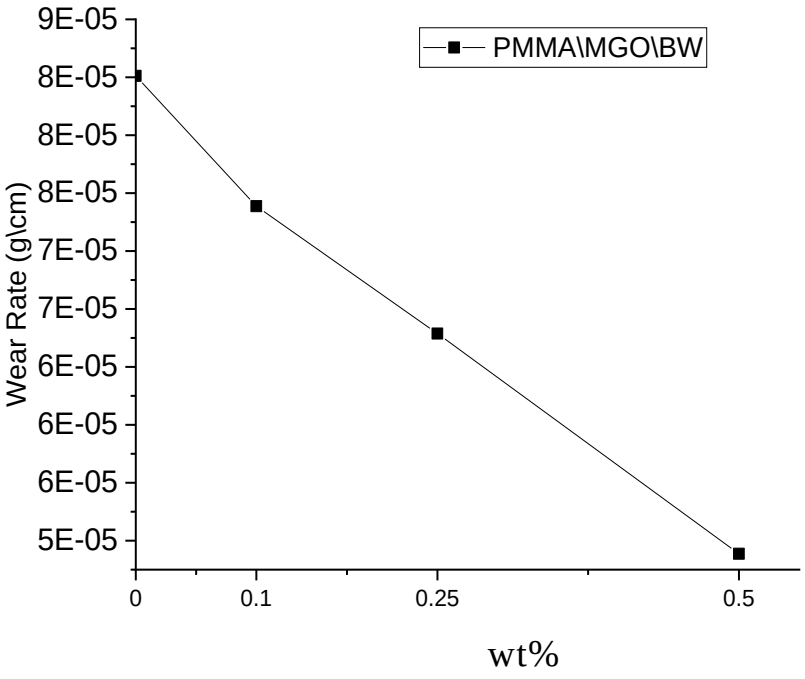

Figure 4.13 Wear rate for PMMA\1 wt% MGO\BW *wt %*

4.6 Pull Off Test

Pull off adhesion testing is widely used to assess the protection coating process. The pull-off strength of manufactured coatings is displayed in Figures 4.14 and 4.15 along with the most common kind of failure. The coating detachment from the surface of glass substrate completely in the form of adhesive failure (coting\ substrate interfacial)

There is no significant increasing in the adhesive strength with increasing the wight percentage of GO in the composite, also the result showed that the nanocomposite with MGO of increasing the brittleness of the resultant coating which can decrease the adhesive bond with glass substrate. The pull-off strength of coatings reinforced with beeswax was the lowest of any of the coating types tested, even lower than that of unreinforced coatings.

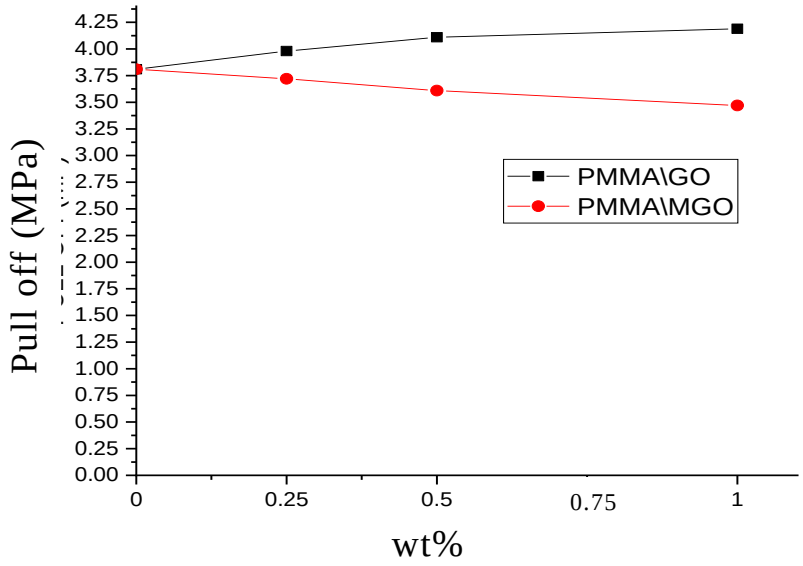

Figure 4.14 Pull Of test for PMMA\GO And PMMA\MGO

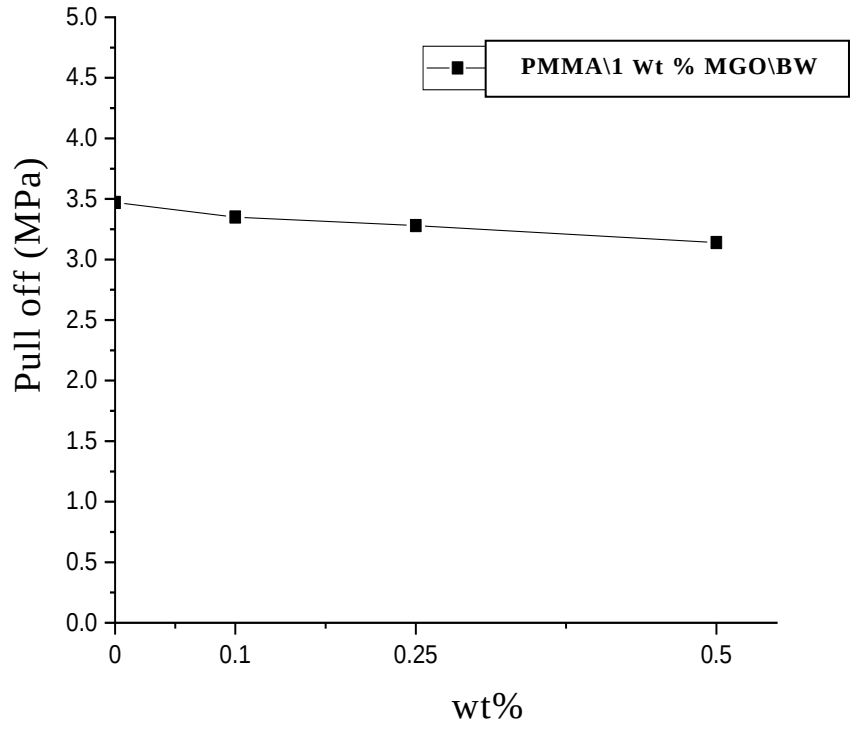

Figure 4.15 Pull Of test for PMMA\GO , PMMA\MGO , PMMA\MGO\BW

4.7 Contact Angel Test

Measuring the contact angle of the finished coating the wettability of the coating was assessed. This test was carried out with distilled water at (30 °C), where the contact angle measured after 30s.Figure 4.16 shows the representative images of contact angels on the pure PMMA and its composites.

The water droplets were rapidly absorbed on the neat PMMA surface data which was taken every ten second, while these droplets on the PMMA\MGO nanocomposites still possessed relatively slightly incrassating contact angle at the same time. It can be seen that the contact angle increased with more MGO nanoparticles addition, PMMA\MGO. while there is slightly decrasing with additon of GO without modification because GO is a haydrophilc

Silane coupling agent is a hydrophobic compound and this agree with [166].

Measurements of the contact angle are used to assess the surface attributes of a composite coating made of PMMA and beeswax that contains 0.1 weight percent of MGO.

Figure 4.16 displays the findings that were gathered from the experiment. This is indicated by the contact angle value of the PMMA\MGO\BW 0.5 has (93°) composites in comparison to the pure PMMA coating (68°) there is increasing 37% in contact angel. This can be attributed to the addition of an optimal amount of GO nanoparticles .All samples using a solid lubricant increased the contact angle. It has been discovered that beeswax samples had a high contact angle with water.

Beeswax is considered to be the most hydrophobic natural substances due to a high content in esters of long-chain fatty alcohols and acids, as well as long-chain alkanes[167].

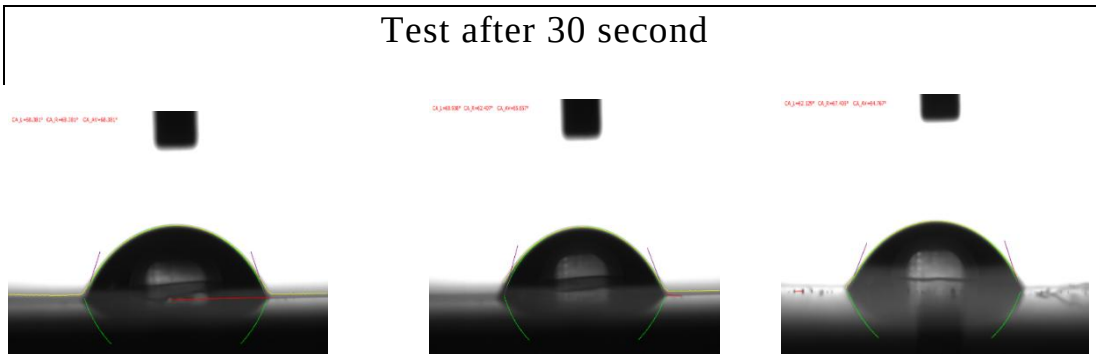

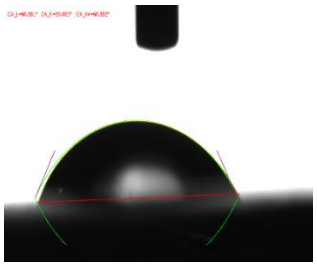

PMMA\GO 1

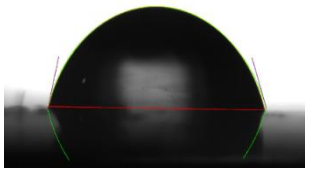

PMMA\MGO 0.25

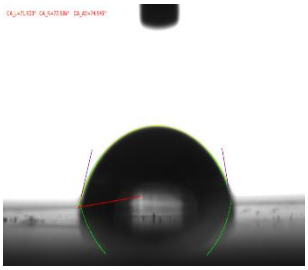

PMMA\MGO 0.5

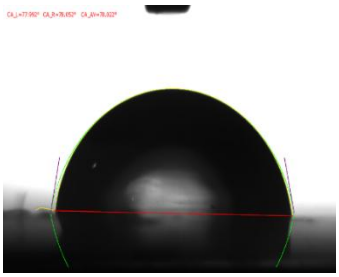

PMMA\MGO 1

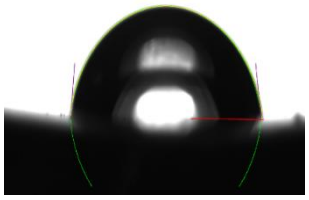

PMMA\MGO\BW 0.1

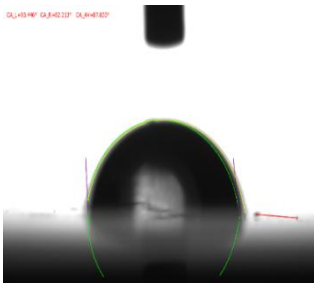

PMMA\MGO\BW 0.25

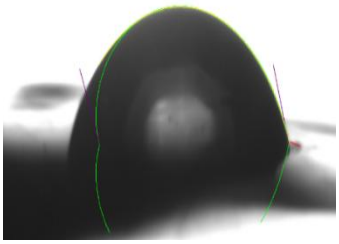

PMMA\MGO\BW 0.5

Figure 4.16 Contact angle of pure PMMA and it's composites (PMMMA\GO , PMMA\MGO, PMMA\1 wt% MGO\BW)

Table 4.2 Contact Angel CAV

Samples	Contact Angel (CAV)
PMMA	68º
PMMA\GO 0.25	66 º
PMMA\GO 0.5	65 º

PMMA\GO 1	61 º
PMMA\MGO 0.25	72 º
PMMA\MGO 0.5	75 º
PMMA\MGO 1	79 º
PMMA\1 wt% MGO\BW 0.1	84 º
PMMA\1 wt %MGO \BW 0.25	88 º
PMMA\1 wt % MGO\BW 0.5	94 º

4.8 Scratch test

Addition of GO and MGO to PMMA can enhanced scratch hardness to 23% and 32% respectively under 0.5 kg probe load as a comparing with pure PMMA. Materials with suitable value of hardness, elastic modules have high scratch hardness as shown in Table 4.3 . It seems that with increasing GO and MGO wight percentage the plastic deformation was reduced.

PMMA reinforced with GO and MGO showed a scratch resistance more than pure PMMA. Addition silane coupling agent can Surface modifications for GO it enhance dispersibility and interfacial interactions between the nanofiller and the matrix due to efficient load transfer using silane, which was responsible for the improvement of several mechanical properties, and this agree with [168] increase in hardness and corresponding enhancement on scratch resistance.

The presence beeswax can reduce the coefficient of friction due to the decreasing of the interfacial shear stress in the contact zone which can increase the scratch resistance. For PMMA\1 wt% MGO\BW were the scratch hardness improved by 68% relative to pure PMMA with

increasing wight percentage of beeswax as shown in Figure 4.17 and Table 4.3

The ability of a polymer coating to resist scratches is contingent upon a number of parameters, including the coating's hardness, mechanical qualities, chain segment structure, dispersion of fillers, and processing [169, 170].

Table 4.3 Scratch hardness for PMMA and its composite (PMMA, PMMA\GO, PMMA\MGO, PMMA\MGO\BW)

Sample	**Scratch hardness value (MPa)**
Pure PMMA	0.0119
PMMA\GO 0.25 wt%	0.0127
PMMA\GO 0.5 wt%	0.0136
PMMA\GO 1 wt%	0.0146
PMMA\MGO 0.25 wt%	0.0136
PMMA\MGO 0.5 wt%	0.0146
PMMA\MGO 1 wt%	0.0157
PMMA\MGO\BW 0.1 wt%	0.0169
PMMA\MGO\BW 0.25 wt%	0.0183
PMMA\MGO\BW 0.5 wt%	0.0199

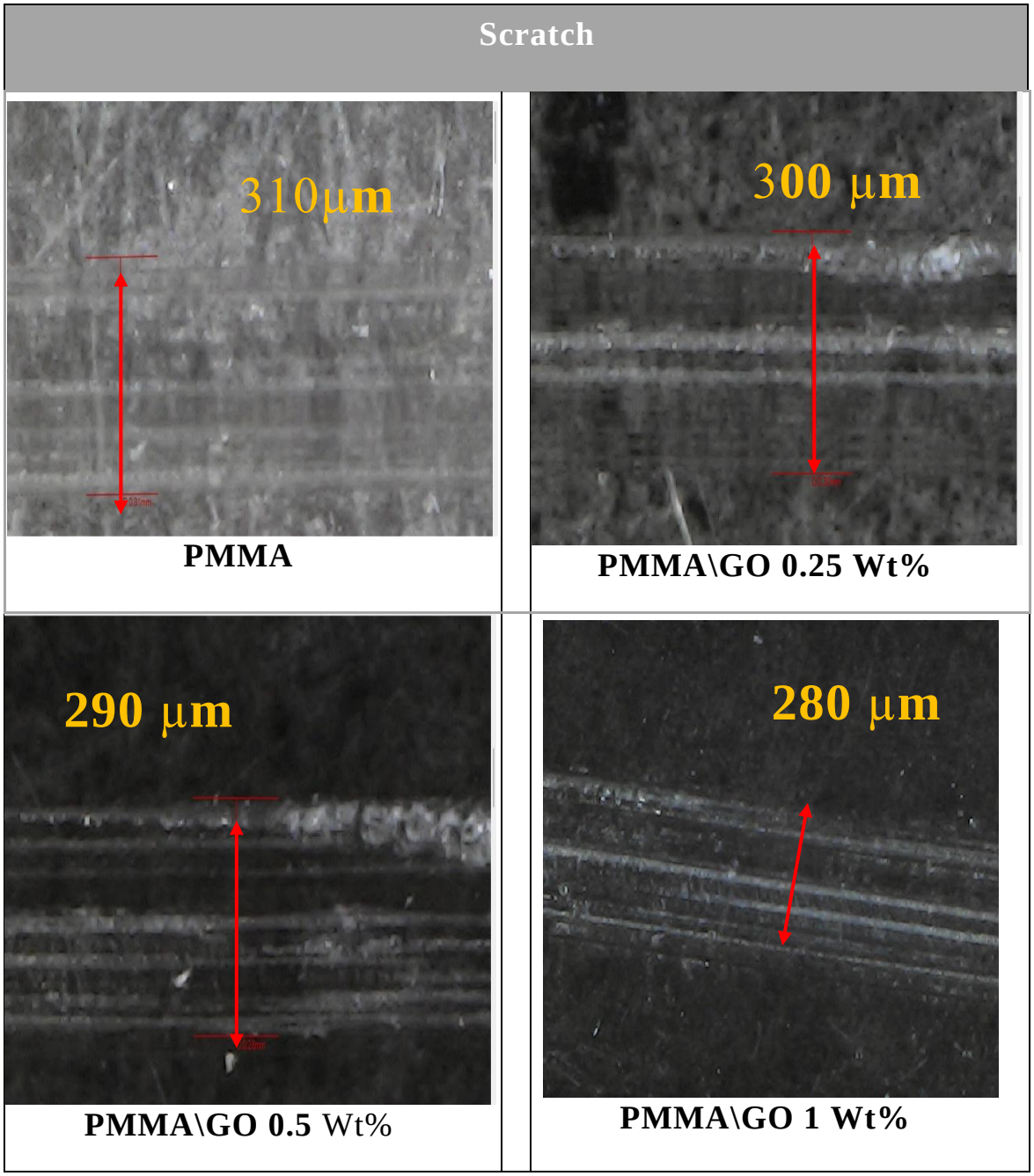

Figure 4.17 Optical images for Scratch hardness for PMMA\GO

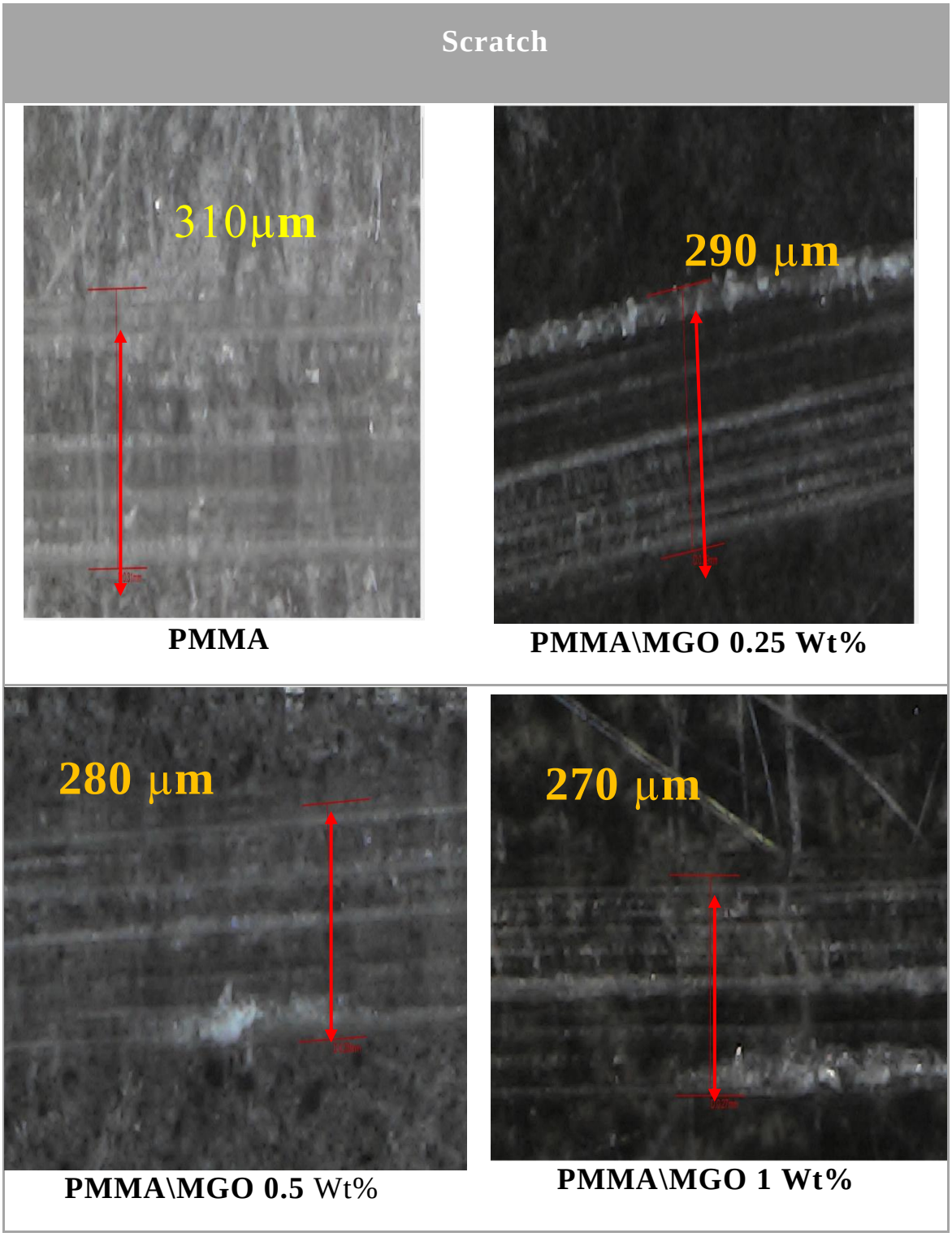

Figure 4.18 Optical images for Scratch hardness for PMMA\MGO

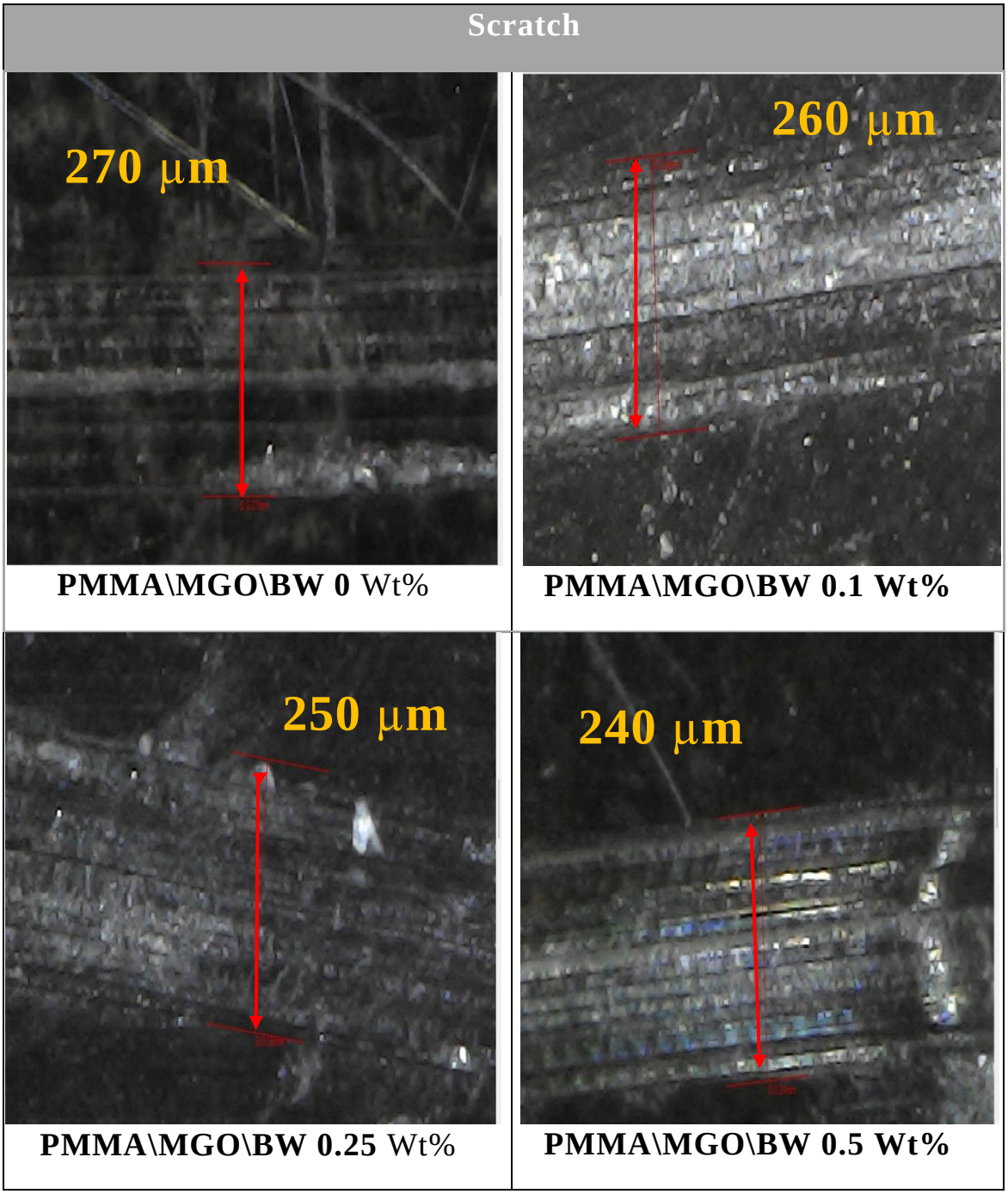

Figure 4.19 Optical images for Scratch hardness for PMMA\MGO\BW

4.9 UV-Vis and Absorption Spectroscopy Result

Absorption of the produced samples is illustrated in Figure 4.20 for the ultraviolet, visible, and infrared areas of the electromagnetic spectrum. The inclusion of graphene oxide created changes in the electrical energy levels that were present within the structure of the polymeric composite material, as demonstrated by the fact that absorbency increased with increasing graphene oxide concentration in the UV area.

These modifications make it possible for the structures to capture potentially dangerous UV radiation and release it as innocuous heat instead of letting it pass through. This is a beneficial advantage which highlights that the composite films have the potential to avoid the hazards of UV-degradation and remain in operation for extended periods of time.

The same pattern of behavior is observed in the visible area (400-800 nm), where the absorbance rose linearly with the amount of graphene oxide present, albeit at lower intensities. This is due to the fact that the radiations which are present in the VIS area have lower energy and longer wavelengths. Additionally, it can be seen that the absorbance throughout the VIS area is relatively constant. This indicates that the prepared films absorb all of the colors that fall within this range at the same rate. Additionally, the combination of graphene oxide and wax improved the absorbency in the infrared region, which made it possible to identify the chemical functional groups.

This indicates that the vibrational and rotational motions of the molecules included inside the composite structures were altered as a direct result of the presence of graphene. And this is in accordance with [171].

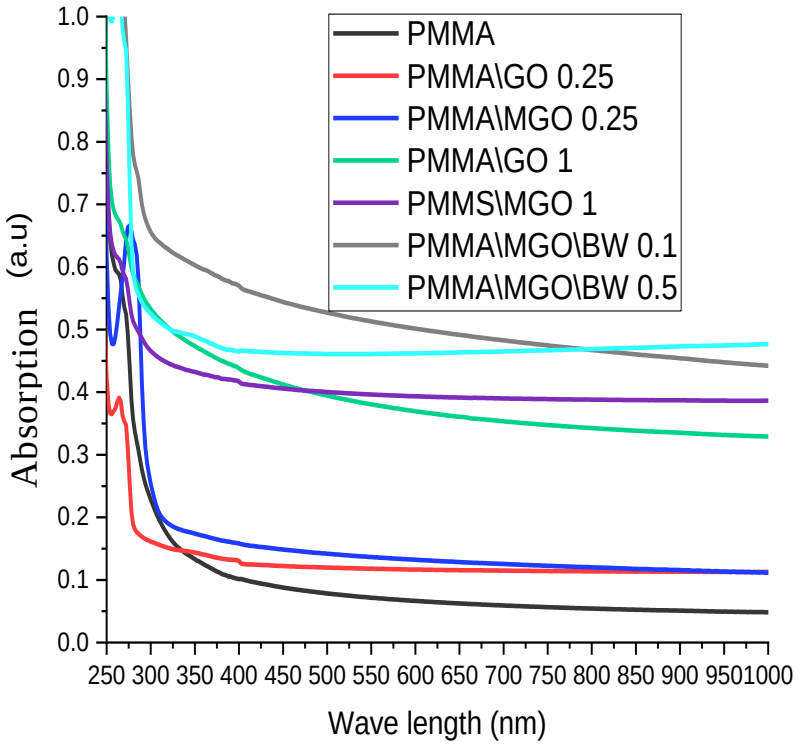

Figure 4.20 UV Absorption

Transmittance decreases with graphene oxide concentration (Figure 4.21). PMMA\GO nanocomposite absorbs UV light between 250 nm and 400 nm, according to UV–Vis spectrum. GO blocks UV and provides UV-shielding. On increasing wt% of GO nanoflakes, UV transmittance reduced without impacting visible range transparency. Adding wax to the composite likewise lowered transparency. Transparency fell from 92% of the very transparent PMMA polymer to 72% of the polymer reinforced with 0.1wt% graphene oxide and 0.5wt% wax, which is acceptable within the visibility range.

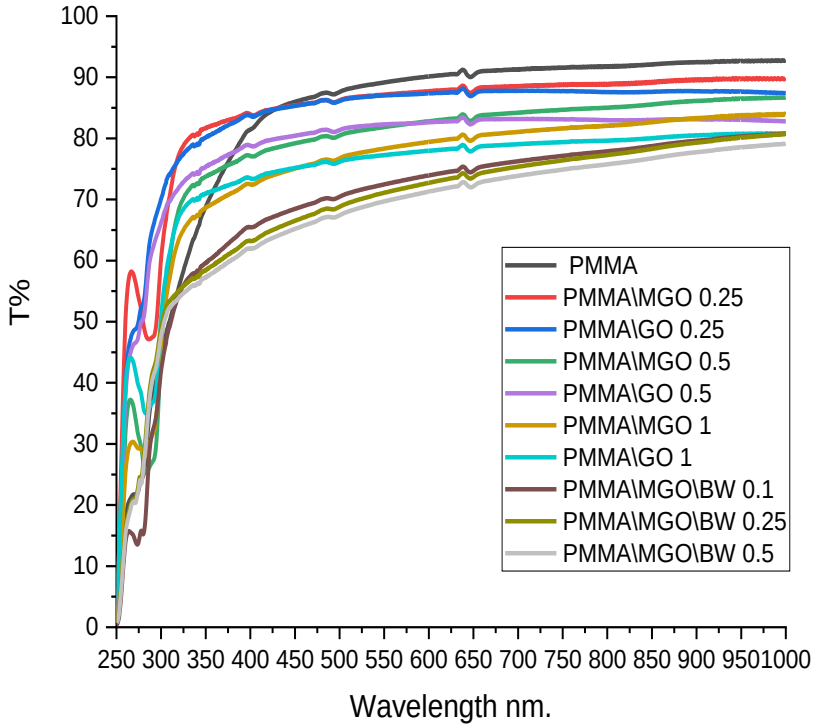

Figure 4.21 UV-VIS Test for All Samples

4.10 Scanning Electron Microscope (SEM)

Scanning electron microscope (SEM) is used to show the morphology and nanoparticle distribution in the polymer matrix (Figure 4.22) it clear that GO nanoparticles are well dispersed through the PMMA matrix and there is a little agglomeration of the nanoparticles in the structure of the polymer .

It can be observed also, in low content GO (0.25 and 0.5%) particles are dispersed homogeneously inside the PMMA matrix with a very few agglomerates. On the other hand, when the filler content increased (1%) agglomeration increased with a reasonable proportion of particles distributed at the nanoscale. As it was observed during sample fabrication, the matrix viscosity significantly increased as nanoparticle concentration increased. Further increases in GO produce an increase in the brittleness of the PMMA matrix.

Additionally, low content MGO (0.5 and 1%) particles are seen to be uniformly dispersed within the PMMA matrix with very few agglomerates. On the other hand, agglomeration increased with a reasonable proportion of particles distributed at the nanoscale as the filler content increased (1%) in the sample. The matrix viscosity significantly increased as the nanoparticle concentration increased, as was seen during sample fabrication. The brittleness of the PMMA matrix increases as GO continues to rise.

The use of hybrid filler (MGO 1wt% with a variety weight percentage of beeswax) had a clear effect in improving the dispersibility of the MGO within the PMMA matrix, which led to a change in the fracture behavior of the surface from plastic deformation to a more elastic behavior. The surface of the MGO was encapsulated with beeswax which ensured that it was completely covered with PMMA matrix, it is abundantly evident that the proportion of wax that was most successful was 0.5 percent. This resulted in an improvement in the mechanical performance of the composite that was created, in addition to an improvement in both the elastic and viscoelastic recovery.

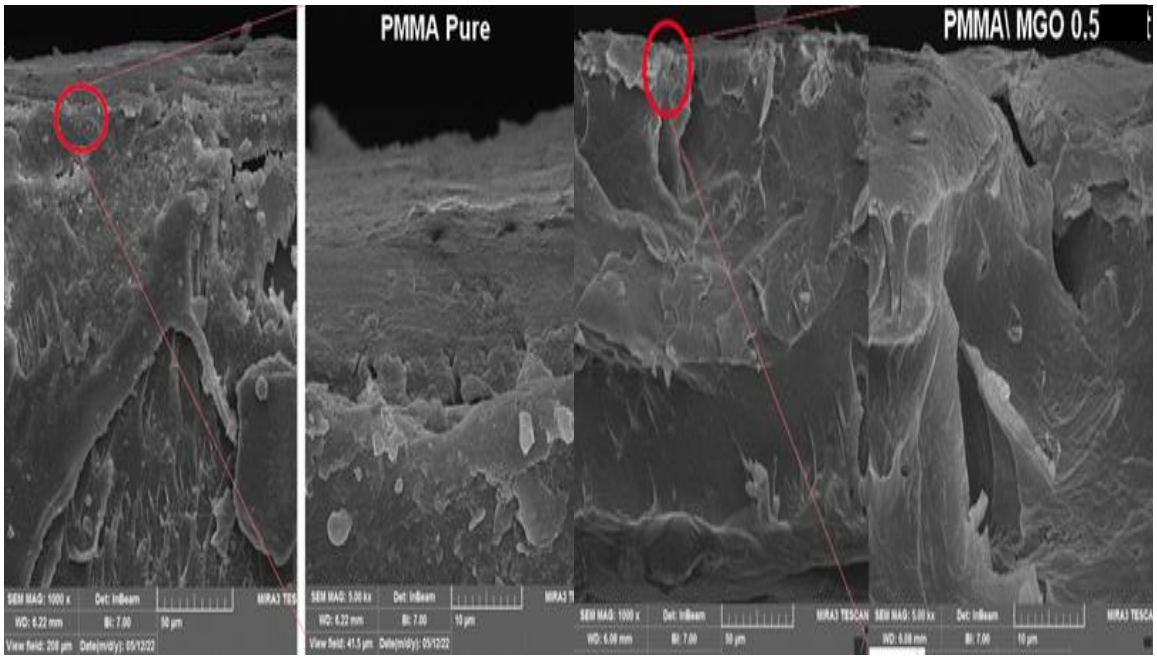
PMMA Pure
PMMA\ MGO 0.5

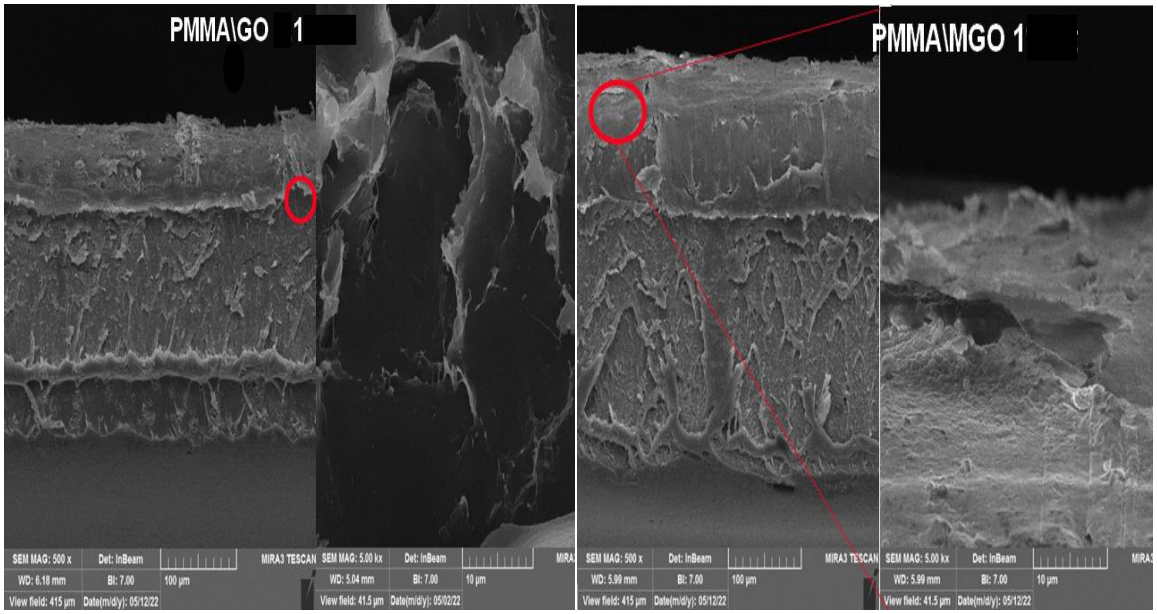
PMMA\GO 1
PMMA\MGO 1

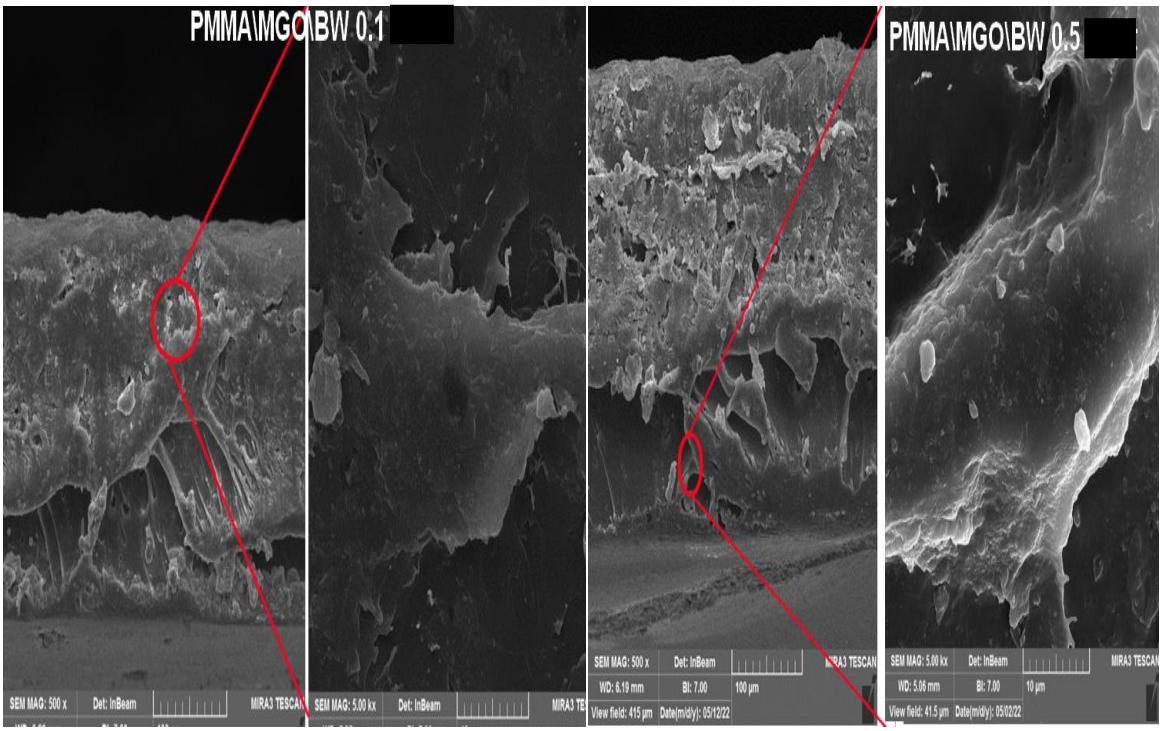

Figure 4.22 SEM Image for pure PMMA and its composite (PMMA , PMMA\MGO 0.5 , PMMA\GO 1 , PMMA\MGO 1 , PMMA\MGO\BW 0.1 , PMMA\MGO\BW 0.5)

4.11: Nano Indention Test:

Nanoindentation is one technique that may be applied to the process of determining the mechanical properties of coating layer [172].

Indentation load versus depth graphs may be used to determine a material's hardness as well as its elastic modulus. Indentation depths, that are less at a given force, are indicative of a material's enhanced hardness.

The indentation unloading response can be determined by the material's elastic modulus. Initial unloading slope is used to measure the elastic modulus of a material; slopes that are steeper indicate that the material is more rigid. According to the load–depth curves, GO causes an increase in both the hardness and elastic modulus of PMMA.

The indentor and flexure setups that were utilized to determine the elastic modulus. There is increase in hardness by 86% for PMMA\GO 1

wt% and 93% for PMMA\MGO wt% in compering with pure PMMA and after addition of beeswax the improving in hardness by 120 % for PMMA\MG\BW 0.5 wt% compering with pure PMMA.

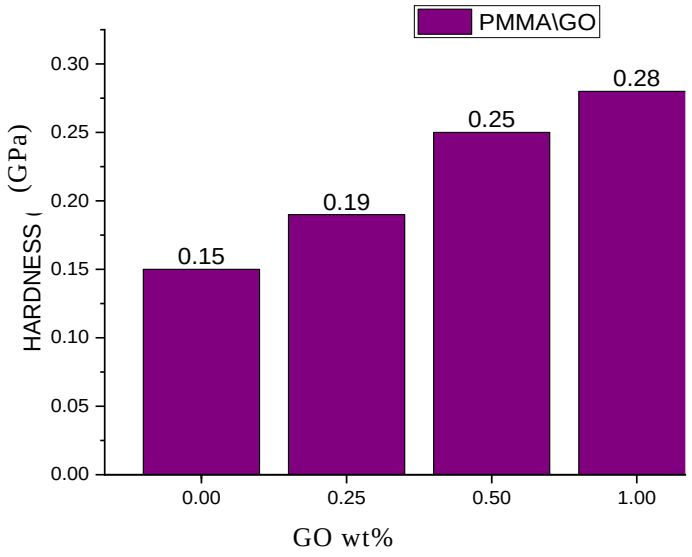

Figure 4.23 Hardness for PMMA\GO

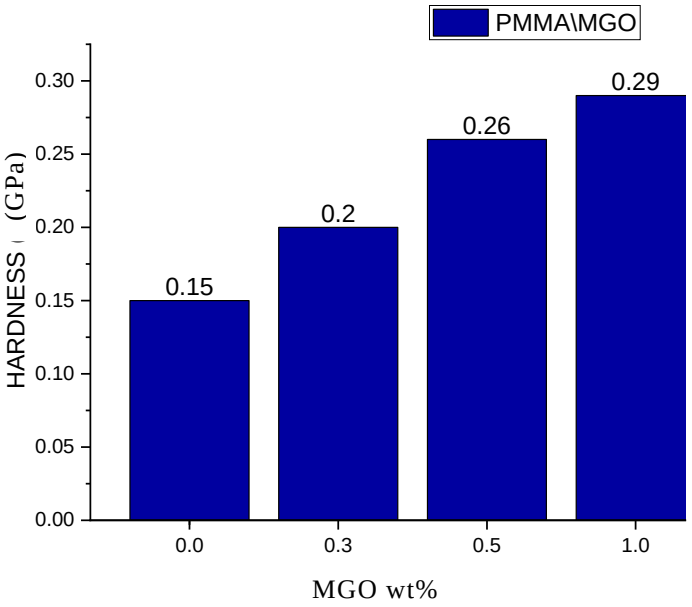

Figure 4.23 Hardness for PMMA\MGO

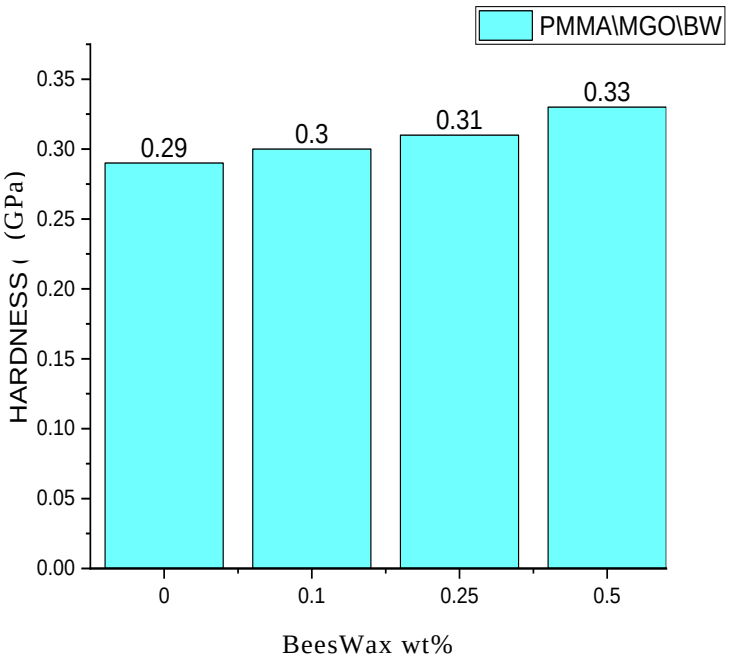

Figure 4.24 Hardness for PMMA\MGO\BW

Figure 4.25 illustrates the elastic modulus of PMMA as well as the nanocomposites made from it. The addition of GO nanoparticles leads to an increase in the material's elastic modulus. The increase in the composites modulus is a reflection of the stress that has been transferred from the PMMA matrix to the high-modulus GO that has been embedded. For this reason, it is preferable to have high interfacial adhesion between the PMMA and the GO in order to stiffen the composite.

Figure 4.26 and 4.27 showed the elastic modulus of PMMA\MGO and PMMA\MGO\BW as well as the nanocomposites made from it. The addition of MGO nanoparticles leads to an increase in the material's elastic modulus also the addition of bees wax can make better distribution for MGO and bees wax increase the recovery of material.

The increase in the composites modulus is a reflection of the stress that has been transferred from the PMMA matrix to the high-modulus MGO and PMMA\MGO\BW that has been embedded. For this reason, it

is preferable to have high interfacial adhesion between the PMMA and the MGO in order to stiffen the composite

According to the adhesive theory of wear, the level of wear resistance has a one-to-one correspondence with the elastic modulus. The true area of contact is reduced when there is a high elastic modulus, which leads to low adhesion and wear. For PMMA\MGO , the result showed that there is also increasing. For addition of wax ,young modulus is also increased.

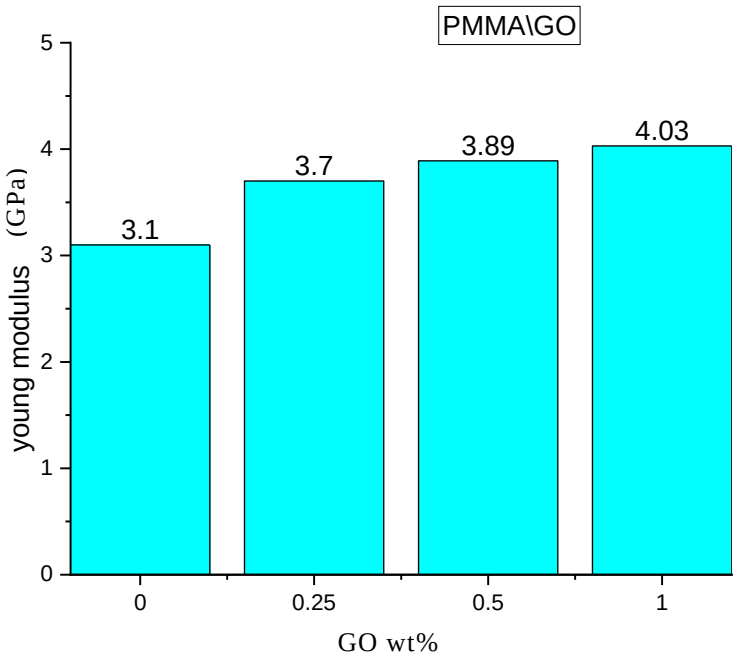

Figure 4.23Youngs Modulus For PMMA\GO

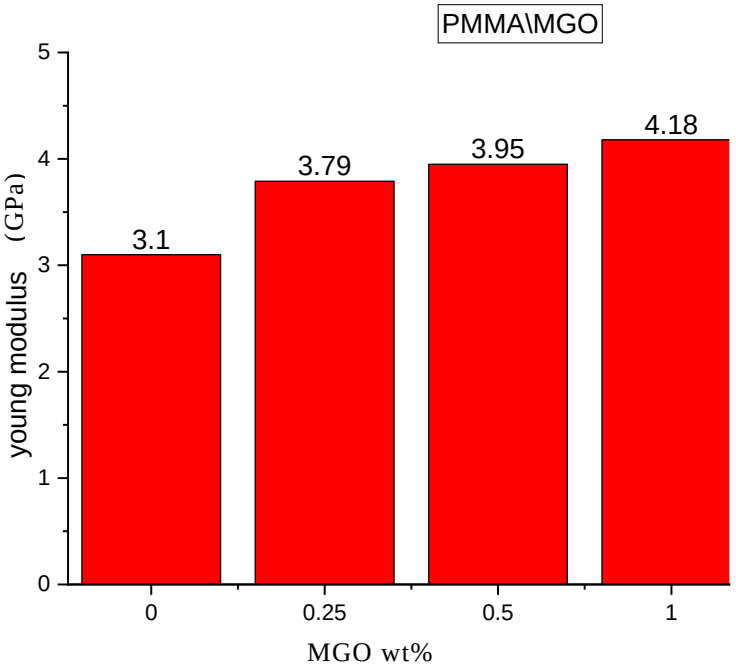

Figure 4.24 Youngs Modulus For PMMA\MGO

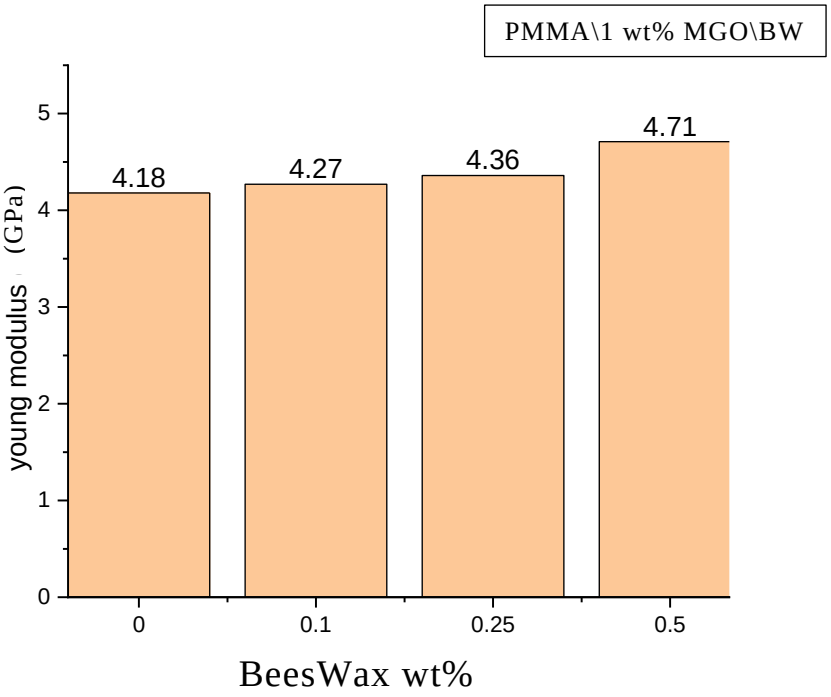

Figure 4.25Youngs Modulus For PMMA\MGO\BW

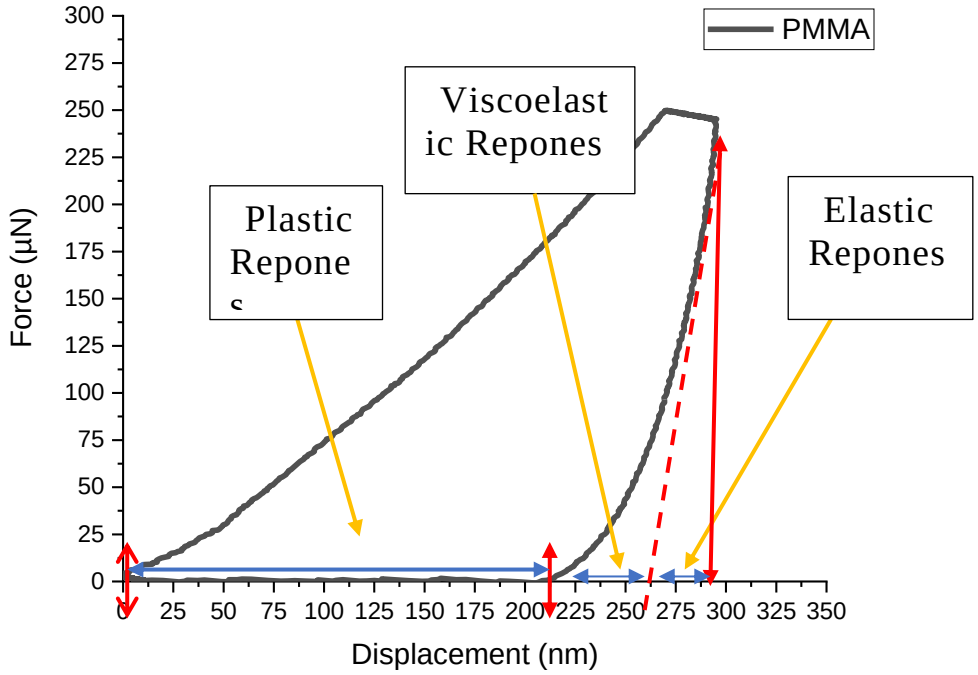

Figure 4.26 Nanoindentation load–displacement curve For PMMA

Figure. 4.29 compares nanoindentation load–displacement curves generated on pure PMMA and PMMA/GO films. viscoelastic contribution and confirm that Oliver–Pharr model may be used to analyze elastic behavior during unloading. Loading and unloading curves showed no discontinuities or steps, suggesting homogenous GO dispersion and no indentation fractures.

Pure PMMA has the lowest indentation force resistance and deepest indentation. The PMMA/GO nanocomposite films' load–displacement curves are all moved to the left, demonstrating that the layered structure increases load resistance. PMMA\1 wt%MGO\BW 0.5 is good for PMMA to increase indent resistance. Figure. 4.31 shows the indentation hardness and elastic modulus for MGO and beeswax increases PMMA elastic modulus and hardness. PMMA\MGO\BW 0.5 wt% elastic modulus and hardness are 28.3% and 90% higher than pure PMMA this agrees with [173].

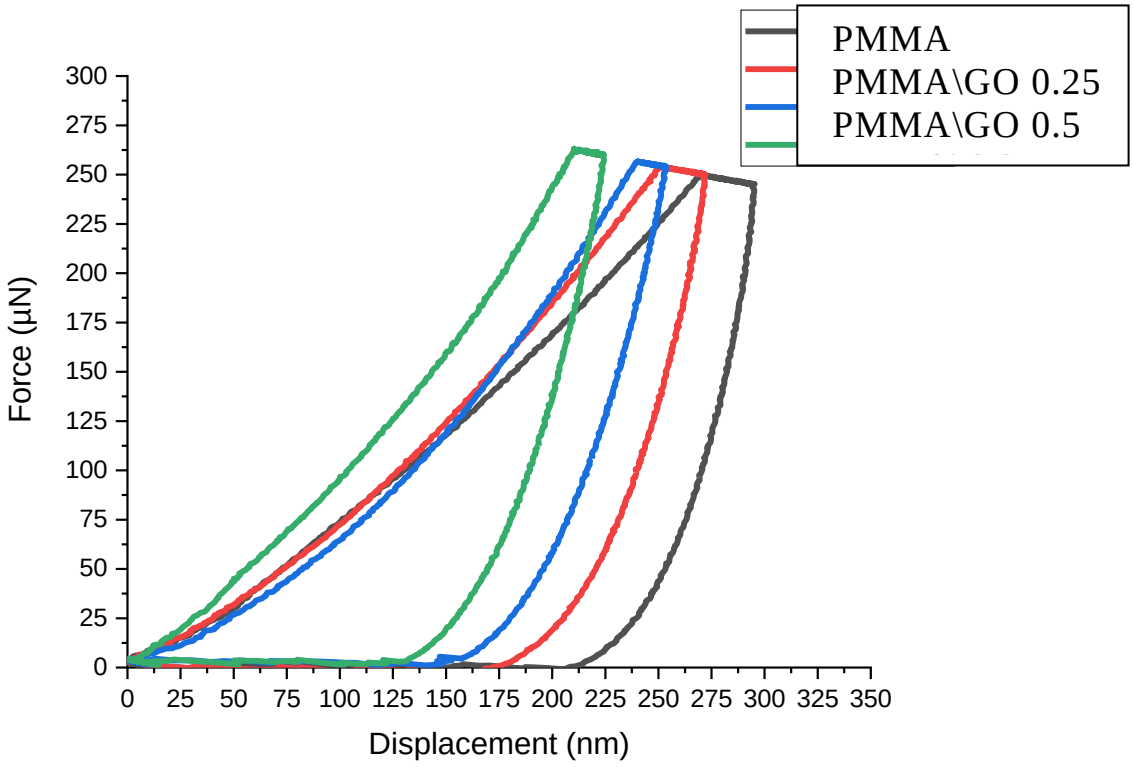

Figure 4.29 Nanoindentation load–displacement curve For PMMA And PMMA\GO

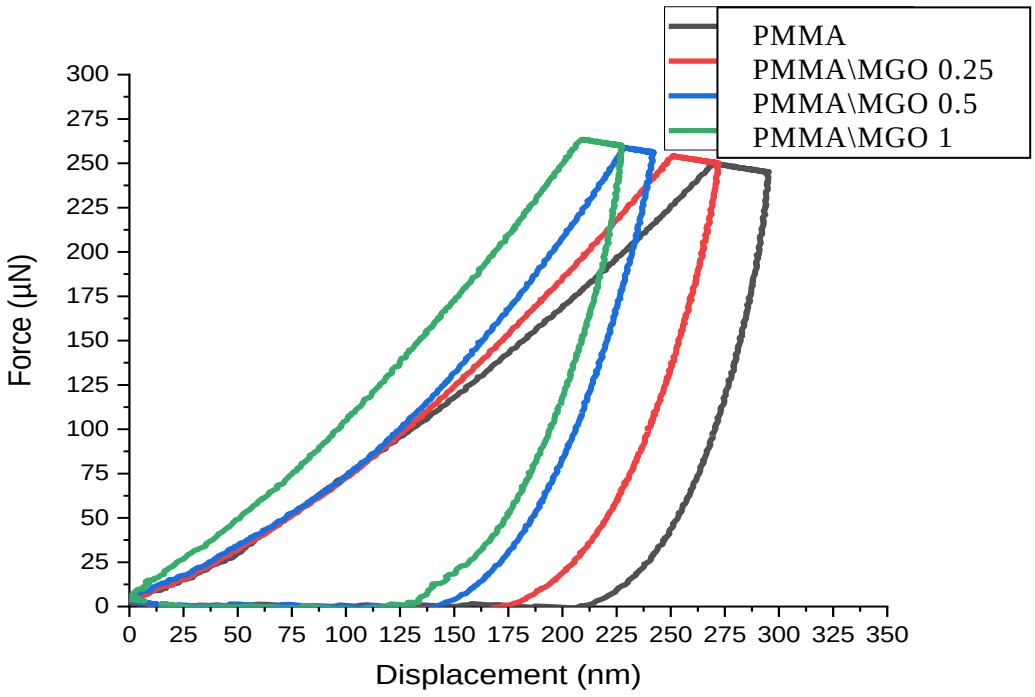

Figure 4.30 Nanoindentation load–displacement curve For PMMA And PMMA\MGO

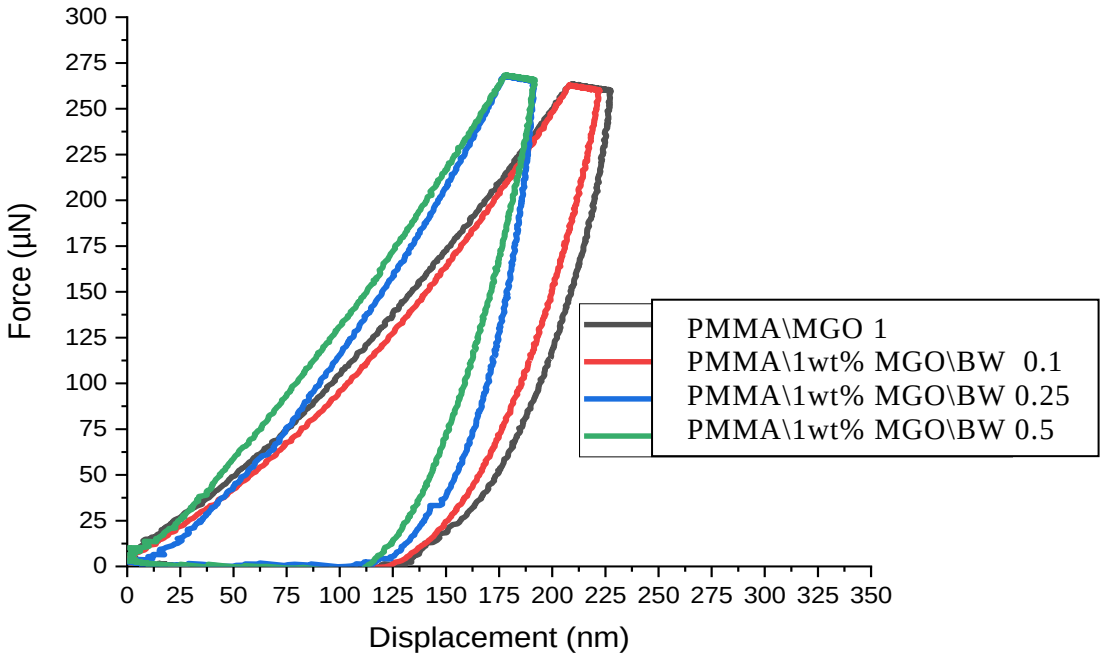

Figure 4.31 Nanoindentation load–displacement curve for PMMA\MGO\BW

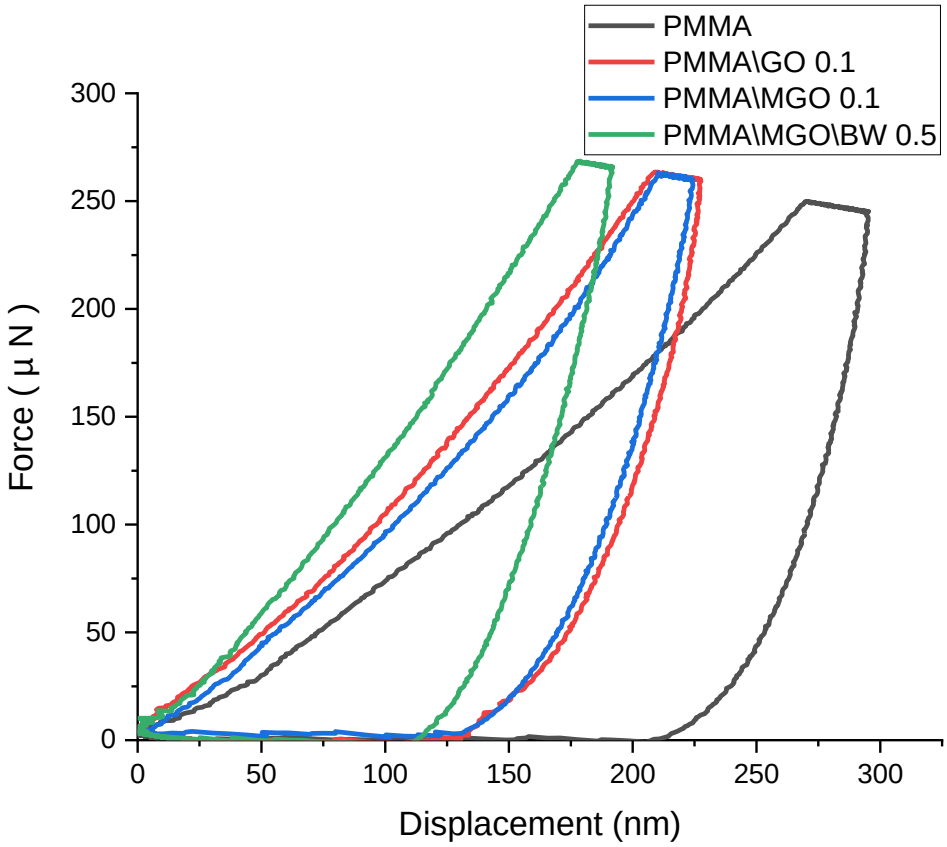

Figure 4.32 Nanoindentation load–displacement curve for samples

Through Table 4.4, Figures 4.29, 4.30, and 4.31 show that the elastic area increases with an increase in the percentage of GO, MGO, and BW as well as for the viscoelastic area, while the plastic area decreases with an increase in the percentage of GO, MGO, and BW. This results in good mechanical properties for the coating in addition to improving its surface properties.

Table 4.4 Plastic, elastic and viscoelastic behavior for PMMA and its composite.

Sample	Elastic ercentage%	Viscoelastic ercentage%	Plastic Percentage%
PMMA	0.178	0.089	0.731
PMMA\GO 0.25	0.238	0.128	0.632
PMMA\GO 0.5	0.248	0.139	0.612
PMMA\GO 1	0.263	0.156	0.581
PMMA\MGO 0.25	0.226	0.131	0.627
PMMA\MGO 0.5	0.251	0.137	0.604
PMMA\MGO 1	0.269	0.159	0.572
PMMA\MGO\BW 0.1	0.274	0.171	0.565
PMMA\MGO\BW 0.25	0.278	0.179	0.553
PMMA\MGO \BW 0.5	0.284	0.187	0.539

Chapter five
Conclusions and Recommendations

5.1 Conclusions

The results of this investigation led to the following conclusion:

1-FTIR results proved, there are just physical interactions but no chemical reactions; interaction, can enhance the desperation and the stability of GO in the nanocomposite.

2-DSC testing, show a rise in T_g with the increasing GO and MGO content. DSC tests are suggestive of the fact that the composite (PMMA/GO, PMMA\MGO, PMMA\MGO\ BW) are good compatible composite and the result showed that there is improvement in T_g with increasing of GO and MGO content.

3-The Hardness shows improvement with the increasing of GO and MGO nanoparticles and BW. PMMA\MGO\BW 0.5 showed increasing in hardness about 110% compere with pure PMMA.

4- Pull off showed adhesive frailer for all sample and shows increasing with addition of GO content but a little decreasing with addition of MGO and BW.

5-Tribological properties include wear and scratch tests. The Wear rate of PMMA was greatly improved with the inclusion of GO and MGO nanoparticles and BW. PMMA\MGO\BW 0.5 showed increase in wear rate by 77% compering with pure PMMA. Friction coefficient showed decreasing by 35% for PMMA\MGO\BW 0.5 compering with pure PMMA. Scratch test shows improvement in scratch hardness with increasing of GO and MGO and with addition of BW PMMA\MGO\BW 0.5 shows increasing by 42% in scratch hardness compering with pure PMMA.

6-UV- VIS Spectroscopy showed that the prepared films have an absorption in the range 300-900 and the highest absorption in the range 300-400, adding GO and MGO increased the absorbance while

the transmittance decreased. PMMA\MGO\BW 0.5 showed decreasing in transparency by 19% compering with pure PMMA.

7- Contact angel showed that there is no much change with addition of GO. because of GO is a hydrophilic. and with addition of MGO the resultant showed a little increasing in contact angel and with addition of BW shows the highest contact angel and change to hydrophobic coating change from 68° for pure PMMA to 94° for PMMA\MGO\BW 0.5.

8- The microstructure analysis (SEM) of the GO, MGO nanoparticles in the PMMA matrix revealed excellent dispersion and little agglomeration due to increasing GO. PMMA\MGO\BW had good coating morphology than other samples.

9- Nano indentation results show that there is increasing in hardness by 120 % for PMMA\MGO\BW 0.5 compere with pure PMMA. and the elastic modules increase by 31% for PMMA\MGO\BW 0.5 compere with pure PMMA. Also, for same sample above the plastic response decreased by 27 %.

5.2 Recommendations

The following suggestions for more research in this area could be helpful:

1- Studying the effects on tribology of the interaction of SiO_2 nanoparticles and other nanoparticles with PMMA.

2- Examining the tribological properties of several high-performance thermoplastic nanomaterials, such as polyether ether ketone (PEEK) and GO.

3- Making blend of two polymers like PET and PMMA

4- Using different coating method, such as spin coating and spry coating.

REFERENCES

References

[1] Goldschmidt, A.; Streitberger, H.-J. *BASF Handbook on Basics of Coating Technology*; William Andrew, 2003.

[2] Ragesh, P.; Ganesh, V. A.; Nair, S. v; Nair, A. S. A Review on 'Self-Cleaning and Multifunctional Materials.' *J Mater Chem A Mater*, **2014**, *2* (36), 14773–14797.

[3] Tai, Z.; Chen, Y.; An, Y.; Yan, X.; Xue, Q. Tribological Behavior of UHMWPE Reinforced with Graphene Oxide Nanosheets. *Tribol Lett*, **2012**, *46* (1), 55–63.

[4] Liston, E. M.; Martinu, L.; Wertheimer, M. R. Plasma Surface Modification of Polymers for Improved Adhesion: A Critical Review. *J Adhes Sci Technol*, **1993**, *7* (10), 1091–1127.

[5] Friedrich, K.; Fakirov, S.; Zhang, Z. *Polymer Composites: From Nano-to Macro-Scale*; Springer Science & Business Media, 2005.

[6] Baker, A.; Mallick, P. K. Composites Engineering Handbook. *Joining and repair of aircraft composite structures. NewYork: Marcel Dekker*, **1997**.

[7] Wang, Q.; Dai, J.; Li, W.; Wei, Z.; Jiang, J. The Effects of CNT Alignment on Electrical Conductivity and Mechanical Properties of SWNT/Epoxy Nanocomposites. *Compos Sci Technol*, **2008**, *68* (7–8), 1644–1648.

[8] Sudeepan, J.; Kumar, K.; Barman, T. K.; Sahoo, P. Study of Tribological Properties of ABS/CaCO3 Polymer Composites Using Taguchi Method. *IOSR Journal of Mechanical and Civil Engineering*, **2014**, *10*, 38–42.

[9] Aldousiri, B.; Shalwan, A.; Chin, C. W. A Review on Tribological Behaviour of Polymeric Composites and Future Reinforcements. *Advances in Materials Science and Engineering*, **2013**, *2013*.

[10] Hemanth, R.; Sekar, M.; Suresha, B. Effects of Fibers and Fillers on Mechanical Properties of Thermoplastic Composites. *Indian Journal of Advances in Chemical Science*, **2014**, *2* (January), 28–35.

[11] Zhang, G.; Chang, L.; Schlarb, A. K. The Roles of Nano-SiO2 Particles on the Tribological Behavior of Short Carbon Fiber Reinforced PEEK. *Compos Sci Technol*, **2009**, *69* (7–8), 1029–1035.

[12] Bonaccorso, F.; Sun, Z.; Hasan, T. A.; Ferrari, A. C. Graphene Photonics and Optoelectronics. *Nat Photonics*, **2010**, *4* (9), 611–622.

References

[13] Barroso-Bujans, F.; Cerveny, S.; Alegría, A.; Colmenero, J. Sorption and Desorption Behavior of Water and Organic Solvents from Graphite Oxide. *Carbon N Y*, **2010**, *48* (11), 3277–3286.

[14] Guo, Y.; Di, C.; Liu, H.; Zheng, J.; Zhang, L.; Yu, G.; Liu, Y. General Route toward Patterning of Graphene Oxide by a Combination of Wettability Modulation and Spin-Coating. *ACS Nano*, **2010**, *4* (10), 5749–5754.

[15] Sun, P.; Zhu, M.; Wang, K.; Zhong, M.; Wei, J.; Wu, D.; Xu, Z.; Zhu, H. Selective Ion Penetration of Graphene Oxide Membranes. *ACS Nano*, **2013**, *7* (1), 428–437.

[16] Lim, W. H.; Yap, Y. K.; Chong, W. Y.; Pua, C. H.; Huang, N. M.; de La Rue, R. M.; Ahmad, H. Graphene Oxide-Based Waveguide Polariser: From Thin Film to Quasi-Bulk. *Opt Express*, **2014**, *22* (9), 11090–11098.

[17] Borini, S.; White, R.; Wei, D.; Astley, M.; Haque, S.; Spigone, E.; Harris, N.; Kivioja, J.; Ryhanen, T. Ultrafast Graphene Oxide Humidity Sensors. *ACS Nano*, **2013**, *7* (12), 11166–11173.

[18] Lyu, M.-Y.; Choi, T. G. Research Trends in Polymer Materials for Use in Lightweight Vehicles. *International journal of precision engineering and manufacturing*, **2015**, *16* (1), 213–220.

[19] Tien, D. H.; Park, J.; Han, S. A.; Ahmad, M.; Seo, Y.; Shin, K. Electrical and Thermal Conductivities of Stycast 1266 Epoxy/Graphite Composites. *Journal of the Korean Physical Society*, **2011**, *59* (4), 2760–2764.

[20] Bartels, T.; Bock, W.; Braun, J.; Busch, C.; Buss, W.; Dresel, W.; Freiler, C.; Harperscheid, M.; Heckler, R.; Hörner, D. Lubricants and Lubrication. *Ullmann's Encyclopedia of Industrial Chemistry*, **2000**.

[21] Har-Even, E.; Brown, A.; Meletis, E. I. Effect of Friction on the Microstructure of Compacted Solid Additive Blends for Polymers. *Wear*, **2015**, *328*, 160–166.

[22] Zuo, Z.; Song, L.; Yang, Y. Tribological Behavior of Polyethersulfone-Reinforced Polytetrafluoroethylene Composite under Dry Sliding Condition. *Tribol Int*, **2015**, *86*, 17–27.

[23] Besnea, M. A. C.; Trufasu, D. C.; Andrei, G.; Bastiurea, M. Estimation of Wear Behavior of Polyphenylene Sulphide Composites Reinforced with Glass/Carbon Fibers, Graphite and Polytetrafluoroethylene, by Pin-on-Disc Test. *Tribology in industry*, **2015**, *37* (1), 88.

References

[24] Delides, C. G. Everyday Life Applications of Polymer Nanocomposites. *Technol. Educ. Inst. West. Maced*, **2016**, No. October, 1–8.

[25] Patil, A.; Lopez, G.; Foxe, M.; Childres, I.; Roecker, C.; Boguski, J.; Jovanovic, I.; Chen, Y. P. Graphene Field Effect Transistors for Detection of Ionizing Radiation. In *IEEE Nuclear Science Symposuim & Medical Imaging Conference*; IEEE, 2010; pp 674–676.

[26] Yoshimura, S.; Ikuse, K.; Tsukazaki, Y.; Kiuchi, M.; Hamaguchi, S. Effect of Ultraviolet Light Irradiation on Etching Process of Poly (Methyl Methacrylate) by Ion Beam Injections. In *Journal of Physics: Conference Series*; IOP Publishing, 2009; Vol. 191, p 012030.

[27] Van, K. D. W. Properties of Polymers. New York: Elsevier 1976.

[28] Gilbert, M. *Brydson's Plastics Materials*; William Andrew, 2016.

[29] Patil, M. T.; Lakshminarasimhan, S. N.; Santhosh, G. Optical and Thermal Studies of Host Poly (Methyl Methacrylate)(PMMA) Based Nanocomposites: A Review. *Mater Today Proc*, **2021**, *46*, 2564–2571.

[30] Lacroix, H. L.; van der Tempel, L. *Thermohygroelastic Properties of Polymethylmethacrylate*; Citeseer, 2007.

[31] Demir, M. M.; Memesa, M.; Castignolles, P.; Wegner, G. PMMA/Zinc Oxide Nanocomposites Prepared by In-situ Bulk Polymerization. *Macromol Rapid Commun*, **2006**, *27* (10), 763–770.

[32] Hashim, H.; Adam, N. I.; Zaki, N. H. M.; Mahmud, Z. S.; Said, C. M. S.; Yahya, M. Z. A.; Ali, A. M. M. Natural Rubber-Grafted with 30% Poly (Methylmethacrylate) Characterization for Application in Lithium Polymer Battery. In *2010 International Conference on Science and Social Research (CSSR 2010)*; IEEE, 2010; pp 485–488.

[33] Dorranian, D.; Abedini, Z.; Hojabri, A.; Ghoranneviss, M. Effects of Oxygen RF Plasma on Properties of Poly Methyl Methacrylate Polymer. *Iranian Physical Journal*, **2008**, *2* (1), 17–21.

[34] Carraher Jr, C. E. *Introduction to Polymer Chemistry*; CRC press, 2017.

[35] Carraher, C. E. *Carraher's Polymer Chemistry*; CRC press, 2017.

[36] Harper, C. A.; Petrie, E. M. *Plastics Materials and Processes: A Concise Encyclopedia*; John Wiley & Sons, 2003.

References

[37] Chang, L.; Woo, E. M. Tacticity Effects on Glass Transition and Phase Behavior in Binary Blends of Poly (Methyl Methacrylate) s of Three Different Configurations. *Polym Chem*, **2010**, *1* (2), 198–202.

[38] Ishitake, K.; Satoh, K.; Kamigaito, M.; Okamoto, Y. From-Syndiotactic-to-Isotactic Stereogradient Methacrylic Polymers by RAFT Copolymerization of Methacrylic Acid and Its Bulky Esters. *Polym Chem*, **2012**, *3* (7), 1750–1757.

[39] Nyangasi, L.; Andala, D.; Onindo, C.; Wanyonyi, A.; Chepngetich, J. Processing Parameters for Electrospinning Poly (Methyl Methacrylate)(PMMA)/Titanium Isopropoxide Composite in a Pump-Free Setup. *Open Research Africa*, **2018**, *1* (27), 27.

[40] Ali, U.; Karim, K. J. B. A.; Buang, N. A. A Review of the Properties and Applications of Poly (Methyl Methacrylate)(PMMA). *Polymer Reviews*, **2015**, *55* (4), 678–705.

[41] Perween, M.; Parmar, D. B.; Bhadu, G. R.; Srivastava, D. N. Polymer–Graphite Composite: A Versatile Use and Throw Plastic Chip Electrode. *Analyst*, **2014**, *139* (22), 5919–5926.

[42] Marcano, D. C.; Kosynkin, D. v; Berlin, J. M.; Sinitskii, A.; Sun, Z.; Slesarev, A.; Alemany, L. B.; Lu, W.; Tour, J. M. Improved Synthesis of Graphene Oxide. *ACS Nano*, **2010**, *4* (8), 4806–4814.

[43] Khan, Z. U.; Kausar, A.; Ullah, H.; Badshah, A.; Khan, W. U. A Review of Graphene Oxide, Graphene Buckypaper, and Polymer/Graphene Composites: Properties and Fabrication Techniques. *Journal of plastic film & sheeting*, **2016**, *32* (4), 336–379.

[44] Cao, Q.; Rogers, J. A. Ultrathin Films of Single-walled Carbon Nanotubes for Electronics and Sensors: A Review of Fundamental and Applied Aspects. *Advanced Materials*, **2009**, *21* (1), 29–53.

[45] Khan, Z. U.; Kausar, A.; Ullah, H.; Badshah, A.; Khan, W. U. A Review of Graphene Oxide, Graphene Buckypaper, and Polymer/Graphene Composites: Properties and Fabrication Techniques. *Journal of plastic film & sheeting*, **2016**, *32* (4), 336–379.

[46] Eda, G.; Chhowalla, M. Chemically Derived Graphene Oxide: Towards Large-area Thin-film Electronics and Optoelectronics. *Advanced materials*, **2010**, *22* (22), 2392–2415.

[47] Brodie, B. C. XIII. On the Atomic Weight of Graphite. *Philos Trans R Soc Lond*, **1859**, No. 149, 249–259.

References

[48] áHummers Jr, W. S. RE ÁOffeman, Preparation of Graphitic Oxide. J. ÁAm. In *Chem. Soc*; 1958; Vol. 80, p 1339.

[49] Shelton, J. C.; Patil, H. R.; Blakely, J. M. Equilibrium Segregation of Carbon to a Nickel (111) Surface: A Surface Phase Transition. *Surf Sci*, **1974**, *43* (2), 493–520.

[50] Becerril, H. A.; Mao, J.; Liu, Z.; Stoltenberg, R. M.; Bao, Z.; Chen, Y. Evaluation of Solution-Processed Reduced Graphene Oxide Films as Transparent Conductors. *ACS Nano*, **2008**, *2* (3), 463–470.

[51] Stankovich, S.; Piner, R. D.; Chen, X.; Wu, N.; Nguyen, S. T.; Ruoff, R. S. Stable Aqueous Dispersions of Graphitic Nanoplatelets via the Reduction of Exfoliated Graphite Oxide in the Presence of Poly (Sodium 4-Styrenesulfonate). *J Mater Chem*, **2006**, *16* (2), 155–158.

[52] Cote, L. J.; Kim, J.; Tung, V. C.; Luo, J.; Kim, F.; Huang, J. Graphene Oxide as Surfactant Sheets. *Pure and Applied Chemistry*, **2010**, *83* (1), 95–110.

[53] Akram, M. W.; Meyer, J. L.; Polycarpou, A. A. Tribological Interactions of Advanced Polymeric Coatings with Polyalkylene Glycol Lubricant and R1234yf Refrigerant. *Tribol Int*, **2016**, *97*, 200–211.

[54] Lee, C. Y.; Bae, J.-H.; Kim, T.-Y.; Chang, S.-H.; Kim, S. Y. Using Silane-Functionalized Graphene Oxides for Enhancing the Interfacial Bonding Strength of Carbon/Epoxy Composites. *Compos Part A Appl Sci Manuf*, **2015**, *75*, 11–17. https://doi.org/https://doi.org/10.1016/j.compositesa.2015.04.013.

[55] Jebur, Sura. K.; Braihi, A. J.; Hassan, A. S. Graphene Effects on the Structural, Morphological and Optical Properties of PEDOT:PSS Thin Films. *Mater Today Proc*, **2022**, *49*, 2733–2740. https://doi.org/https://doi.org/10.1016/j.matpr.2021.09.255.

[56] Corcione, C. E.; De Simone, N.; Santarelli, M. L.; Frigione, M. Protective Properties and Durability Characteristics of Experimental and Commercial Organic Coatings for the Preservation of Porous Stone. *Prog Org Coat*, **2017**, *103*, 193–203.

[57] Poh, T. Y.; Ali, N.; mac Aogáin, M.; Kathawala, M. H.; Setyawati, M. I.; Ng, K. W.; Chotirmall, S. H. Inhaled Nanomaterials and the Respiratory Microbiome: Clinical, Immunological and Toxicological Perspectives. *Part Fibre Toxicol*, **2018**, *15* (1), 1–16.

References

[58] Komarneni, S. Nanocomposites. *J Mater Chem*, **1992**, *2* (12), 1219–1230.

[59] Delides, C. G. Everyday Life Applications of Polymer Nanocomposites. *Technol. Educ. Inst. West. Maced*, **2016**, No. October, 1–8.

[60] Omanović-Mikličanin, E.; Badnjević, A.; Kazlagić, A.; Hajlovac, M. Nanocomposites: A Brief Review. *Health Technol (Berl)*, **2020**, *10* (1), 51–59.

[61] Shameli, K.; Ahmad, M. bin; Jazayeri, S. D.; Sedaghat, S.; Shabanzadeh, P.; Jahangirian, H.; Mahdavi, M.; Abdollahi, Y. Synthesis and Characterization of Polyethylene Glycol Mediated Silver Nanoparticles by the Green Method. *Int J Mol Sci*, **2012**, *13* (6), 6639–6650.

[62] Han, J. T.; Cho, K. Nanoparticle-Induced Enhancement in Fracture Toughness of Highly Loaded Epoxy Composites over a Wide Temperature Range. *J Mater Sci*, **2006**, *41* (13), 4239–4245.

[63] Wu, C. L.; Zhang, M. Q.; Rong, M. Z.; Friedrich, K. Tensile Performance Improvement of Low Nanoparticles Filled-Polypropylene Composites. *Compos Sci Technol*, **2002**, *62* (10–11), 1327–1340.

[64] Jordan, J.; Jacob, K. I.; Tannenbaum, R.; Sharaf, M. A.; Jasiuk, I. Experimental Trends in Polymer Nanocomposites—a Review. *Materials science and engineering: A*, **2005**, *393* (1–2), 1–11.

[65] Wu, Y.-P.; Jia, Q.-X.; Yu, D.-S.; Zhang, L.-Q. Modeling Young's Modulus of Rubber–Clay Nanocomposites Using Composite Theories. *Polym Test*, **2004**, *23* (8), 903–909.

[66] Collins, M. N.; Nechifor, M.; Tanasă, F.; Zănoagă, M.; McLoughlin, A.; Stróżyk, M. A.; Culebras, M.; Teacă, C.-A. Valorization of Lignin in Polymer and Composite Systems for Advanced Engineering Applications–a Review. *Int J Biol Macromol*, **2019**, *131*, 828–849.

[67] Verdejo, R.; Bernal, M. M.; Romasanta, L. J.; Lopez-Manchado, M. A. Graphene Filled Polymer Nanocomposites. *J Mater Chem*, **2011**, *21* (10), 3301–3310.

[68] Terrones, M.; Martín, O.; González, M.; Pozuelo, J.; Serrano, B.; Cabanelas, J. C.; Vega-Díaz, S. M.; Baselga, J. Interphases in Graphene Polymer-based Nanocomposites: Achievements and Challenges. *Advanced Materials*, **2011**, *23* (44), 5302–5310.

[69] Kuilla, T.; Bhadra, S.; Yao, D.; Kim, N. H.; Bose, S.; Lee, J. H. Recent Advances in Graphene Based Polymer Composites. *Prog Polym Sci*, **2010**, *35* (11), 1350–1375.

References

[70] An, X.; Simmons, T.; Shah, R.; Wolfe, C.; Lewis, K. M.; Washington, M.; Nayak, S. K.; Talapatra, S.; Kar, S. Stable Aqueous Dispersions of Noncovalently Functionalized Graphene from Graphite and Their Multifunctional High-Performance Applications. *Nano Lett*, **2010**, *10* (11), 4295–4301.

[71] Du, J.; Cheng, H. The Fabrication, Properties, and Uses of Graphene/Polymer Composites. *Macromol Chem Phys*, **2012**, *213* (10-11), 1060–1077.

[72] Kuilla, T.; Bhadra, S.; Yao, D.; Kim, N. H.; Bose, S.; Lee, J. H. Recent Advances in Graphene Based Polymer Composites. *Prog Polym Sci*, **2010**, *35* (11), 1350–1375.

[73] Zhang, H.-B.; Zheng, W.-G.; Yan, Q.; Jiang, Z.-G.; Yu, Z.-Z. The Effect of Surface Chemistry of Graphene on Rheological and Electrical Properties of Polymethylmethacrylate Composites. *Carbon N Y*, **2012**, *50* (14), 5117–5125.

[74] Taher, A. A.; Oraibi, A. H.; Abd Ali, F. A. M.; Jaber, H. J. Mechanical Properties of Graphene Oxide/Polyvinyl Chloride Composite Film.

[75] Gonçalves, G.; Marques, P. A. A. P.; Barros-Timmons, A.; Bdkin, I.; Singh, M. K.; Emami, N.; Grácio, J. Graphene Oxide Modified with PMMA via ATRP as a Reinforcement Filler. *J Mater Chem*, **2010**, *20* (44), 9927–9934.

[76] Pei, S.; Cheng, H.-M. The Reduction of Graphene Oxide. *Carbon N Y*, **2012**, *50* (9), 3210–3228.

[77] Singh, V.; Joung, D.; Zhai, L.; Das, S.; Khondaker, S. I.; Seal, S. Graphene Based Materials: Past, Present and Future. *Prog Mater Sci*, **2011**, *56* (8), 1178–1271.

[78] An, X.; Simmons, T.; Shah, R.; Wolfe, C.; Lewis, K. M.; Washington, M.; Nayak, S. K.; Talapatra, S.; Kar, S. Stable Aqueous Dispersions of Noncovalently Functionalized Graphene from Graphite and Their Multifunctional High-Performance Applications. *Nano Lett*, **2010**, *10* (11), 4295–4301.

[79] Kim, H.; Miura, Y.; Macosko, C. W. Graphene/Polyurethane Nanocomposites for Improved Gas Barrier and Electrical Conductivity. *Chemistry of materials*, **2010**, *22* (11), 3441–3450.

[80] Bao, C.; Song, L.; Xing, W.; Yuan, B.; Wilkie, C. A.; Huang, J.; Guo, Y.; Hu, Y. Preparation of Graphene by Pressurized Oxidation and Multiplex Reduction and Its Polymer Nanocomposites by Masterbatch-Based Melt Blending. *J Mater Chem*, **2012**, *22* (13), 6088–6096.

References

[81] Potts, J. R.; Lee, S. H.; Alam, T. M.; An, J.; Stoller, M. D.; Piner, R. D.; Ruoff, R. S. Thermomechanical Properties of Chemically Modified Graphene/Poly (Methyl Methacrylate) Composites Made by in Situ Polymerization. *Carbon N Y*, **2011**, *49* (8), 2615–2623.

[82] An, X.; Simmons, T.; Shah, R.; Wolfe, C.; Lewis, K. M.; Washington, M.; Nayak, S. K.; Talapatra, S.; Kar, S. Stable Aqueous Dispersions of Noncovalently Functionalized Graphene from Graphite and Their Multifunctional High-Performance Applications. *Nano Lett*, **2010**, *10* (11), 4295–4301.

[83] Zaman, I.; Kuan, H.; Meng, Q.; Michelmore, A.; Kawashima, N.; Pitt, T.; Zhang, L.; Gouda, S.; Luong, L.; Ma, J. A Facile Approach to Chemically Modified Graphene and Its Polymer Nanocomposites. *Adv Funct Mater*, **2012**, *22* (13), 2735–2743.

[84] Pitkethly, M. J. Nanomaterials–the Driving Force. *Materials today*, **2004**, *7* (12), 20–29.

[85] Kubacka, A.; Serrano, C.; Ferrer, M.; Lünsdorf, H.; Bielecki, P.; Cerrada, M. L.; Fernández-García, M.; Fernández-García, M. High-Performance Dual-Action Polymer− TiO2 Nanocomposite Films via Melting Processing. *Nano Lett*, **2007**, *7* (8), 2529–2534.

[86] Szabó, T.; Berkesi, O.; Forgó, P.; Josepovits, K.; Sanakis, Y.; Petridis, D.; Dékány, I. Evolution of Surface Functional Groups in a Series of Progressively Oxidized Graphite Oxides. *Chemistry of materials*, **2006**, *18* (11), 2740–2749.

[87] Suk, J. W.; Piner, R. D.; An, J.; Ruoff, R. S. Mechanical Properties of Monolayer Graphene Oxide. *ACS Nano*, **2010**, *4* (11), 6557–6564.

[88] Dai, J.-F.; Wang, G.-J.; Ma, L.; Wu, C.-K. Surface Properties of Graphene: Relationship to Graphene-Polymer Composites. *Rev. Adv. Mater. Sci*, **2015**, *40* (1), 60–71.

[89] Gómez-Navarro, C.; Burghard, M.; Kern, K. Elastic Properties of Chemically Derived Single Graphene Sheets. *Nano Lett*, **2008**, *8* (7), 2045–2049.

[90] Wang, J.; Wang, X.; Xu, C.; Zhang, M.; Shang, X. Preparation of Graphene/Poly (Vinyl Alcohol) Nanocomposites with Enhanced Mechanical Properties and Water Resistance. *Polym Int*, **2011**, *60* (5), 816–822.

[91] Kuila, T.; Bose, S.; Hong, C. E.; Uddin, M. E.; Khanra, P.; Kim, N. H.; Lee, J. H. Preparation of Functionalized Graphene/Linear Low Density Polyethylene Composites by a Solution Mixing Method. *Carbon N Y*, **2011**, *49* (3), 1033–1037.

[92] Jia, C.; Chen, P.; Liu, W.; Li, B.; Wang, Q. Surface Treatment of Aramid Fiber by Air Dielectric Barrier Discharge Plasma at Atmospheric Pressure. *Appl Surf Sci*, **2011**, *257* (9), 4165–4170.
[93] Hussain, S.; Yorucu, C.; Ahmed, I.; Hussain, R.; Chen, B.; Khan, M. B.; Siddique, N. A.; Rehman, I. U. Surface Modification of Aramid Fibres by Graphene Oxide Nano-Sheets for Multiscale Polymer Composites. *Surf Coat Technol*, **2014**, *258*, 458–466.
[94] Szabó, T.; Berkesi, O.; Forgó, P.; Josepovits, K.; Sanakis, Y.; Petridis, D.; Dékány, I. Evolution of Surface Functional Groups in a Series of Progressively Oxidized Graphite Oxides. *Chemistry of materials*, **2006**, *18* (11), 2740–2749.
[95] Bourlinos, A. B.; Gournis, D.; Petridis, D.; Szabó, T.; Szeri, A.; Dékány, I. Graphite Oxide: Chemical Reduction to Graphite and Surface Modification with Primary Aliphatic Amines and Amino Acids. *Langmuir*, **2003**, *19* (15), 6050–6055.
[96] Stankovich, S.; Dikin, D. A.; Piner, R. D.; Kohlhaas, K. A.; Kleinhammes, A.; Jia, Y.; Wu, Y.; Nguyen, S. T.; Ruoff, R. S. Synthesis of Graphene-Based Nanosheets via Chemical Reduction of Exfoliated Graphite Oxide. *Carbon N Y*, **2007**, *45* (7), 1558–1565.
[97] Dreyer, D. R.; Park, S.; Bielawski, C. W.; Ruoff, R. S. The Chemistry of Graphene Oxide. *Chem Soc Rev*, **2010**, *39* (1), 228–240.
[98] Botas, C.; Pérez-Mas, A. M.; Álvarez, P.; Santamaría, R.; Granda, M.; Blanco, C.; Menéndez, R. Optimization of the Size and Yield of Graphene Oxide Sheets in the Exfoliation Step. *Carbon N Y*, **2013**, *63*, 576–578.
[99] Weinberg, N. L.; Reddy, T. B. Electrochemical Oxidation of the Surface of Graphite Fibres. *J Appl Electrochem*, **1973**, *3* (1), 73–75.
[100] Colmenares, J. C.; Luque, R.; Campelo, J. M.; Colmenares, F.; Karpiński, Z.; Romero, A. A. Nanostructured Photocatalysts and Their Applications in the Photocatalytic Transformation of Lignocellulosic Biomass: An Overview. *Materials*, **2009**, *2* (4), 2228–2258.
[101] Kim, F.; Cote, L. J.; Huang, J. Graphene Oxide: Surface Activity and Two-dimensional Assembly. *Advanced Materials*, **2010**, *22* (17), 1954–1958.
[102] Adeel, M.; Bilal, M.; Rasheed, T.; Sharma, A.; Iqbal, H. M. N. Graphene and Graphene Oxide: Functionalization and Nano-Bio-Catalytic System for Enzyme Immobilization and

Biotechnological Perspective. *Int J Biol Macromol*, **2018**, *120*, 1430–1440.

[103] Bourlinos, A. B.; Gournis, D.; Petridis, D.; Szabó, T.; Szeri, A.; Dékány, I. Graphite Oxide: Chemical Reduction to Graphite and Surface Modification with Primary Aliphatic Amines and Amino Acids. *Langmuir*, **2003**, *19* (15), 6050–6055.

[104] Compton, O. C.; Nguyen, S. T. Graphene Oxide, Highly Reduced Graphene Oxide, and Graphene: Versatile Building Blocks for Carbon-based Materials. *small*, **2010**, *6* (6), 711–723.

[105] Mattevi, C.; Eda, G.; Agnoli, S.; Miller, S.; Mkhoyan, K. A.; Celik, O.; Mastrogiovanni, D.; Granozzi, G.; Garfunkel, E.; Chhowalla, M. Evolution of Electrical, Chemical, and Structural Properties of Transparent and Conducting Chemically Derived Graphene Thin Films. *Adv Funct Mater*, **2009**, *19* (16), 2577–2583.

[106] Gokhale, A. A.; Lu, J.; Lee, I. Immobilization of Cellulase on Magnetoresponsive Graphene Nano-Supports. *J Mol Catal B Enzym*, **2013**, *90*, 76–86.

[107] Niyogi, S.; Bekyarova, E.; Itkis, M. E.; McWilliams, J. L.; Hamon, M. A.; Haddon, R. C. Solution Properties of Graphite and Graphene. *J Am Chem Soc*, **2006**, *128* (24), 7720–7721.

[108] Ikhe, A. B.; Kale, A. B.; Jeong, J.; Reece, M. J.; Choi, S.-H.; Pyo, M. Perfluorinated Polysiloxane Hybridized with Graphene Oxide for Corrosion Inhibition of AZ31 Magnesium Alloy. *Corros Sci*, **2016**, *109*, 238–245.

[109] Li, J.; Cui, J.; Yang, J.; Ma, Y.; Qiu, H.; Yang, J. Silanized Graphene Oxide Reinforced Organofunctional Silane Composite Coatings for Corrosion Protection. *Prog Org Coat*, **2016**, *99*, 443–451.

[110] Liu, J.; Yu, Q.; Yu, M.; Li, S.; Zhao, K.; Xue, B.; Zu, H. Silane Modification of Titanium Dioxide-Decorated Graphene Oxide Nanocomposite for Enhancing Anticorrosion Performance of Epoxy Coatings on AA-2024. *J Alloys Compd*, **2018**, *744*, 728–739.

[111] Fotovvati, B.; Namdari, N.; Dehghanghadikolaei, A. On Coating Techniques for Surface Protection: A Review. *Journal of Manufacturing and Materials processing*, **2019**, *3* (1), 28.

[112] Krebs, F. C. Fabrication and Processing of Polymer Solar Cells: A Review of Printing and Coating Techniques. *Solar energy materials and solar cells*, **2009**, *93* (4), 394–412.

References

[113] Siemann, U. Solvent Cast Technology–a Versatile Tool for Thin Film Production. In *Scattering methods and the properties of polymer materials*; Springer, 2005; pp 1–14.

[114] Yilbas, B.; Al-Sharafi, A.; Ali, H. *Self-Cleaning of Surfaces and Water Droplet Mobility*; Elsevier, 2019.

[115] Brinker, C. J.; Scherer, G. W. *Sol-Gel Science: The Physics and Chemistry of Sol-Gel Processing*; Academic press, 2013.

[116] Sahu, N.; Parija, B.; Panigrahi, S. Fundamental Understanding and Modeling of Spin Coating Process: A Review. *Indian Journal of Physics*, **2009**, *83* (4), 493–502.

[117] Steele, A.; Bayer, I.; Loth, E. Inherently Superoleophobic Nanocomposite Coatings by Spray Atomization. *Nano Lett*, **2009**, *9* (1), 501–505.

[118] Mohammadnezhad, G.; Dinari, M.; Soltani, R. The Preparation of Modified Boehmite/PMMA Nanocomposites by in Situ Polymerization and the Assessment of Their Capability for Cu 2+ Ion Removal. *New Journal of Chemistry*, **2016**, *40* (4), 3612–3621.

[119] Pujari, S. P.; Scheres, L.; Marcelis, A. T. M.; Zuilhof, H. Covalent Surface Modification of Oxide Surfaces. *Angewandte Chemie International Edition*, **2014**, *53* (25), 6322–6356.

[120] Pauthe, M.; Phalippou, J.; Corriu, R.; Leclercq, D.; Vioux, A. Silica Xerogels Containing a Functional Group at Silicon. *J Non Cryst Solids*, **1989**, *113* (1), 21–30.

[121] Palimi, M. J.; Rostami, M.; Mahdavian, M.; Ramezanzadeh, B. Surface Modification of Fe2O3 Nanoparticles with 3-Aminopropyltrimethoxysilane (APTMS): An Attempt to Investigate Surface Treatment on Surface Chemistry and Mechanical Properties of Polyurethane/Fe2O3 Nanocomposites. *Appl Surf Sci*, **2014**, *320*, 60–72.

[122] Chen, Y.; Zhou, S.; Chen, G.; Wu, L. Preparation and Characterization of Polyester/Silica Nanocomposite Resins. *Prog Org Coat*, **2005**, *54* (2), 120–126.

[123] Wells, F. B. Hive Product Uses--Beeswax, 5. *American Bee Journal (USA)*, **1977**.

[124] Tulloch, A. P. Beeswax—Composition and Analysis. *Bee world*, **1980**, *61* (2), 47–62.

[125] Sabat, G.; Gouda, N.; Mahapatra, P. M.; Mahakhud, R.; Panda, A. K. Co-Pyrolysis of Beeswax with Different Consumer Plastics for Synergetic Production of Sustainable Fuel Oil. *Sustainable Energy Technologies and Assessments*, **2022**, *53*, 102493.

References

[126] Morgan, J.; Townley, S.; Kemble, G.; Smith, R.; . Measurement of Physical and Mechanical Properties of Beeswax. *Materials science and technology*, **2002**, *18* (4), 463–467.

[127] Gerdeen, J. C.; Rorrer, R. A. L. *Engineering Design with Polymers and Composites*; CRC Press, 2011; Vol. 30.

[128] Menezes, P. L.; Nosonovsky, M.; Ingole, S. P.; Kailas, S. V.; Lovell, M. R. *Tribology for Scientists and Engineers*; Springer, 2013.

[129] Bobzin, K.; Bartels, T.; Mang, T. *Industrial Tribology: Tribosystems, Friction, Wear and Surface Engineering, Lubrication*; John Wiley & Sons, 2011.

[130] Abdelbary, A.; Nasr, M. N. A. Fatigue Wear of Polyamides with Surface Defects under Different Loading Conditions. *Advances in materials Research*, **2016**, *5* (3), 193.

[131] Sawyer, W. G.; Argibay, N.; Burris, D. L.; Krick, B. A. Mechanistic Studies in Friction and Wear of Bulk Materials. *Annu. Rev. Mater. Res*, **2014**, *44* (1), 395–427.

[132] Abdelbary, A. *Wear of Polymers and Composites*; Woodhead Publishing, 2015.

[133] Friedrich, K.; Schlarb, A. K. *Tribology of Polymeric Nanocomposites: Friction and Wear of Bulk Materials and Coatings*; Elsevier, 2011.

[134] Fischer, A.; Bobzin, K. *Friction, Wear and Wear Protection*; John Wiley & Sons, 2009; Vol. 10.

[135] Blau, P. J. *Friction Science and Technology: From Concepts to Applications*; CRC press, 2008.

[136] Varenberg, M. Towards a Unified Classification of Wear. Friction, 1 (4), 330 340. 2013.

[137] Rebai, H. Tribology and Machine Elements. **2014**.

[138] Adebisi, A. A.; Maleque, M. A. Modelling Aspect of Corrosive Wear under Biodiesel. In *Proceedings of Regional Tribology Conference 2011: RTC2011*; Malaysian Tribology Society, 2011; p 162.

[139] Bahadur, S.; Schwartz, C. The Effect of Nanoparticle Fillers on Transfer Film Formation and the Tribological Behavior of Polymers Tribology of Polymeric Nanocomposites. *Friction and Wear of Bulk Materials and Coatings:*, **2013**, 23–48.

[140] Grellmann, W.; Seidler, S. *Polymer Testing*; Carl Hanser Verlag GmbH Co KG, 2022.

[141] Chau, J. L. H.; Hsieh, C.-C.; Lin, Y.-M.; Li, A.-K. Preparation of Transparent Silica–PMMA Nanocomposite Hard Coatings. *Prog Org Coat*, **2008**, *62* (4), 436–439.

[142] Jeon, S. J.; Lee, J. J.; Kim, W.; Chang, T. S.; Koo, S. M. Hard Coating Films Based on Organosilane-Modified Boehmite Nanoparticles under UV/Thermal Dual Curing. *Thin Solid Films*, **2008**, *516* (12), 3904–3909.

[143] Gonçalves, G.; Marques, P. A. A. P.; Barros-Timmons, A.; Bdkin, I.; Singh, M. K.; Emami, N.; Grácio, J. Graphene Oxide Modified with PMMA via ATRP as a Reinforcement Filler. *J Mater Chem*, **2010**, *20* (44), 9927–9934.

[144] Kim, J.; Im, H.; Cho, M. H. Tribological Performance of Fluorinated Polyimide-Based Nanocomposite Coatings Reinforced with PMMA-Grafted-MWCNT. *Wear*, **2011**, *271* (7–8), 1029–1038.

[145] Gonçalves, G.; Cruz, S. M. A.; Ramalho, A.; Grácio, J.; Marques, P. A. A. P. Graphene Oxide versus Functionalized Carbon Nanotubes as a Reinforcing Agent in a PMMA/HA Bone Cement. *Nanoscale*, **2012**, *4* (9), 2937–2945.

[146] Yang, X.; Wang, X.; Yang, J.; Li, J.; Wan, L. Functionalization of Graphene Using Trimethoxysilanes and Its Reinforcement on Polypropylene Nanocomposites. *Chem Phys Lett*, **2013**, *570*, 125–131.

[147] Stojanović, D. B.; Brajović, L.; Orlović, A.; Dramlić, D.; Radmilović, V.; Uskoković, P. S.; Aleksić, R. Transparent PMMA/Silica Nanocomposites Containing Silica Nanoparticles Coating under Supercritical Conditions. *Prog Org Coat*, **2013**, *76* (4), 626–631.

[148] Hu, K.; Kulkarni, D. D.; Choi, I.; Tsukruk, V. v. Graphene-Polymer Nanocomposites for Structural and Functional Applications. *Prog Polym Sci*, **2014**, *39* (11), 1934–1972.

[149] Hu, J.; Jia, X.; Li, C.; Ma, Z.; Zhang, G.; Sheng, W.; Zhang, X.; Wei, Z. Effect of Interfacial Interaction between Graphene Oxide Derivatives and Poly (Vinyl Chloride) upon the Mechanical Properties of Their Nanocomposites. *J Mater Sci*, **2014**, *49* (7), 2943–2951.

[150] Harb, S. v; dos Santos, F. C.; Pulcinelli, S. H.; Santilli, C. v; Knowles, K.; Hammer, P. Protective Coatings Based on PMMA–Silica Nanocomposites Reinforced with Carbon Nanotubes. *Carbon nanotubes–current progress of their polymer composites. 1st ed. Rijeka, Croatia: Intech*, **2016**, 195–225.

[151] Al-Kawaz, A.; Rubin, A.; Badi, N.; Blanck, C.; Jacomine, L.; Janowska, I.; Pham-Huu, C.; Gauthier, C. Tribological and Mechanical Investigation of Acrylic-Based Nanocomposite

Coatings Reinforced with PMMA-Grafted-MWCNT. *Mater Chem Phys*, **2016**, *175*, 206–214.

[152] Hu, H.; Zhao, S.; Sun, G.; Zhong, Y.; You, B. Evaluation of Scratch Resistance of Functionalized Graphene Oxide/Polysiloxane Nanocomposite Coatings. *Prog Org Coat*, **2018**, *117*, 118–129.

[153] Nazri, S. R. B.; Liu, W.-W.; Khe, C.-S.; Hidayah, N. M. S.; Teoh, Y.-P.; Voon, C. H.; Lee, H. C.; Adelyn, P. Y. P. Synthesis, Characterization and Study of Graphene Oxide. In *AIP Conference Proceedings*; AIP Publishing LLC, 2018; Vol. 2045, p 020033.

[154] Loste, J.; Lopez-Cuesta, J.-M.; Billon, L.; Garay, H.; Save, M. Transparent Polymer Nanocomposites: An Overview on Their Synthesis and Advanced Properties. *Prog Polym Sci*, **2019**, *89*, 133–158.

[155] Boussehel, H. Influence of 3-(Trimethoxysilyl) Propyl Methacrylate Coupling Agent Treatment of Olive Pomace Flour Reinforced Polystyrene Composites. *Revue des Composites et des Matériaux Avancés*, **2019**, *29* (6).

[156] Shah, S.; Shaikh, H.; Hafeez, S.; Malik, M. I. Synthesis of 3-(Trimethoxysilyl) Propyl Methacrylate Functionalized Graphene Oxide Based Mixed Matrix Membrane and Its Application for O2/N2 Separation. *Pakistan Journal of Analytical & Environmental Chemistry*, **2020**, *21* (1), 44–53.

[157] Chathuranga, H.; Wasalathilake, K. C.; Marriam, I.; MacLeod, J.; Zhang, Z.; Bai, R.; Lei, Z.; Li, Y.; Liu, Y.; Yang, H. Preparation of Bioinspired Graphene Oxide/PMMA Nanocomposite with Improved Mechanical Properties. *Compos Sci Technol*, **2021**, *216*, 109046.

[158] Matinlinna, J. P.; Özcan, M.; Lassila, L. V. J.; Vallittu, P. K. The Effect of a 3-Methacryloxypropyltrimethoxysilane and Vinyltriisopropoxysilane Blend and Tris (3-Trimethoxysilylpropyl) Isocyanurate on the Shear Bond Strength of Composite Resin to Titanium Metal. *Dental Materials*, **2004**, *20* (9), 804–813.

[159] Chen, W.; Yan, L.; Bangal, P. R. Chemical Reduction of Graphene Oxide to Graphene by Sulfur-Containing Compounds. *The Journal of Physical Chemistry C*, **2010**, *114* (47), 19885–19890.

[160] Ramesh, S.; Leen, K. H.; Kumutha, K.; Arof, A. K. FTIR Studies of PVC/PMMA Blend Based Polymer Electrolytes. *Spectrochim Acta A Mol Biomol Spectrosc*, **2007**, *66* (4–5), 1237–1242.

References

[161] Lee, C. Y.; Bae, J.-H.; Kim, T.-Y.; Chang, S.-H.; Kim, S. Y. Using Silane-Functionalized Graphene Oxides for Enhancing the Interfacial Bonding Strength of Carbon/Epoxy Composites. *Compos Part A Appl Sci Manuf*, **2015**, *75*, 11–17.

[162] Rajitha, K.; Mohana, K. N. S.; Nayak, S. R.; Hegde, M. B.; Madhusudhana, A. M. An Efficient and Eco-Friendly Anti-Corrosive System Based on Beeswax-Graphene Oxide Nanocomposites on Mild Steel in Saline Medium. *Surfaces and Interfaces*, **2020**, *18*, 100393.

[163] Li, Y.; Guo, H. Crosslinked Poly (Methyl Methacrylate) with Perfluorocyclobutyl Aryl Ether Moiety as Crosslinking Unit: Thermally Stable Polymer with High Glass Transition Temperature. *RSC Adv*, **2020**, *10* (4), 1981–1988.

[164] Harper, C. A.; Petrie, E. M. *Plastics Materials and Processes: A Concise Encyclopedia*; John Wiley & Sons, 2003.

[165] Sura Kamel Jebur Zamel, B.; Jabbar Braihi Assist Ali Salah Hassan, A. *Comparing Study for PEDOT:PSS/Graphene and PEDOT:PSS/Graphene with Isopropyl Alcohol Nanocomposite Thin Films by Spin Coating Technique Supervised By*.

[166] Geng, Y.; Li, S.; Hou, D.; Zhang, W.; Jin, Z.; Li, Q.; Luo, J. Fabrication of Superhydrophobicity on Foamed Concrete Surface by GO/Silane Coating. *Mater Lett*, **2020**, *265*, 127423.

[167] Buchwald, R.; Breed, M. D.; Greenberg, A. R. The Thermal Properties of Beeswaxes: Unexpected Findings. *Journal of Experimental Biology*, **2008**, *211* (1), 121–127.

[168] Shin, K.-Y.; Hong, J.-Y.; Lee, S.; Jang, J. Evaluation of Anti-Scratch Properties of Graphene Oxide/Polypropylene Nanocomposites. *J Mater Chem*, **2012**, *22* (16), 7871–7879.

[169] Zhang, S. L.; Tsou, A. H.; Li, J. C. M. Scratching Behavior of Elastomeric Poly (Dimethylsiloxane) Coatings. *J Polym Sci B Polym Phys*, **2002**, *40* (14), 1530–1537.

[170] Prandato, E.; Livi, S.; Melas, M.; Auclair, J.; Verney, V.; Fleury, E.; Méchin, F. Effect of Bio-based Monomers on the Scratch Resistance of Acrylate Photopolymerizable Coatings. *J Polym Sci B Polym Phys*, **2015**, *53* (5), 379–388.

[171] Kamel, S.; Braihi, A.; Hassan, A. Graphene Effects on the Structural, Morphological and Optical Properties of PEDOT:PSS Thin Films. *Mater Today Proc*, **2021**, *49*. https://doi.org/10.1016/j.matpr.2021.09.255.

[172] Cai, D.; Jin, J.; Yusoh, K.; Rafiq, R.; Song, M. High Performance Polyurethane/Functionalized Graphene Nanocomposites with Improved Mechanical and Thermal Properties. *Compos Sci Technol*, **2012**, *72* (6), 702–707.

References

[173] Zhu, Y.; Wang, H.; Zhu, J.; Chang, L.; Ye, L. Nanoindentation and Thermal Study of Polyvinylalcohol/Graphene Oxide Nanocomposite Film through Organic/Inorganic Assembly. *Appl Surf Sci*, **2015**, *349*, 27–34.

الخلاصة

يتضمن هذا العمل تحضير ودراسة طلاء بوليمري شفاف له خصائص ترايبولوجية جيدة. بالإضافة إلى ذلك ، تحسين الخصائص الميكانيكية للطلاء بالاضافة لذالك يكون الطلاء المقوى بالجسيمات النانوية لديه القدرة على امتصاص الأشعة فوق البنفسجية مع الحفاظ على الشفافية.

ان تقليل معامل الاحتكاك لتعزيز سلوك مقاومة البلى للطلاء لتطبيقات شاشات الهاتف المحمول والكمبيوتر أيضًا زيادة العمر الافتراضي لأغطية مصابيح السيارة والزجاج والنوافذ البلاستيكية وطلاء الخلايا الشمسية.

وقد تم استخدام تقنية الصب بالمحلول لإنشاء الطلاء المركب النانوي المصنوع من أكسيد الجرافين والبوليمر. كما تم اختبار الخصائص الترايبولوجية والميكانيكية لاضافة اكسيد الجرافين وتأثير الجسيمات النانوية GO و GO المعالج. بالإضافة إلى ذلك ، تم فحص تأثير إضافة شمع العسل على الخصائص الميكانيكية ، والبنية المجهرية ، والترايبولوجية لـ (PMMA).

تم إنشاء طلاء مركب من مادة PMMA مع جسيمات GO و MGO النانوية بنسب وزنية مختلفة (0 ، 0.25 ، 0.5 ، 1) % وكذلك تم تحضير عينات الطلاء بنسب اضافة 1 % من MGO مع نسب وزنية مختلفة من شمع العسل بنسب وزنية (0.25,0.5, 0.1 نسبة وزنية %. تم إجراء الفحوصات حيث تم تقييم توزيع النانو ونوع الكسر باستخدام طرق الفحص المجهري الإلكتروني (SEM). وقد تم فحص التركيب الكيميائي لـ PMMA وطلاء المركب النانوي باستخدام طريقة (FTIR) كما تم إجراء اختبارات الصلادة و FTIR و DSC و UV و Nanoindentation وفحص الترطيب واختبارات الالتصاق للعينات. والصلادة والبلا ومعامل الاحتكاك .وقد تم فحص الخصائص الميكانيكية لطلاء PMMA ومع إضافة الجسيمات النانوية .للتحقق من العلاقة بين السلوك الترايبولوجي والسلوك الميكانيكي.

أظهرت النتائج أن إدراج جسيمات MGOو GO النانوية أدى إلى تحسين خواص طلاء PMMA.كذلك كان لشمع العسل دور في تحسين الخواص الميكانيكية والترايبولوجية للطلاء. تم العثور على معدل البلى ومعامل الاحتكاك للطلاء المركب PMMA أقل بكثير من تلك الخاصة بـ طلاء PMMA النقي. انخفض معامل

الاحتكاك بنسبة 26% بلنسبة لعينة PMMA\1% wt MGO\BW 0.5 وان هذه العينة لها اقل معدل بلى ومعامل احتكاك.

وفقًا لبيانات البنية المجهرية، كان للمعالجة بالموجات فوق الصوتية دور مهم في تحقيق تشتت ممتاز وتقليل تكتل الجسيمات النانوية. كما انه قد كان هناك تحسن ملحوظ ، كما يتضح من نتائج الخواص الميكانيكية مثل الصلابة ، ومعامل المرونة ، والالتصاق. تشير نتائج اختبارات قابلية البلل إلى أن إضافة شمع العسل أدى إلى تحسين مقاومة البلل لمادة PMMA .

وبين فحص UV ان اضافة الجرافين اوكسايد ساعد على امتصاص الاشعة فوق البنفسجية لطلاء PMMA المركب. كما ان الشفافية قد قلت مع زيادة نسبة اوكسايد الجرافين وشمع العسل .وبلنسبة لاختبار الصلادة (فكرز) فقد تم تحسين الصلابة بنسبة 55% لعينة PMMA\1% wt MGO\BW 0.5.كذلك تم تحسين معامل المرونة بنسبة 38٪ لعينة PMMA\1% Wt MGO\BW 0.5، زاد T_g بحوالي 20٪ بالنسبة لـ PMMA \ MGO 1 بالمقارنة مع PMMA النقي.

وزارة التعليم العالي والبحث العلمي
جامعـــــــــــــــــة بابـــــــــــــــــــل
كليـــــــــــــــة هنـــــــــــــــدسة المواد
قسم البوليمر والصناعات البتروكيمياوية

تحضير ودراسة الخواص الترايبولوجية والميكانيكية لطلاء مركب نانوي بوليمري شفاف

رسالة

مقدمه إلى قسم هندسة البوليمر في كلية هندسة المواد/ جامعة بابل وهي جزء من متطلبات نيل درجة ماجستير في هندسة المواد / البوليمر

من قبل

احمد فاضل عباس هادي

بكالوريوس هندسة المواد / هندسة البوليمر والصناعات البتروكيمياوية

بإشراف

أ.م.د. عمار عماد كاظم **أ.د. ذو الفقار كريم مزعل**

1444 هـ. **2023 م.**